

UNCLASSIFIED

AD NUMBER

AD916279

LIMITATION CHANGES

TO:

Approved for public release; distribution is unlimited.

FROM:

Distribution authorized to U.S. Gov't. agencies only; Test and Evaluation; AUG 1973. Other requests shall be referred to Army Air Mobility Research and Development Lab., Fort Eustis, VA.

AUTHORITY

USAAMRDL ltr 30 Mar 1982

THIS PAGE IS UNCLASSIFIED

**THIS REPORT HAS BEEN DELIMITED
AND CLEARED FOR PUBLIC RELEASE
UNDER DOD DIRECTIVE 5200.20 AND
NO RESTRICTIONS ARE IMPOSED UPON
ITS USE AND DISCLOSURE.**

DISTRIBUTION STATEMENT A

**APPROVED FOR PUBLIC RELEASE;
DISTRIBUTION UNLIMITED.**

7

AD 916279

AD

USAAMRDL TECHNICAL REPORT 73-62A
DESIGN GUIDE HANDBOOK FOR THE DESIGN OF
BALLISTIC-DAMAGE-TOLERANT SHORT-FIBER-MOLDED
AIRCRAFT FLIGHT CONTROL SYSTEM COMPONENTS

VOLUME I

DESIGN CRITERIA, CONCEPTS, TOOLING,
FABRICATION, TESTING, AND EVALUATION

By

D. C. Cully

T. J. Boller

August 1973

DDC
RECEIVED
JAN 25 1974
REGISTERED
B

EUSTIS DIRECTORATE
U. S. ARMY AIR MOBILITY RESEARCH AND DEVELOPMENT LABORATORY
FORT EUSTIS, VIRGINIA

CONTRACT DAAJ02-70-C-0062
GOODYEAR AEROSPACE CORPORATION
AKRON, OHIO



Distribution limited to U.S. Government agencies only; test and evaluation; August 1973. Other requests for this document must be referred to the Eustis Directorate, U.S. Army Air Mobility Research and Development Laboratory, Fort Eustis, VA 23604.

DISCLAIMERS

The findings in this report are not to be construed as an official Department of the Army position unless so designated by other authorized documents.

When Government drawings, specifications, or other data are used for any purpose other than in connection with a definitely related Government procurement operation, the United States Government thereby incurs no responsibility nor any obligation whatsoever; and the fact that the Government may have formulated, furnished, or in any way supplied the said drawings, specifications, or other data is not to be regarded by implication or otherwise as in any manner licensing the holder or any other person or corporation, or conveying any rights or permission, to manufacture, use, or sell any patented invention that may in any way be related thereto.

Trade names cited in this report do not constitute an official endorsement or approval of the use of such commercial hardware or software.

DISPOSITION INSTRUCTIONS

Destroy this report when no longer needed. Do not return it to the originator.



DEPARTMENT OF THE ARMY
U. S. ARMY AIR MOBILITY RESEARCH & DEVELOPMENT LABORATORY
EUSTIS DIRECTORATE
FORT EUSTIS, VIRGINIA 23604

This report was prepared by Goodyear Aerospace Corporation under the terms of Contract DAAJ02-70-C-0062. It is presented in two volumes:

Volume I - Design Criteria, Concepts, Tooling, Fabrication, Testing, and Evaluation (Unclassified)

Volume II - Ballistic Data (Classified Confidential)

This effort is the third phase of a three-phase program to advance the state of the art of providing small-arms ballistic protection for Army aircraft critical components. The approach consists of using a short-fiber plastic composite and a compression-molded fabrication technique to develop ballistic-damage-tolerant flight control components that are competitive with current standard components from the standpoint of weight, strength, ease of fabrication, reliability, and cost. The Phase III effort reported herein involved the preparation of a handbook for the design of survivable flight control components using a short-fiber moldable composite material and covering fabrication and test requirements of components made from such material.

The technical monitor for this contract was Mr. Stephen Pociluyko of the Military Operations Technology Division.

Task 1F162203A15003
Contract DAAJ02-70-C-0062
USAAMRDL Technical Report 73-62A
August 1973

DESIGN GUIDE HANDBOOK FOR THE DESIGN OF
BALLISTIC-DAMAGE-TOLERANT SHORT-FIBER-MOLDED
AIRCRAFT FLIGHT CONTROL SYSTEM COMPONENTS

VOLUME I - DESIGN CRITERIA, CONCEPTS, TOOLING,
FABRICATION, TESTING, AND EVALUATION

GER 15881, Volume I

By
D. C. Cully
T.J. Boller

Prepared by

Goodyear Aerospace Corporation
Akron, Ohio

for

EUSTIS DIRECTORATE
U. S. ARMY AIR MOBILITY RESEARCH AND
DEVELOPMENT LABORATORY
FORT EUSTIS, VIRGINIA

Distribution limited to U.S. Government agencies only;
test and evaluation; August 1973. Other requests for
this document must be referred to the Eustis Directorate,
U.S. Army Air Mobility Research and Development
Laboratory, Fort Eustis, VA 23604.

ABSTRACT

This design guide has been prepared to provide the design engineer, structural analyst, manufacturing engineer, and test engineer with the engineering know-how and technology to design, analyze, manufacture, and test ballistic-damage-tolerant flight control components molded of a short-fiber glass-epoxy composite material. The design guide provides data on the effects of variable material parameters such as resin type, fiber length, fiber type, fiber finish, and composite thickness on the ballistic response of the composite (i. e., the extent of damage and residual load capacity after damage). Fully tumbled caliber .30 ball M2 and untumbled caliber .50 AP M2 projectiles were evaluated at several impact temperatures and velocities. Methods of design to maximize ballistic tolerance and design analysis techniques are described. Designs, tooling and manufacturing techniques, and a test and evaluation program for three typical flight control components are presented.

The design guide is organized in two volumes. The greatest amount of the design guide information is unclassified and is presented in this document (Volume I) to facilitate its availability and use by individual designers. The essential classified information is presented in Volume II (Confidential document) for sources of pertinent and/or related information that may be required by the designer.

PRECEDING PAGE BLANK-NOT FILMED

FOREWORD

This document was prepared by Goodyear Aerospace Corporation, Akron, Ohio, under U.S. Army Contract DAAJ02-70-C-0062, Task 1F162203A15003, for the Eustis Directorate, U.S. Army Air Mobility Research and Development Laboratory. Mr. Stephen Pociluyko was the Contracting Officer's Technical Representative.

This report covers the Design Guide Handbook effort accomplished in Phase III - Design Guide and Composite Material Specification - of the project for the Development of Ballistic-Damage-Tolerant Flight Control Components Molded of a Short-Fiber Reinforced Composite Material. The design guide is organized in two volumes. The contract period under which this volume of the design guide (Volume I) was prepared extended from November 1972 through April 1973.

Mr. D. C. Cully was responsible for the organization and content of the design guide and was the program manager for Goodyear Aerospace Corporation. Mr. T. J. Boller provided the technical data for the design analysis of ballistic response and the structural design analysis.

PRECEDING PAGE BLANK-NOT FILMED

TABLE OF CONTENTS

	<u>Page</u>
ABSTRACT	iii
FOREWORD	v
LIST OF ILLUSTRATIONS	ix
LIST OF TABLES	xiv
INTRODUCTION AND DESCRIPTION	1
Program Background	1
Purpose of Design Guide	1
Scope and Organization	2
AIRCRAFT VULNERABILITY/SURVIVABILITY FACTORS	3
BALLISTIC THREATS	5
MATERIAL CONSIDERATIONS AND BALLISTIC RESPONSE	7
General	7
Effect of Composite Constituent Materials	7
Effect of Ballistic Parameters	13
Effect of Material Thickness	13
Cyclic Tensile Fatigue	17
Combined Stress-Impact	19
DESIGN ANALYSIS OF BALLISTIC RESPONSE	20
Damage Analysis	20
Design Allowables	26
Design Criteria for Cyclic Loading	27
Analytical Methods for Design	31
COMPONENT DESIGN	37
Design Concepts	37
Typical Component Designs	37
Design Criteria	39
Design Configurations	43

	<u>Page</u>
Structural Design Analysis	49
Weight Comparison	56
TOOLING AND FABRICATION	57
General	57
Idle Bell Crank Tooling	58
Aft Bell Crank Tooling	58
Quadrant Assembly Tooling	58
Fabrication of Components	65
TESTING AND EVALUATION	78
Test and Evaluation Criteria	78
Description of the Test Program	79
Test Fixtures and Equipment	81
Component Fit Checks	81
Preliminary Proof Loading	88
Category 1 Tests	88
Category 2 Tests	101
Category 3 Tests	104
Category 4 Tests	111
Category 5 Tests	123
Category 6 Tests	123
Category 7 Tests	126
Summary of Test Results	132
LITERATURE CITED	134
APPENDIX - COMPOSITE MATERIAL SYSTEMS PROPERTIES . .	136
DISTRIBUTION	147

LIST OF ILLUSTRATIONS

<u>Figure</u>		<u>Page</u>
1	Typical Surface Ballistic Damage Characteristics of the Composite Materials	10
2	Comparison of Post-Damage Tensile Properties - Composites Reinforced With S-2 and E Glass	12
3	Effect of Fiber Content on the Strength of the Composite Materials	12
4	Load-N Curves for Undamaged and Ballistically Damaged 1/8-Inch-Thick Composite Material	18
5	Tensile Fatigue Curves for the Undamaged Composite	29
6	Tensile Fatigue Curves for the Damaged Composite	30
7	Tensile Fatigue Curves for Undamaged and Damaged Composites as a Percentage of Static Strength	32
8	Fatigue Design Curves (A-Basis) for the Composite	33
9	Typical Design Curves for Ballistic-Damage-Tolerant Components	36
10	Typical Components Molded of a Short-Fiber Composite Material	39
11	Specific Design Details for Components Molded of a Short-Fiber Glass-Epoxy Composite Material	40
12	Loading Conditions for the Ballistic-Damage-Tolerant Components	42
13	Design of CH-47C Ballistic-Damage-Tolerant Idler Bell Crank	45
14	Design of CH-47C Ballistic-Damage-Tolerant Aft Pylon Upper Bell Crank	47

<u>Figure</u>		<u>Page</u>
15	Design of UH-1B/D Ballistic-Damage-Tolerant Quadrant Assembly	51
16	Areas of High Stress in Undamaged Components	53
17	Areas of High Stress in Ballistically Damaged Components	54
18	Design of Compression-Molding Tool for Idler Bell Crank	59
19	Procedure for Removing Component From Three-Piece Tool	61
20	Matched-Die Steel Tooling for Idler Bell Crank	62
21	Design of Compression-Molding Tool for Aft Bell Crank	63
22	Matched-Die Steel Tooling for Aft Bell Crank	65
23	Design of Compression-Molding Tool for Quadrant Sheave	67
24	Matched-Die Steel Tooling for Quadrant Sheave	69
25	Design of Compression-Molding Tool for Quadrant Crank	70
26	Matched-Die Steel Tooling for Quadrant Crank	71
27	Schematic Diagram of Typical Fiber Glass Roving Impregnation Equipment	71
28	Schematic Diagram of Typical Rotary Roving Cutting Equipment	72
29	Turner Model M-600 Roving Chopper	72
30	Various Fabrication Stages of Idler Bell Crank	74
31	Preforming Chopped-Fiber Molding Material for Quadrant Sheave	75

<u>Figure</u>		<u>Page</u>
32	Completed Preform for Quadrant Sheave	76
33	Molded Quadrant Sheave on Knock-Out Pins in Tool . .	77
34	Completed Quadrant Sheave Removed From Tool . . .	77
35	Test Program for Molded Flight Control Components .	80
36	Fatigue Test Fixtures and Component Installations . .	82
37	Universal Ballistic Test Fixture and Component Installations	83
38	Comparison of Ballistic-Damage-Tolerant Flight Control Components With Their Metal Counterparts	84
39	Two Molded Idler Bell Cranks Installed in CH-47C Training Unit	85
40	Molded Aft Bell Crank Installed in CH-47C Training Unit	86
41	Molded Quadrant Assembly Installed in UH-1D Aircraft .	87
42	Load-Deflection Curves, Proof and Ultimate Loading - Aft Bell Crank	89
43	Load-Deflection Curve, Proof and Ultimate Loading - Idler Bell Crank	90
44	Load-Deflection Curve, Proof and Ultimate Loading - Quadrant Assembly	91
45	Fatigue Test Setup for Quadrant Assembly	93
46	Schematic of Ballistic Test Range Facility	94
47	Quadrant Assembly Mounted in the Test Fixture at the Ballistic Test Range	95
48	Temperature Recorder and Gun Mount Used in Ballistic Testing	96

<u>Figure</u>		<u>Page</u>
49	High-Speed Motion-Picture Sequences, Caliber .30 and Caliber .50 Ballistic Impacts - Aft Bell Crank	97
50	High-Speed Motion-Picture Sequences, Caliber .30 Ballistic Impacts - Quadrant Assembly	98
51	High-Speed Motion-Picture Sequences, Caliber .30 and Caliber .50 Ballistic Impacts - Idler Bell Crank	99
52	Caliber .30 Ballistic Impact Under Load - Quadrant Assembly	100
53	Load-Deflection Curve, Failure Loading - Idler Bell Crank	106
54	Load-Deflection Curve, Failure Loading - Aft Bell Crank	107
55	Load-Deflection Curve, Failure Loading - Quadrant Assembly	108
56	Quadrant Assembly After Category 3 Failure Load Test	109
57	Quadrant Assembly After Vibration Testing	113
58	Location of Cracks in Test Specimens for Crack Propagation Tests	114
59	Initial Crack in Idler Bell Crank After 6000 Operational Load Cycles	116
60	Idler Bell Crank Loaded to Failure - Crack Propagation Test	117
61	Initial Crack in Aft Bell Crank After 6000 Operational Load Cycles	118
62	Aft Bell Crank Loaded to Failure - Crack Propagation Test	119
63	Load-Deflection Curve, Crack Propagation Loading - Aft Bell Crank	120

<u>Figure</u>		<u>Page</u>
64	Crack Propagation Curve - Aft Bell Crank	120
65	Initial Crack in Crank of Quadrant Assembly After 6000 Operational Load Cycles	121
66	Quadrant Assembly Loaded to Failure - Crack Propaga- tion Test	122
67	Idler Bell Crank Fire-Resistance Test	128
68	Quadrant Assembly Fire-Resistance Test (Crank Area) . .	129
69	Burning and Extent of Fire Damage in the Crank Area of the Quadrant Assembly	130
70	Quadrant Assembly Fire-Resistance Test (Groove ² Rim Area)	131
71	Typical Tensile Stress-Strain Curves for the Composite Material System	138
72	Typical Compression Stress-Strain Curves for the Com- posite Material System	139
73	Typical Panel Shear Stress-Strain Curves for the Com- posite Material System	140
74	Flexural Strength Design Curves for the Composite Material System	141
75	Interlaminar Shear Strength Design Curves for the Com- posite Material System	142
76	Tensile Strength Design Curves for the Composite Material System	143
77	Compressive Strength Design Curves for the Composite Material System	144
78	Panel Shear Strength Design Curves for the Composite Material System	145
79	Bearing Strength Design Curves for the Composite Material System	146

LIST OF TABLES

<u>Table</u>		<u>Page</u>
I	Effects of Material Variables on Undamaged and Caliber .30 Ballistically Damaged Composites	9
II	Summary of Visual Area and Volume Ballistic Damage on the Composite Material	14
III	Summary of Visual Transverse Ballistic Damage on the Composite Material	15
IV	Summary of Residual Load Capacities of the Composite Material	15
V	Summary of Area, Volume, and Transverse Ballistic Damage on 3.5-Inch-Wide Composite Material	16
VI	Summary of Residual Load Capacities and Estimated Ballistic Limits of 3.5-Inch-Wide Composite Material . .	16
VII	Environmental and Loading Effects on Tensile Properties of the Undamaged Composite	21
VIII	Influence of Test Variables on the Residual Load Capacity and Effective Damage Length of the Caliber .30 Impacted Composite	23
IX	Environmental and Loading Effects on Tensile Properties of the Caliber .30 Impacted Composite	24
X	Summary of Load-Carrying Abilities of Undamaged and Caliber .30 Ballistically Damaged Composites	25
XI	Influence of Test Variables on the Residual Load Capacity and Effective Damage Length of the Caliber .50 Impacted Composite	27
XII	Design Allowable Property Values for the Composite . . .	28
XIII	Development of Effective Damage Length Criteria	34
XIV	Summary of Structural Design Analysis - Calculated Minimum Margins of Safety	55

<u>Table</u>		<u>Page</u>
XV	Component Weight Comparisons	56
XVI	Sequence of Category 2 Tests	101
XVII	Summary of Category 2 Test Results	103
XVIII	Sequence of Category 3 Tests	104
XIX	Summary of Category 3 Test Results	110
XX	Sequence of Category 4 Tests	111
XXI	Comparison of Failure Loads With Maximum Design Loads and Operational Loads - Crack Propagation Tests	123
XXII	Summary of Fuel and Oil Immersion Test Results	125
XXIII	Summary of Fire-Resistance Test Results	127
XXIV	Summary of Test Results	133
XXV	Composite Material Constituents	136
XXVI	Summary of Key Properties for Composite Material System	137

INTRODUCTION AND DESCRIPTION

PROGRAM BACKGROUND

U.S. Army aircraft, and in particular rotary-wing aircraft, have in the past decade been expected to perform combat roles where they have been exposed to extremely high concentrations of enemy small-arms ground fire. The intensity and magnitude of these weapon effects on the aircraft structure have exceeded the levels envisioned for the aircraft when originally designed and produced. As a result, high aircraft loss rates have been experienced that have promoted extensive research and testing to develop effective means of increasing aircraft survivability.

Several programs have been conducted to evaluate many different techniques and concepts for providing ballistic protection to combat aircraft. Conceptual approaches evaluated have included development of structural and parasitic armor designs, which, while effective, result in high weight and cost penalties.

One concept that has shown promise is a technique developed for limiting or minimizing the extent of structural damage from small-arms projectile impacts. This technique of ballistic-damage tolerance is a concept that permits the impacting projectile to perforate the structural component with minimum energy transfer and, consequently, minimum structural damage. The approach consists of using redundant load paths, high-fracture-resistant materials, and sufficiently large (in area) structural sections. Components of high ballistic-damage tolerance can be designed through the use of this concept. The majority of the specific applications of this concept will be in the flight control components and other primary and secondary structural aircraft fittings. Ballistic-damage tolerance is one of the first techniques that should be examined in the design process, inasmuch as this concept can provide a significant degree of improved survivability for the least weight and cost.

PURPOSE OF DESIGN GUIDE

The purpose of the design guide is to provide aircraft engineers in the fields of design, structural analysis, and manufacturing with the basic design, ballistic, strength, and manufacturing data necessary for the design of high-confidence-level, ballistic-damage-tolerant flight control system components. It is structured to acquaint designers and structural engineers with a new technology utilizing a short-fiber glass reinforced molded composite material and the methodology required for cost-effective designs. It is not the purpose of this design guide to present

new control system concepts or new analytical techniques. It requires of the designer a good working knowledge and experience in the conventional design and analytical procedures.

SCOPE AND ORGANIZATION

The scope of this document encompasses the definition of aircraft vulnerability/survivability and the threat levels for which protection has been evaluated. Several engineering disciplines that are utilized in the design of ballistic-damage-tolerant components are discussed in detail within the technical areas listed below.

- Aircraft vulnerability and survivability
- Ballistic threats
- Effect of material parameters on ballistic response
- Cyclic fatigue response
- Analysis of ballistic response
- Design criteria
- Component designs
- Component tooling and fabrication
- Component testing and evaluation

The design guide is organized on a sequential functional level based on logical consideration of component design. The data presented reflect the current status of the material and ballistic response characteristics.

Special care has been taken to present the maximum amount of design information in an unclassified document to facilitate its availability and use by designers. The essential classified information is presented in Volume II (Confidential document). References to Volume II are made throughout this document (Volume I) for sources of pertinent and/or related information that may be required by the designer.

AIRCRAFT VULNERABILITY/SURVIVABILITY FACTORS

Aircraft vulnerability is defined as:

"That quantitative measure of an aircraft's response to a given hostile weapon effect, and the encounter condition, that results in attrition, crew injury, or inability to perform those functions essential to achieve combat mission objectives."9

Of specific concern here is the vulnerability of the flight control system and other structural components.

Aircraft survivability is defined as:

"That measure of an aircraft's capability to continue to function after being hit by hostile weapon systems. This includes those design and performance features that enable an aircraft, by avoidance, suppression, or tolerance techniques, to degrade a hostile force's ability to use its weapons effectively."9

We will specifically consider design and performance techniques to achieve survivability.

Frequently, the terms "survivability" and "vulnerability" have been used interchangeably, but they are not synonymous. The probability of an aircraft's survivability in combat is dependent primarily on three factors: (1) the probability of detection, (2) the probability of a hit, and (3) the probability of a kill, given a hit.

Each of these factors is important, and each should be considered regardless of the enemy weapons employed. An increase in survivability is gained by a reduction in the probability of being detected, being hit, or being killed. The probability of being detected is influenced by terrain, weather, speed, altitude, radar reflectivity, noise, etc. The probability of being hit when detected is influenced by altitude, speed, size of aircraft, etc. Many of these influencing factors (for example, altitude, speed, and size of aircraft) are dictated by the mission of the aircraft and cannot be altered significantly. However, a factor that is just as important as or perhaps even more important than any of these in terms of combat survival is the ability of the aircraft to withstand the effects of hits from enemy gunfire.

It is the latter approach to survivability that we will develop in this document. When the aircraft has been detected and ballistically impacted,

what techniques has the designer employed and made a part of the aircraft structure, particularly the flight control system or other structural components, which will assure survivability?

BALLISTIC THREATS

The ballistic threats for which protection has been evaluated are the impacts from small-arms ground fire. Some of the types of weapons used in small-arms fire are the caliber .30 ball and armor-piercing (AP) and caliber .50 AP projectiles. Tracer and incendiary rounds of both types are also included in the threat.

Ballistic impacts on standard metal aircraft structural and flight control components can cause several responses; the responses vary according to the character of the metal used, the design of the component, and the velocity, mass, and attitude of the impacting projectile. The metal may be either brittle or ductile; the design of the component may be of marginal or abundant structural adequacy; and the impacting projectile may hit the component in a very vulnerable area or in a highly damaging attitude.

When the projectile strikes the component, the impact imparts energy to the component which must be expended in one or more of several fashions. If the component is brittle, the impact may propagate a crack and cause component failure or in some cases cause the component to shatter. If the component is ductile, the impact may bend or otherwise deform the component and jam its operational function. If the component is structurally marginal and the hit is in a vulnerable area, the impact may remove sufficient structure to cause failure of the component under subsequent dynamic structural loading.

The ballistic response of nonmetallic components molded of fiber-reinforced composite materials differs greatly from that of the metal materials. Indeed, composite materials perform differently depending on the form in which the fiber is present and the specific design features of the component.

Long-fiber composites (e.g., those employing filament-winding or filament-woven fabric lay-up techniques), while of excellent strength, may exhibit poor ballistic response and extensive damage as the energy moves along the fibers, tearing them from the composite. Some woven fabric materials show good ballistic-response properties; however, these materials are often used in sandwich constructions, for cost and strength considerations, in which they tend to delaminate with oblique impacts.

Composites molded of short-fiber reinforced plastics have been found to possess unique properties that provide a sound basis for the design of ballistic-damage-tolerant components.

During the course of experimentation and analysis of ballistic damage on the short-fiber molded components, it was found that the usual worst-case threat analysis situation of highest kinetic energy ($KE = 1/2 m V^2$) does not apply. This premise is based on the assumption that maximum damage will occur with the high-kinetic-energy projectile impact. Because the molded composite permits the projectile to penetrate the components with very little energy transfer into the components or linkages, the projectile velocity and mass factors are not significantly contributory to ballistic damage. Tests of projectile impacts of various velocities and masses have confirmed this conclusion. The important ballistic factor for this type of components is the footprint, or projected area, of the impacting projectile. Therefore, the size and attitude of the projectile control the worst-case analysis. Consideration of the probability of various attitudes for specific size projectiles cannot be ignored. For the objectives of this design guide, it has been decided that the fully tumbled caliber .30 and untumbled caliber .50 projectiles will collectively provide the best test data for practical design of ballistic-damage-tolerant flight control components. This guide presents designs of such components that would survive damage by tumbled caliber .30 ball projectiles; it does not consider caliber .30 AP because the tumbled ball is considered to be more damaging than AP to short-fiber plastic composite type components. Ball-type ammunition has more plasticity and tumbles more easily than AP ammunition, which tends to penetrate aircraft structure in an untumbled path. It can be shown that the incidence of tumbled caliber .30 projectile impacts is significant for examination of in-service ballistic damage. The caliber .50 projectiles show a lower incidence of tumbled hits. The greater mass, energy, and velocity relationship of the caliber .50 projectile makes it more difficult to tumble through aircraft structure.¹

MATERIAL CONSIDERATIONS AND BALLISTIC RESPONSE

GENERAL

The material system evaluated for developing the ballistic-damage tolerance concept consists of a composite molded of short-fiber glass-epoxy materials. This material system is capable of being molded in matched-die steel tooling to provide the dimensional shape with adequate strength and rigidity for use as in-service flight control components and other structural components.

The material requirements are simply stated as the need for a reliable material that will withstand ballistic impacts with minimum damage and/or maximum strength.

The strength and ballistic response of any composite material system are a function of the properties of the constituent materials. Ballistic response can be measured in many ways; however, the most significant measurements are the extent of damage (a dimensional measurement of the damage area size or volume of the impacted material) and the residual load capacity (the retained load-carrying capability after impact).

EFFECT OF COMPOSITE CONSTITUENT MATERIALS

The constituent material variables of short-fiber reinforced composites that may affect ballistic response are numerous and include (1) the resin matrix strength, modulus, and toughness properties; (2) the reinforcing fiber strength; (3) fiber length; (4) fiber finish; (5) fiber-to-resin ratio; (6) fiber diameter; (7) fiber orientation; (8) fiber bundle size; and (9) molded composite thickness. Three of these parameters were believed to have the most influence on ballistic response: (1) resin type, (2) fiber finish, and (3) fiber length. These three parameters were extensively evaluated.

The resin matrix must carry out several important functions to allow the composite to effectively resist structural loads. These functions include transferring the load between the fibers and providing strength and rigidity in the directions normal to the fibers. The epoxy resins provide an optimum combination of properties based on these considerations and consequently are most appropriate as matrix materials for high-strength composites.

The three epoxy resin systems evaluated were (1) an epoxy novalac with intermediate tensile strength and toughness; (2) a bisphenol-A epoxy flexibilized with a long-chain aliphatic epoxide, exhibiting intermediate strength and low modulus but high elongation and toughness; and (3) a cyclopentyl-ether epoxy with high strength and modulus, low elongation, and intermediate toughness.

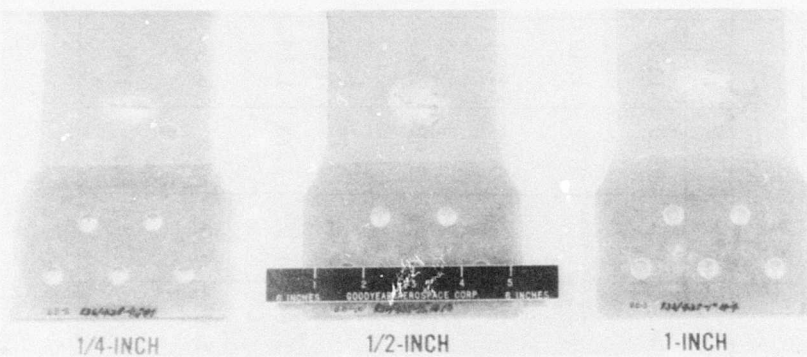
The fiber glass finishes evaluated were (1) a compatible finish, which provides high strength coupling between the glass fiber and the resin matrix; (2) an incompatible finish, which was expected to provide poor coupling; and (3) an intermediate compatibility finish.

The fiber lengths evaluated were 1/4, 1/2, and 1 inch. These lengths gave a broad range of strengths and were most commonly used for short-fiber product moldings.

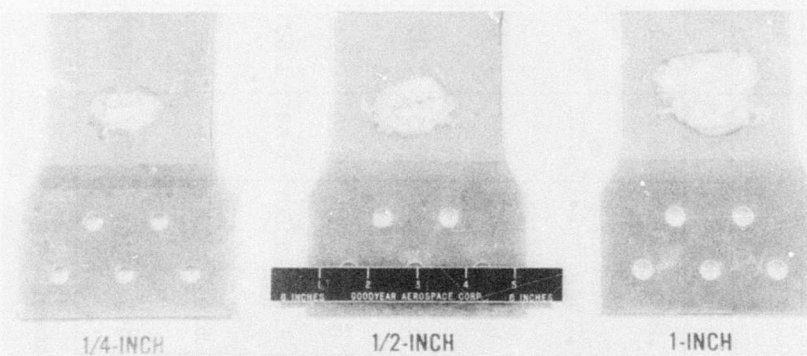
The effects of these variations in the three material parameters on several structural and ballistic responses of the composites are summarized in Table I. Several significant results are evident from the data summary in Table I:

1. Fiber length has by far the most significant effect on both the structural properties and the ballistic response as measured by residual load capacity. The shortest fiber lengths result in the minimum ballistic damage but the lowest strength. The longest fiber lengths result in the highest strength but the maximum ballistic damage (see Figure 1).
2. Resin type did not significantly affect the composite strength; however, variations in extent of damage and residual strength were noted. Due to the large amount of variability existing in the data, no conclusive trends were evident regarding the selection of a resin type.
3. A compatible fiber finish would appear to result in a somewhat better composite strength; however, the effect on extent of damage and residual load capacity is not significant.
4. Short-fiber molded composites exhibiting the property extremes of (1) high undamaged strength and/or low extent of damage and (2) low undamaged strength and/or high extent of damage do not always conform to the expected corresponding results of (1) low strength + high damage = low residual load capacity and (2) high strength + low damage = high residual load capacity. Therefore, visual extent of damage per se is not a totally reliable criterion on which to judge the post-damage properties of short-fiber components.

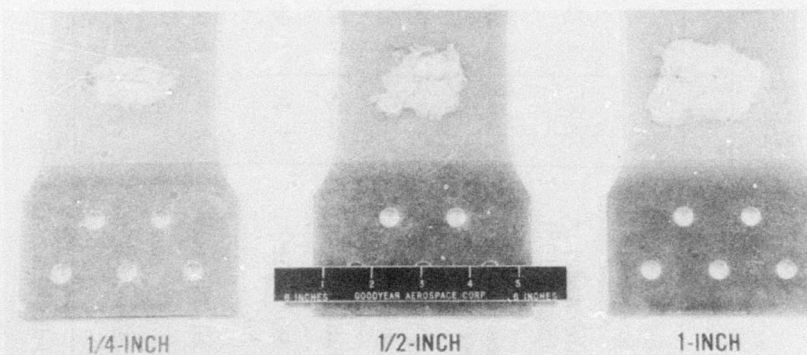
TABLE I. EFFECTS OF MATERIAL VARIABLES ON UNDAMAGED AND CALIBER .30 BALLISTICALLY DAMAGED COMPOSITES													
Parameter	Fiber Length (in.)			Fiber Finish and Resin Type									
				Compatible			Intermediate Compatible			Incompatible			
	1	1/2	1/4	A	B	C	A	B	C	A	B	C	
Ultimate Tensile Strength, Undamaged (psi x 10 ³)	21.5	17.1	15.5	19.7	20.2	20.9	17.1	15.9	16.7	17.8	18.9	14.3	
Initial Tensile Modulus, Undamaged (psi x 10 ⁶)	3.85	3.73	3.76	3.50	3.13	4.37	3.55	3.40	4.23	3.76	3.62	4.49	
Front Surface Ballistic Damage Area (in. ²)	1.01	0.95	0.81	0.95	0.87	0.88	1.10	0.81	0.77	1.06	0.97	0.91	
Back Surface Ballistic Damage Area (in. ²)	3.77	2.39	1.62	2.62	2.18	2.45	2.87	2.59	2.44	2.93	2.69	2.57	
Damage Volume (in. ³)	0.28	0.20	0.15	0.21	0.19	0.20	0.24	0.20	0.19	0.23	0.22	0.20	
Transverse Ballistic Damage (in.)	1.86	1.68	1.53	1.68	1.60	1.68	1.80	1.61	1.64	1.77	1.73	1.67	
Residual Load Capacity (lb x 10 ³)	8.3	5.5	4.1	5.4	6.1	7.0	5.4	6.1	5.9	5.9	6.9	5.5	
Strength-to-Weight Ratio (in. x 10 ³)	260	174	130	174	197	224	170	188	186	183	217	171	
A = Intermediate strength and modulus (epoxy novalac).													
B = Intermediate strength and low modulus (flexibilized epoxy).													
C = High strength and modulus (cyclopentyl-ether epoxy).													



A. Front Surface Damage: Epoxy-Novalac Resin, Compatible Fiber Finish



B. Back Surface Damage: Epoxy-Novalac Resin, Compatible Fiber Finish



C. Back Surface Damage: Flexibilized Epoxy Resin, Incompatible Fiber Finish

Figure 1. Typical Surface Ballistic Damage Characteristics of the Composite Materials.

Fiber diameter, fiber strength, and fiber content were the three other material parameters evaluated. The results of these evaluations are given below.

1. Fiber diameter has no significant effect on the strength or the ballistic response of short-fiber composites.
2. Fiber strength does have a pronounced effect on the undamaged composite strength and modulus and on the residual load capacity after damage. S-2 glass fiber composites exhibit 15 to 30 percent higher strength than that of the E glass composites, as shown in Figure 2. Fiber strength has no significant effect on the extent of damage.
3. Fiber content has no significant effect on the composite strength or the ballistic response within the range evaluated: levels ranging from 44 to 64 volume percent (v/o). Composites with fiber content levels higher than 64 v/o are of poor quality and those with levels below 45 v/o lose strength properties rapidly. A level of 53 v/o is the optimum fiber volume percent for the best physical properties, processability, and ballistic response. (See Figure 3.)

All of the materials used in the composite material systems evaluations were produced with randomly oriented fibers. The random orientation and discontinuous nature of the fiber in the composite result in properties that have a tendency to be variable. The complexity of the component to be fabricated also adds to the variation of properties in the final part. Therefore, the ability of a material to mold a complex part while maintaining its consistent properties and moldability plays an important role in the selection of the material system for this program. The material system selected for use in the design of ballistic-damage-tolerant components consists of 1/2-inch-long glass fibers with a compatible finish in an epoxy-novalac resin matrix. This system may not yield the highest static properties, but its selection was based on achieving the best combination of the following characteristics:

- Minimum damage resulting from ballistic tests
- Superior load-carrying capacity under combined stress-impact effects
- Ease of premolding for complex shapes
- Ease of fabrication with a minimum of fiber crippling
- Better producibility and repeatability

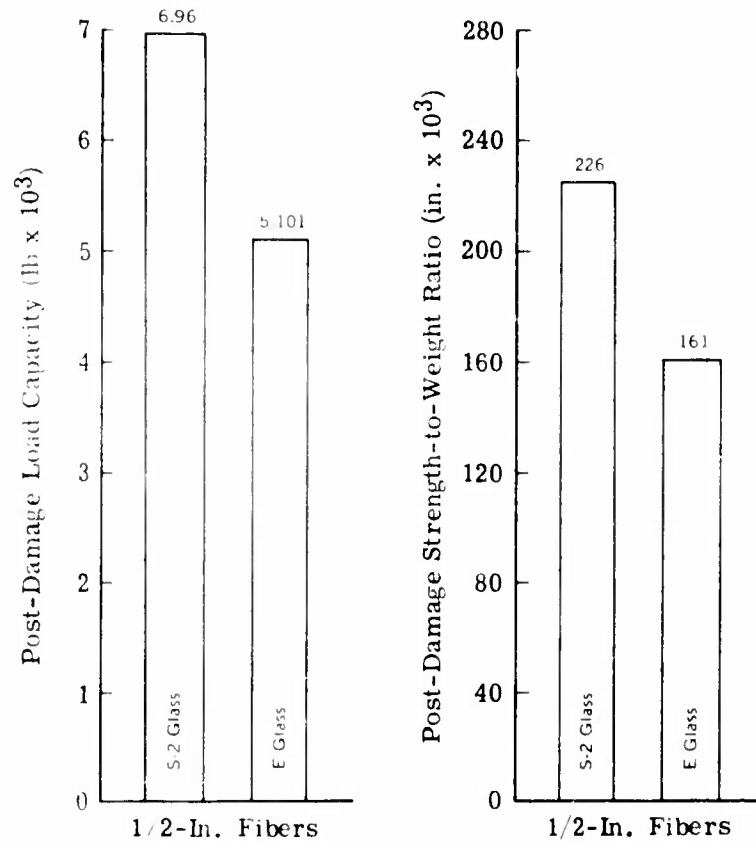


Figure 2. Comparison of Post-Damage Tensile Properties - Composites Reinforced With S-2 and E Glass.

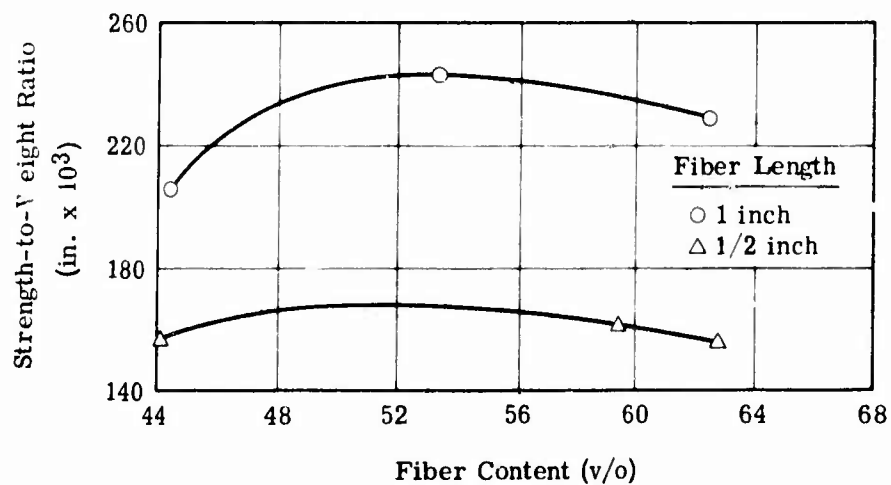


Figure 3. Effect of Fiber Content on the Strength of the Composite Materials.

EFFECT OF BALLISTIC PARAMETERS

Certain ballistic parameters including projectile mass, velocity, impacting attitude, and temperature at impact can affect the ballistic response of the composite materials. Tests were conducted using both fully tumbled caliber .30 ball M2 and untumbled caliber .50 AP M2 projectiles. The extent of visual area and volume ballistic damage on the impacted specimens is summarized in Table II. It can be seen that the caliber .50 projectile causes significantly less damage than the caliber .30 projectile. The extent of the caliber .30 damage is approximately twice the amount of the caliber .50 damage. This same relationship applies to the extent of transverse ballistic damage, which is summarized in Table III. The transverse damage measurements in Table III also show marginally greater damage when impacts occur at 160°F. The residual load capacities of the composite material after ballistic damage are summarized in Table IV. The data summary shows that the specimens impacted with the caliber .50 projectile retain greater load capacities than those impacted with the caliber .30 projectile.

With regard to the velocity of the projectile, the tests show rather wide variability in the residual load capacity but insignificant differences in the extent of damage. Multiple-regression analysis of the residual strength data shows that the damage increases and the residual load capacity decreases as the V₅₀ of the material is approached, at which velocity level all of the energy remaining in the projectile is transmitted to the component. However, the V₅₀ of structural sections of the short-fiber composite is so low (less than the range of 600 to 1300 ft/sec, depending on thickness) that the energy of impact transmitted to the component is also low.

EFFECT OF MATERIAL THICKNESS

Material thickness also affects the ballistic response of the composite material. The extent of ballistic damage is directly proportional to the thickness of the material. The extent of area, volume, and transverse ballistic damage on the 1/8-, 1/4-, and 3/8-inch-thick materials is summarized in Table V. It can be seen that the thicker specimens exhibit more extensive damage than the thin specimens.

The residual load capacities of the three material thicknesses after ballistic damage are summarized in Table VI. Residual load capacity is independent of impacting temperature, but is directly proportional to thickness. The percentage of retained strength of any thickness is not significantly different.

TABLE II. SUMMARY OF VISUAL AREA AND VOLUME BALLISTIC DAMAGE ON THE COMPOSITE MATERIAL^a

Velocity (ft/sec)	Caliber .50 Impacts			Caliber .30 Impacts		
	Temperature (°F)			Temperature (°F)		
	-80	RT	160	-80	RT	160
A. Front Surface Area (in. ²)						
1200	-	-	-	1.00	-	-
1500	0.56	0.51	0.51	1.13	0.85	0.97
1800	0.65	0.50	0.59	1.16	0.93	1.14
2100	0.59	0.52	0.58	1.24	1.22	1.16
2400	-	-	-	-	-	1.13
B. Back Surface Area (in. ²)						
1200	-	-	-	3.00	-	-
1500	1.51	1.40	1.36	2.49	2.40	2.62
1800	1.40	1.21	1.26	3.15	2.55	2.89
2100	1.32	1.34	1.20	2.54	2.50	2.34
2400	-	-	-	-	-	2.36
C. Volume (in. ³)						
1200	-	-	-	0.242	-	-
1500	0.126	0.114	0.109	0.221	0.195	0.217
1800	0.124	0.101	0.110	0.258	0.209	0.244
2100	0.115	0.108	0.106	0.231	0.226	0.211
2400	-	-	-	-	-	0.206
^a All specimens were 1/8 inch thick and 3.5 inches wide. (Typical specimens are illustrated in Figure 1, page 10.)						

TABLE III. SUMMARY OF VISUAL TRANSVERSE BALLISTIC DAMAGE ON THE COMPOSITE MATERIAL ^a						
Velocity (ft/sec)	Caliber .50 Impacts			Caliber .30 Impacts		
	Temperature (°F)			Temperature (°F)		
	-80	RT	160	-80	RT	160
A. Front Surface Transverse Damage (in.)						
1200	-	-	-	1.46	-	-
1500	0.97	0.90	0.83	1.44	1.32	1.35
1800	0.90	0.81	0.85	1.42	1.34	1.64
2100	1.02	0.89	0.99	1.47	1.58	1.50
2400	-	-	-	-	-	1.61
B. Back Surface Transverse Damage (in.)						
1200	-	-	-	2.22	-	-
1500	1.78	1.85	1.50	2.09	2.07	1.84
1800	1.67	1.71	1.58	2.21	2.17	2.12
2100	1.90	1.57	1.69	1.94	2.02	1.96
2400	-	-	-	-	-	1.97
^a All specimens were 1/8 inch thick and 3.5 inches wide.						

TABLE IV. SUMMARY OF RESIDUAL LOAD CAPACITIES OF THE COMPOSITE MATERIAL ^a						
Velocity (ft/sec)	Caliber .50 Impacts			Caliber .30 Impacts		
	Temperature (°F)			Temperature (°F)		
	-80	RT	160	-80	RT	160
1200	-	-	-	5320	-	-
1500	7203	7930	7173	6097	5610	5820
1800	7305	7937	7487	6050	5795	4973
2100	7362	8150	7250	5867	5367	5653
2400	-	-	-	-	-	4463
^a All test specimens were 1/8 inch thick and 3.5 inches wide. All values are in pounds.						

TABLE V. SUMMARY OF AREA, VOLUME, AND TRANSVERSE BALLISTIC DAMAGE ON 3.5-INCH-WIDE COMPOSITE MATERIAL^a

Material Thickness (in.)	Area and Volume Damage			Transverse Damage		
	Temperature (°F)			Temperature (°F)		
	-80	RT	160	-80	RT	160
	A. Front Surface Area (in. ²)			A. Front Surface (in.)		
1/8	0.85	0.76	0.81	1.30	1.08	1.19
1/4	0.99	1.25	1.33	1.38	1.51	1.54
3/8	1.58	1.55	1.49	1.72	1.62	1.61
	B. Back Surface Area (in. ²)			B. Back Surface (in.)		
1/8	2.45	2.60	2.53	2.00	1.94	1.97
1/4	3.51	3.71	3.81	2.43	2.51	2.49
3/8	4.79	4.52	4.47	2.77	2.69	2.62
	C. Volume (in. ³)			C. Avg Front/Back Surface (in.)		
1/8	0.196	0.193	0.195	1.65	1.51	1.58
1/4	0.545	0.579	0.631	1.91	2.01	2.02
3/8	1.126	1.085	1.062	2.26	2.16	2.12

^aMaterial was impacted with tumbled caliber .30 ball M2 projectiles at a nominal velocity of 1500 ft/sec.

TABLE VI. SUMMARY OF RESIDUAL LOAD CAPACITIES AND ESTIMATED BALLISTIC LIMITS OF 3.5-INCH-WIDE COMPOSITE MATERIAL^a

Material Thickness (in.)	Residual Load Capacities (lb)			Estimated Ballistic Limits (ft/sec)		
	Temperature (°F)			Temperature (°F)		
	-80	RT	160	-80	RT	160
1/8	5,043	6,890	5,967	589	578	584
1/4	10,537	10,430	10,180	978	956	1,017
3/8	15,650	15,203	16,123	1,231	1,188	1,216

^aMaterial was impacted with tumbled caliber .30 ball M2 projectiles at a nominal velocity of 1500 ft/sec.

Residual projectile velocity measurements were taken to be used in calculating the ballistic limit based on the following expression:

$$\text{Ballistic limit} = \sqrt{V_I^2 - V_R^2}$$

where V_I = impact velocity, ft/sec

V_R = residual velocity, ft/sec

The ballistic limit is defined as the projectile defeat velocity of any given material thickness. Table VI shows that the effect of temperature on ballistic limit is minimal. However, the ballistic limit is strongly dependent on material thickness. The 3/8-inch-thick material exhibited approximately twice the value of projectile defeat capability than that of the 1/8-inch-thick material. Although the ballistic defeat capabilities of the various material thicknesses are of minimal consideration in design, the degree of ballistic damage caused by the impacting projectile at different material thicknesses must be given careful attention. There is an increase of approximately 50 percent in damage area with each 1/8-inch increase in thickness. However, this increase in damage area does not translate into a relative decrease in residual load capacity. In general, the thinnest possible section that is structurally satisfactory should be used in the design of components.

CYCLIC TENSILE FATIGUE

In designing flight control components, consideration must be given to the effect of repeated operational cyclic loading. Data are available on the cyclic fatigue capability of the material in both the undamaged and damaged conditions. Figure 4 shows the plots of load-N curves for the material in the undamaged and damaged conditions. The following conclusions were drawn from analysis of the fatigue data:

1. An endurance limit (stress) exists below which cyclic tensile loading has no apparent effect on the composite.
2. Specimens tested above the endurance limit (10 to 20 percent of the ultimate strength) develop cracks within the first 4 percent of the fatigue life.

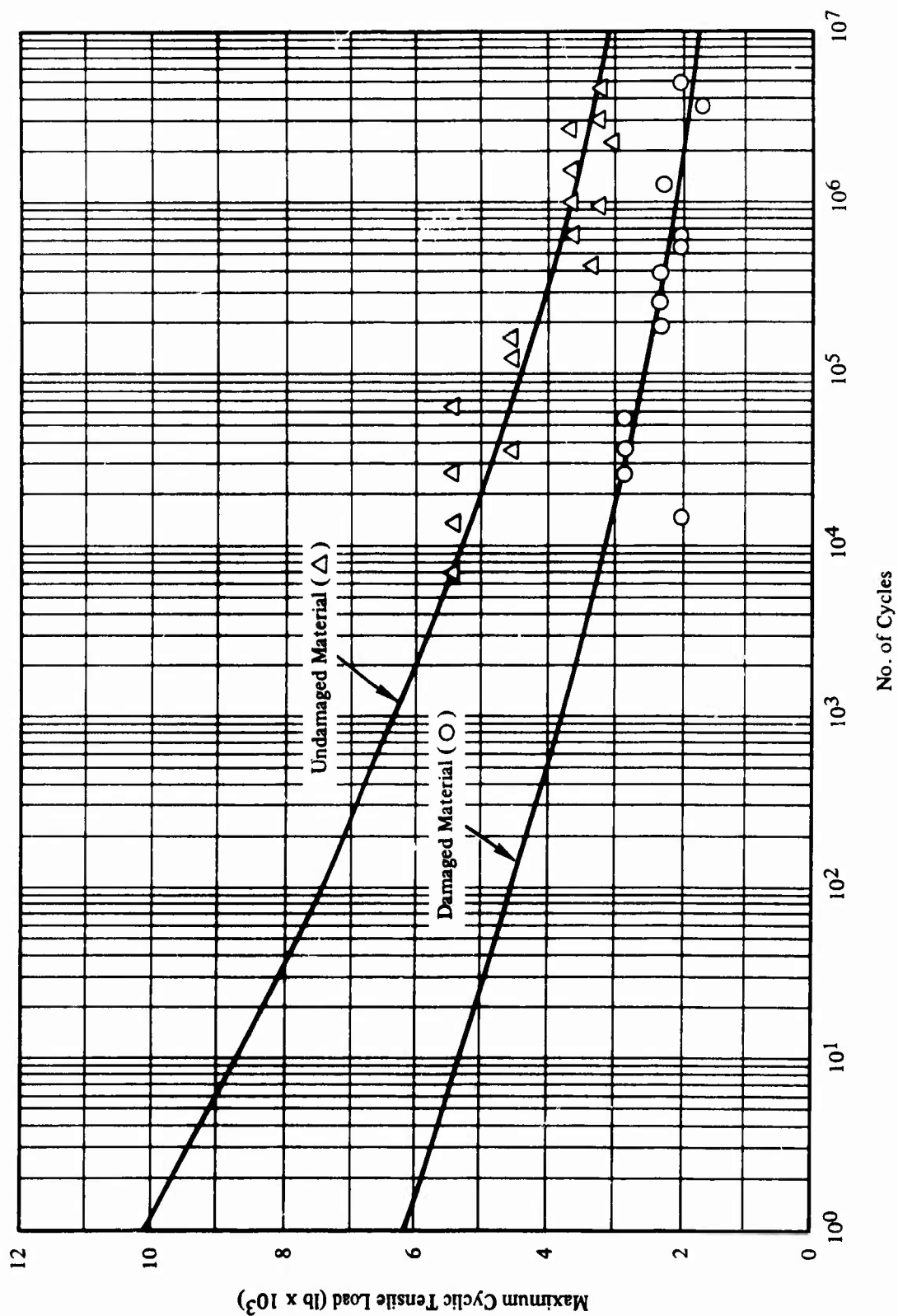


Figure 4. Load-N Curves for Undamaged and Ballistically Damaged 1/8-Inch-Thick Composite Material.

COMBINED STRESS-IMPACT

Flight control components must be able to survive an impact while under load at the most critical operating temperature. Tests were conducted to determine the threshold stress level at which 1/8-inch-thick material would fail catastrophically when impacted with a tumbled caliber .30 ball M2 projectile at 160°F. To determine this value, the following method was used.

The initial specimen of the composite was preloaded to approximately 90 percent of the damaged strength at 160°F. An up-and-down method was then employed, wherein the preload level was changed based on the response of the preceding specimen. If the previous specimen failed catastrophically, the preload was reduced for the following specimen. Conversely, if the preceding specimen survived, the preload was increased for the next test. After each reversal in response (failure/no failure/failure), a constantly decreasing change was made in preload level.

The threshold stress was determined by arithmetically averaging the highest individual preloads resulting in specimen survival with a like number of the lowest preloads producing catastrophic failure. A value of 6727 psi was calculated as the threshold stress level at 160°F. This value appears to be reasonable based on the minimum stress of 6591 psi for failure in any one test. The analysis of the data shows that the combined effects of stress and impact at 160°F produce the most critical condition that can be imposed on a short-fiber composite. The data showed that an average specimen damaged at low prestress (35 percent of ultimate) and tested at 160°F could sustain 3707 pounds. An average specimen at the threshold stress would sustain 2950 pounds, or a concentration factor of 0.80.

DESIGN ANALYSIS OF BALLISTIC RESPONSE

DAMAGE ANALYSIS

The effective use of the visual area and volume ballistic damage data, the visual transverse ballistic damage data, and the residual load capacity data for predicting the damage response of a component requires the development of useful analytical techniques. Attempts to directly relate the visual and transverse ballistic damage data to the damage response have proved unreliable and impractical. The damage patterns do not correlate well with the residual load capacity measurements. The response data are significantly influenced by test and material variables.

The successful design of any structural component requires a basic knowledge of the materials used in the design and an accurate definition of the external loads that will be applied to the component. The loading requirements are established by analysis of the flight operational loads of yaw, thrust, maneuvering, payload, landing, and any unusual loads due to servo-action or hydraulic bleed-down. Static and cyclic loads that are applied to the component before, during, and after ballistic impact must also be considered.

The most effective design of a component that must survive in a ballistic-damage environment is the design requiring the minimum original section (width and thickness). Determination of the required original section that will retain sufficient residual load capacity after ballistic damage requires the knowledge of two factors: namely, the basic strength of the material and the amount of material removed by ballistic impact under any given ballistic and environmental condition. This latter factor relates to the extent of effective damage rather than visual damage. The effects of damage can then best be determined based on the loss in strength after damage. For a specified specimen thickness, the length of composite material, transverse to the load path, that is lost due to perforation and is equivalent to the measured loss in strength is expressed in terms of a value defined as the "effective damage length."

The residual load capacity and the effective damage length are influenced by test and material variables. These variables include the preload level in the component prior to impact, the projectile velocity and orientation, material thickness, and orientation of the reinforcing fibers. Regression analysis was used to calculate the residual load capacity for various data sets in which one variable was changed while all others were held constant. By using the load capacity of the undamaged composite, the effective damage length was computed from the loss in material strength.

Effective damage lengths have been determined for fatigue life and the combined effects of preload and ballistic impact at 160°F.

Table VII presents a summary of the tensile strength, modulus, and cyclic fatigue properties for undamaged specimens. Included are the effects of temperature, fiber alignment, thickness, and three levels of cyclic loading. Also presented are the strength factors that represent the ratio of each property to the basic tensile strength at room temperature.

TABLE VII. ENVIRONMENT AND LOADING EFFECTS ON TENSILE PROPERTIES OF THE UNDAMAGED COMPOSITE		
Parameter	Property Value	Strength Factor
1. Undamaged Ultimate Tensile Strength (psi)		
a. Basic Value, σ_s^a	22,950	1.000
b. Temperature Effect		
At -80°F	24,650	1.074
At 75°F	22,950	1.000
At 160°F	14,620	0.637
c. Edge Alignment		
Center, σ_c	21,800	0.950
Edge, σ_e	24,400	1.063
d. Thickness Effect		
1/16 inch	22,400	0.976
1/4 inch	23,400	1.020
3/8 inch	23,200	1.011
2. Modulus of Elasticity (psi x 10 ⁶)		
a. Basic Value, E_s^a	3.59	1.000
b. Temperature Effect		
At -80°F	3.61	1.006
At 160°F	2.21	0.616
c. Edge Alignment		
Center	3.32	0.925
Edge	3.84	1.070
3. Fatigue Strength (psi) ^a		
At 2,000 cycles	13,710	0.597
At 100,000 cycles	10,011	0.436
At 10,000,000 cycles	6,949	0.303
^a Standard specimens, 1/8 inch thick and 3.5 inches wide, at 75°F.		

The effects of the ballistic and composite variables on the load-carrying ability and the effective damage length are given in Table VIII for the tumbled caliber .30 ball M2 impacted composite.

The data in Table VIII indicate that residual load capacities and, consequently, effective damage length are relatively insensitive to changes in specimen temperature during ballistic impact. Residual load capacity increases directly with preload. The effect of this variable seems contrary to the combined stress-impact results discussed on page 19. However, it is important to recognize that there was one significant difference in test procedure between the combined stress-impact investigation and the balance of the ballistic tests. In the combined stress-impact investigation, the specimen preload was maintained for at least 5 minutes unless failure occurred earlier. In all other tests, the preload was removed within 20 seconds after ballistic impact. One possible explanation for this trend is that the effective stiffness of the specimen increases directly with preload. This would reduce the amount of damage caused by bending in the specimen. The residual load capacity is affected to some degree by impact velocity, peaking at a value of approximately 2000 ft/sec. Lower residual load capacities can be expected with the lower velocity impacts.

The ballistic response of the composite was not significantly affected by changes in footprint length.

Effective damage length increases directly with specimen thickness. Variations in rotation angle of the projectile have only a minor influence on effective damage length. The geometry of the projectile - the small l/d ratio and the cylindrical base - probably is responsible for this minor effect. An angular rotation of 30 degrees reduces the effective length of the projectile only 7 percent compared with 13.5 percent for an infinitely large l/d ratio.

Selected residual load capacity and effective damage length values from Table VIII are summarized in Table IX to show the effects of temperature, thickness, and velocity. Also presented are the appropriate values for damage fatigue and combined stress-impact conditions.

The data reported were utilized to establish the part width required to carry various loads before and after tumbled caliber .30 ball M2 projectile impact. In this analysis, it was assumed that the composite would be 1/8 inch thick and consist only of randomly oriented material. This latter constraint was imposed since there is no assurance that a significant degree of fiber alignment will be present in the compression-molded flight control components.

TABLE VIII. INFLUENCE OF TEST VARIABLES ON THE RESIDUAL LOAD CAPACITY AND EFFECTIVE DAMAGE LENGTH OF THE CALIBER .30 IMPACTED COMPOSITE

Temp ^a (°F)	Velocity ^b (ft/sec)	Ultimate Preload ^c (pct)	Footprint Length ^d (in.)	Thickness ^e (in.)	Rotation Angle ^f (deg)	Impact Location ^g (in.)	Specific Gravity ^h	Residual Load Capacity (lb)	Damage Length (in.)
-80	1500	25	1.10	0.125	90	1.755	1.907	5,762	1.564
-5	↓	↓	↓	↓	↓	↓	↓	5,846	1.533
70	↓	↓	↓	↓	↓	↓	↓	5,767	1.562
115	↓	↓	↓	↓	↓	↓	↓	5,641	1.607
160	↓	↓	↓	↓	↓	↓	↓	5,457	1.674
70	900	25	1.10	0.125	90	1.755	1.907	4,297	2.080
↓	1200	↓	↓	↓	↓	↓	↓	5,123	1.793
↓	1500	↓	↓	↓	↓	↓	↓	5,767	1.562
↓	1800	↓	↓	↓	↓	↓	↓	6,084	1.458
↓	2100	↓	↓	↓	↓	↓	↓	5,929	1.503
↓	2400	↓	↓	↓	↓	↓	↓	5,156	1.781
70	1500	15	1.10	0.125	90	1.755	1.907	5,893	1.516
↓	↓	25	↓	↓	↓	↓	↓	5,767	1.562
↓	↓	35	↓	↓	↓	↓	↓	6,260	1.393
↓	↓	45	↓	↓	↓	↓	↓	7,371	0.987
70	1500	25	1.10	0.125	90	1.755	1.907	5,767	1.562
↓	↓	↓	1.00	↓	↓	↓	↓	5,601	1.622
↓	↓	↓	0.90	↓	↓	↓	↓	5,521	1.651
↓	↓	↓	0.80	↓	↓	↓	↓	5,524	1.650
↓	↓	↓	0.70	↓	↓	↓	↓	5,612	1.618
70	1500	25	1.10	0.125	90	1.755	1.907	5,767	1.562
↓	↓	↓	↓	0.250	↓	↓	↓	10,605	1.765
↓	↓	↓	↓	0.375	↓	↓	↓	13,920	1.979
70	1500	25	1.10	0.125	90	1.755	1.907	5,767	1.562
↓	↓	↓	↓	↓	75 or 125	↓	↓	5,659	1.601
↓	↓	↓	↓	↓	60 or 120	↓	↓	5,374	1.703
↓	↓	↓	↓	↓	45 or 135	↓	↓	5,026	1.827
↓	↓	↓	↓	↓	30 or 150	↓	↓	4,764	1.919
70	1500	25	1.10	0.125	90	1.755	1.907	5,757	1.562
↓	↓	↓	↓	↓	↓	1.655	↓	5,225	1.756
↓	↓	↓	↓	↓	↓	1.555	↓	4,835	1.894
↓	↓	↓	↓	↓	↓	1.355	↓	4,741	1.927

^a Temperature is defined as the specimen temperature at impact (°F).

^b Velocity is defined as the projectile velocity at impact (ft/sec).

^c Ultimate preload is defined as the specimen preload as a percentage of undamaged strength at the test temperature.

^d Footprint length is defined as the measure of the degree of projectile tumble at the time of impact (in.).

^e Thickness is defined as the average specimen thickness in the test area (in.).

^f Rotation angle is defined as the in-plane rotational angle of the projectile. Tip of projectile at 12 o'clock, angle = 0°; at 3 o'clock (transverse), angle = 90°.

^g Impact location is defined as the distance from the edge of the specimen to the point of impact (in.).

^h Specific gravity is defined as the measured specific gravity of the specimen used in residual load capacity calculations.

TABLE IX. ENVIRONMENT AND LOADING EFFECTS ON TENSILE PROPERTIES OF THE CALIBER .30 IMPACTED COMPOSITE		
Parameter	Property Value	Effective Damage Length (in.)
1. Undamaged Ultimate Tensile Load, P_u (lb)	10,070	-
2. Post-Damage Load, P_d (lb) ^a		
a. Temperature Effect at 1500 Ft/Sec		
At -80°F	5,762	1.564
At 75°F	5,767	1.562
At 160°F	5,457	1.674
b. Thickness Effect at 75°F and 1500 Ft/Sec		
1/8 inch	5,767	1.562
1/4 inch	10,605	1.765
3/8 inch	13,920	1.979
c. Velocity Effect at 75°F		
At 1500 ft/sec	5,767	1.562
At 1800 ft/sec	6,084	1.463
At 2100 ft/sec	5,929	1.503
3. Damaged Fatigue at 75°F (lb)		
At 2,000 cycles	3,600	1.480
At 10,000,000 cycles	1,730	1.590
4. Combined Stress-Impact: Load Capacity at Catastrophic Failure (lb) ^a	2,950	1.960
^a Standard specimens, 1/8 inch thick and 3.5 inches wide.		

The load-carrying abilities of the composite are presented in Table X for six operational conditions. The first condition, static strength at 75°F, represents the simple case where the composite is not subjected to ballistic impact. The part widths required to carry the static tensile loads are determined, therefore, from undamaged specimen property data.

**TABLE X. SUMMARY OF LOAD-CARRYING ABILITIES OF
UNDAMAGED AND CALIBER .30 BALLISTICALLY
DAMAGED COMPOSITES**

Condition	Load (lb)	Required Width (in.)
Static Strength at 75°F	Basic strength → 21,800 psi	
	1,000	0.367
	2,000	0.734
	5,000	1.835
	10,000	3.670
Post-Damage Strength at 75°F	Damage length → 1.562 in.	
	1,000	1.929
	2,000	2.296
	5,000	3.397
	10,000	5.232
Fatigue Strength at 75°F and 2000 Cycles	Fatigue strength → 13,020 psi	
	1,000	0.614
	2,000	1.228
	5,000	3.070
	10,000	6.140
Post-Damage Fatigue Strength at 75°F and 2000 Cycles	Damage length → 1.480 in.	
	1,000	2.094
	2,000	2.708
	5,000	4.550
	10,000	7.620
Static Strength at 160°F	160°F strength → 13,900 psi	
	1,000	0.576
	2,000	1.152
	5,000	2.880
	10,000	5.760
Combined Stress-Impact at 160°F	Damage length → 1.960 in.	
	1,000	2.536
	2,000	3.112
	5,000	4.840
	10,000	7.720

The second condition defines post-damage strength at 75°F. When the composite is impacted at room temperature with fully tumbled caliber .30 ball M2 projectiles at 1500 ft/sec, the part width must be increased by an amount equal to the effective damage length given in Table X under these ballistic conditions.

The third condition defines the width of composite required to sustain 2000 fatigue cycles at various load levels before projectile impact. The fatigue strength of randomly oriented material reported in Table X was determined from property data on undamaged specimens given in Table VII. Specifically, the values were obtained by multiplying the fatigue strength of the standard specimens by the strength factor for center material.

If 2000 operational cycles are applied to the composites after ballistic damage, the part widths associated with the fourth condition are needed to carry the loads indicated. These widths were determined by adding the effective damage length given in Table X to the part width required for the undamaged fatigue condition.

The final condition relates to the combination of applied stress and impact, where the part is ballistically impacted while under tensile load at 160°F.

The residual load capacities and the associated damage lengths for 1/8-inch-thick standard specimens impacted with the caliber .50 projectiles are presented in Table XI.

DESIGN ALLOWABLES

The design allowables for the short-fiber molding material to be used for the design of the composite components have been established for all of the usual physical properties. For each property evaluated in the study, the technique of regression analysis was used to develop a mathematical function of property versus temperature in the range from -65°F to +160°F. Based on the standard deviation of the test values, an A-basis lower statistical tolerance limit was developed that will be exceeded 99 percent of the time with a confidence level of 95 percent. Table XII lists the average test value, the minimum test value, and the lower tolerance limit (design allowable value) for each property at -80°F, 75°F, and 160°F. The minimum design allowable value for each property occurs at 160°F; therefore, these values are the design allowables that should be used in the design analysis. Because of the small number of test samples and the high percentile of confidence probability levels selected, the design allowables are known to be conservative.

TABLE XI. INFLUENCE OF TEST VARIABLES ON THE RESIDUAL LOAD CAPACITY AND EFFEC- TIVE DAMAGE LENGTH OF THE CALIBER .50 IMPACTED COMPOSITE			
Variable	Level	Residual Load Capacity (lb)	Damage Length (in.)
Temperature (°F)	-80	6685	1.238
	5	7102	1.086
	70	7518	0.933
	115	7768	0.842
	160	8017	0.751
Velocity (ft/sec)	1500	7518	0.933
	1800	7842	0.815
	2100	7970	0.768
Preload (percent of ultimate)	25	7378	0.984
	35	7518	0.933
	45	7657	0.882
	55	7796	0.832
Impact Location (in.)	1.755	7518	0.933
	1.655	7610	0.900
	1.555	7668	0.878
	1.355	7669	0.878

The static test data for the composite material system are presented in the appendix in the form of tabular and graphic summaries.

DESIGN CRITERIA FOR CYCLIC LOADING

Since components must be capable of withstanding cyclic loads both before and after ballistic damage, it is necessary to establish fatigue design criteria for use in structural design analysis. These criteria have been established from the tensile fatigue data by using the regression analysis technique. This technique results in a fundamental regression function based on the Weibull function equation:¹

$$S_{\max} = (\sigma_u - S_E) e^{-k (\log_e N)^M} + S_E$$

The mean values and the lower tolerance limits for both the undamaged and the damaged composites have been computed from the regression functions. These curves are shown in Figures 5 and 6.

TABLE XII. DESIGN ALLOWABLE PROPERTY VALUES
FOR THE COMPOSITE

Mechanical Properties	Test Temp (°F)	Avg Test Values (psi)	Min Test Values (psi)	Design Allowable Values (psi)
Interlaminar Shear Strength	-80	7,453	6,420	5,000
	75	7,833	6,940	5,380
	160	5,106	4,380	2,654
Flexure Strength	-80	54,180	48,250	28,258
	75	50,326	42,390	24,405
	160	34,485	27,480	8,563
Tensile Strength	-80	24,241	19,310	16,253
	75	20,086	18,210	12,098
	160	17,378	14,580	9,390
Compressive Strength	-80	49,056	42,110	35,169
	75	36,476	31,340	22,589
	160	23,958	20,980	10,071
Panel Shear Strength	-80	23,680	22,690	19,542
	75	17,350	15,240	13,281
	160	15,390	14,810	11,319
Bearing Strength	-80	81,460	78,080	58,633
	75	65,970	56,000	43,344
	160	43,580	38,160	20,757
Tensile Modulus	-80	3.74×10^6	-	-
	75	3.41×10^6	-	-
	160	2.57×10^6	-	-
Adhesive Tensile Strength	-80	4,137	3,350	2,557
	-	-	-	-
	160	3,586	3,150	2,006
Adhesive Shear Strength	-80	1,596	1,451	1,015
	75	1,597	1,269	1,016
	160	1,704	1,630	1,123

To develop these regression functions, a one-cycle load and an endurance limit load were required. For the one-cycle load, an average of the static tensile test data was used. There was no way to include the variability of this point into the regression function without a great deal of mathematical development that was beyond the scope of this program. As a result, the

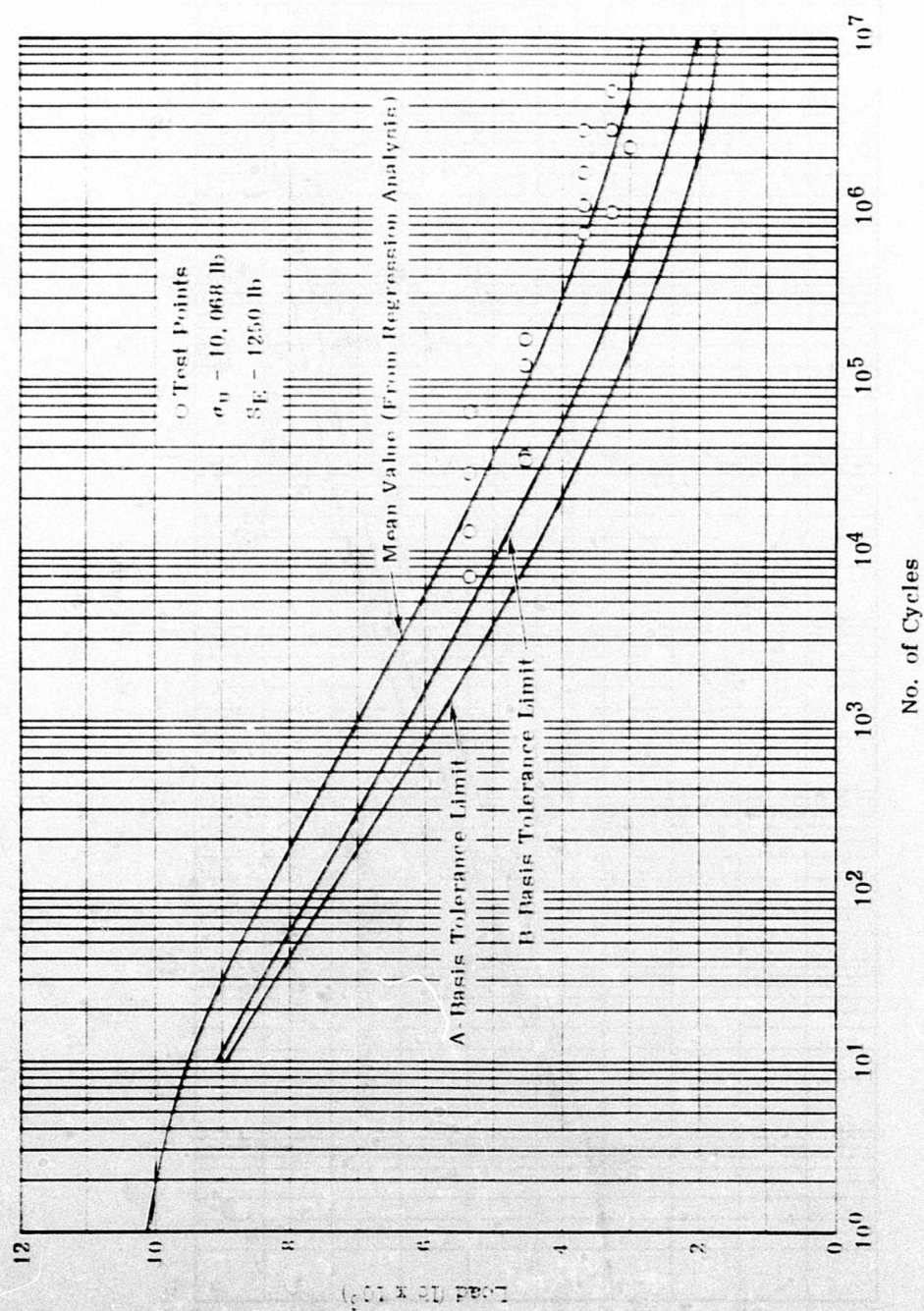


Figure 5. Tensile Fatigue Curves for the Undamaged Composite.

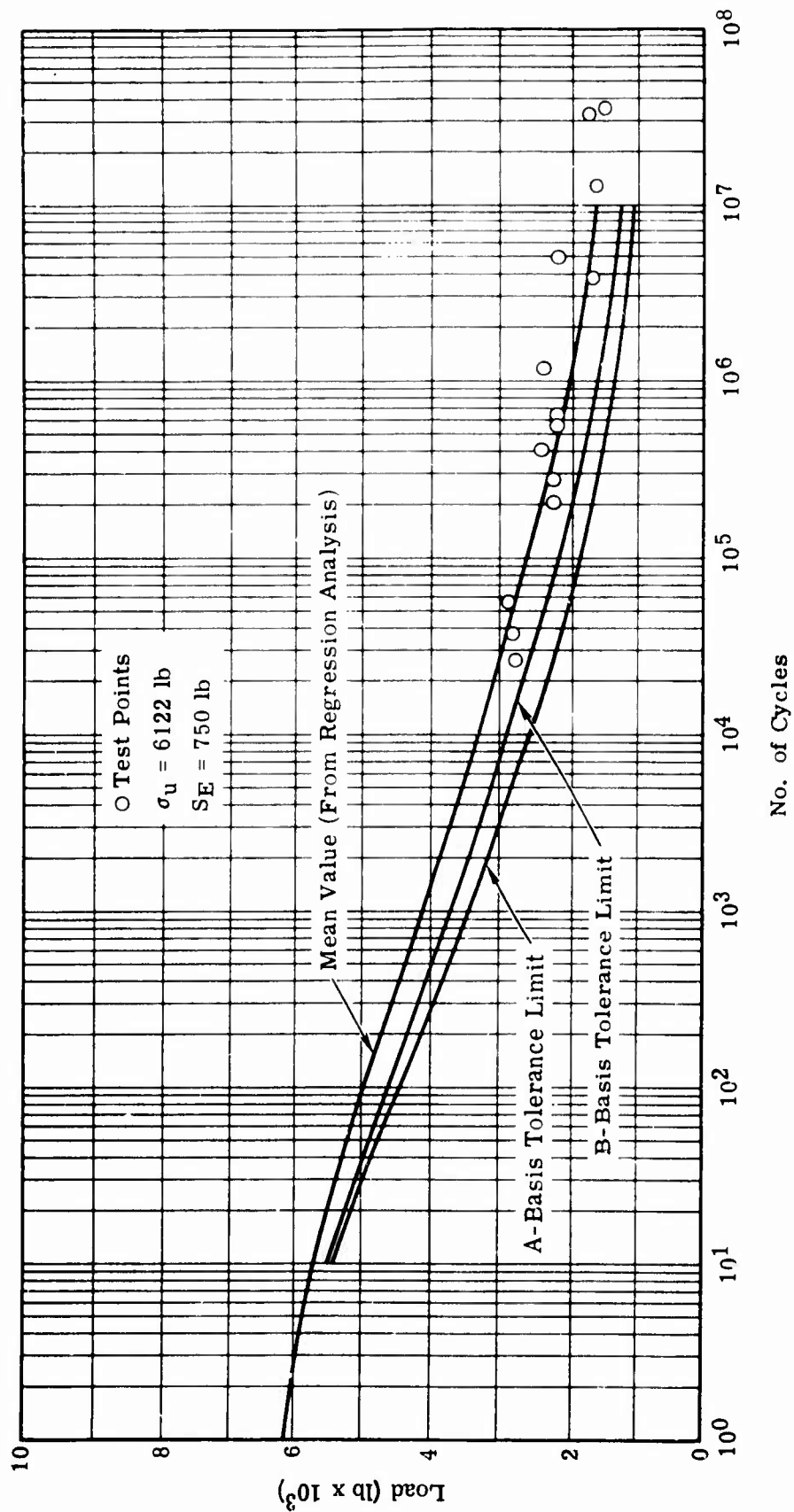


Figure 6. Tensile Fatigue Curves for the Damaged Composite.

lower tolerance limit for low number of cycles may not be entirely reliable. A comparison of the curves in Figures 5 and 6 is shown in Figure 7, which plots the same information as a percentage of the one-cycle strength. Figure 7 shows that the curves for undamaged and damaged composites are almost identical. This would indicate that if the one-cycle value is known, a curve of load versus number of cycles can be developed based on the data in Figure 7. Therefore, to develop a conservative design allowable for fatigue throughout the total range from one to 10^7 cycles, the following approach was used. The lower tolerance limit from the static load information was used as the lower tolerance limit for one cycle, and a complete lower tolerance curve was developed from the mean value curve of Figure 7. This curve is superimposed over the lower tolerance curve developed from the fatigue data, adjusted for temperature and the randomly oriented center material only, and the lower value is used as a design curve. The fatigue design curves at 75° and 160°F developed in this manner are shown in Figure 8. The following tensile fatigue criteria were established from these curves:

- 2000 cycles at 160°F = 5910 psi
- 5×10^6 cycles at 160°F = 2400 psi
- 10^7 cycles at 160°F = 2240 psi
- Endurance limit at 160°F = 1067 psi

ANALYTICAL METHODS FOR DESIGN

After the effects of ballistic damage have been established, it is necessary to develop a design analysis method. One method is to assume that an effective length of damage as designated in Table VIII is removed by the ballistic impact and that the remaining portion of the structure is available, undamaged, to resist the loads. The allowable stresses in the remaining, undamaged material can then be established as the lower tolerance limits and are given as the design allowables presented in Table XII.

In the case of cyclic loads, the normalized curves for the undamaged and damaged tests were similar. Therefore, if the effective length of damaged material is removed, the remainder of the material would be expected to react to the cyclic loads according to the curves of Figure 7. Since the mean value curve for the damaged fatigue specimens was slightly below the curve for the undamaged specimens, the normalized damaged curve was used to plot the curves shown in Figure 8, which are the curves to be used for component design under damage fatigue conditions.

For specific conditions, the effective damage length must be determined by combining the various computed values of Table VIII. An example of how the effective damage length criteria are calculated is given in the following paragraphs.

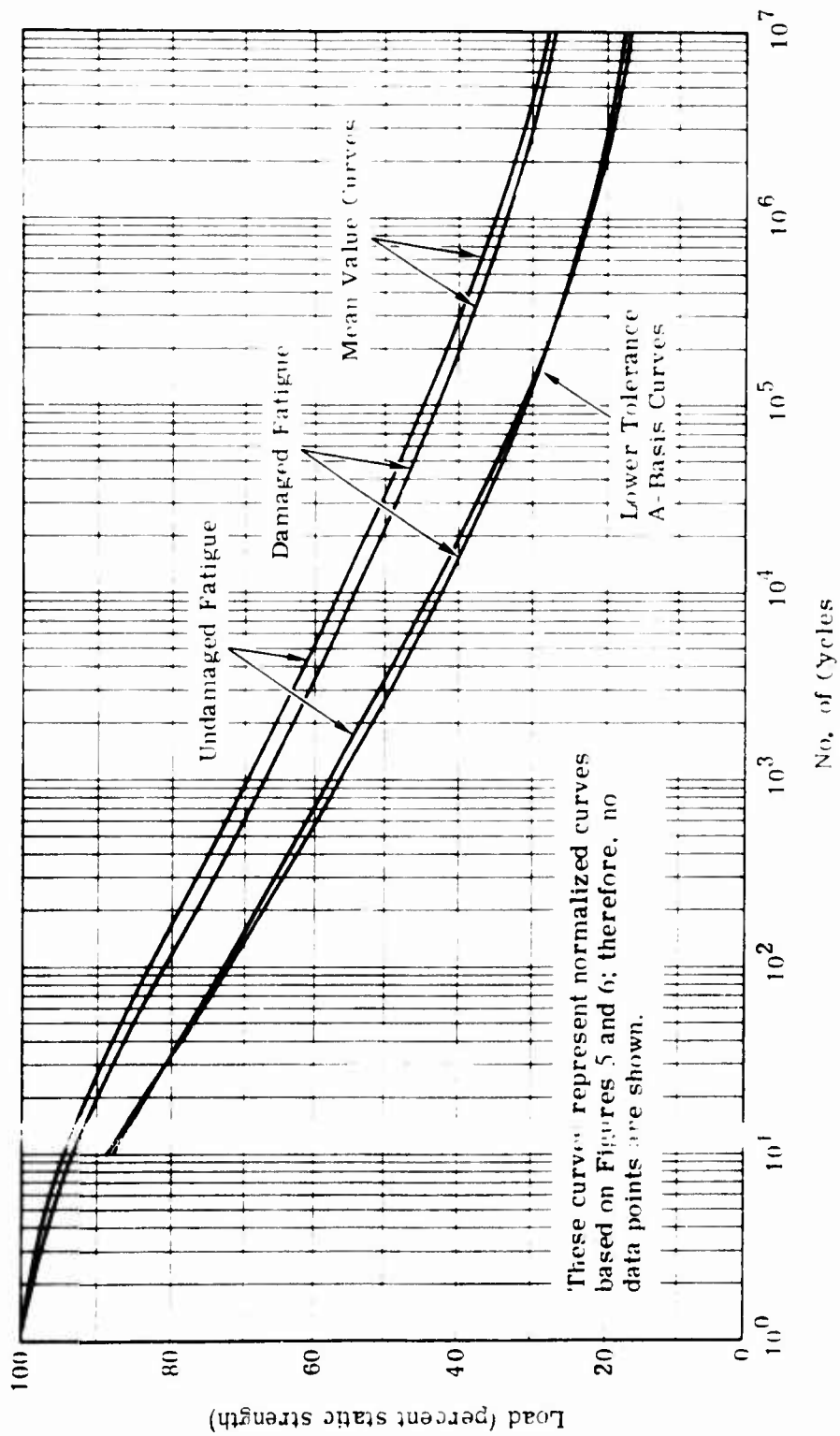


Figure 7. Tensile Fatigue Curves for Undamaged and Damaged Composites as a Percentage of Static Strength.

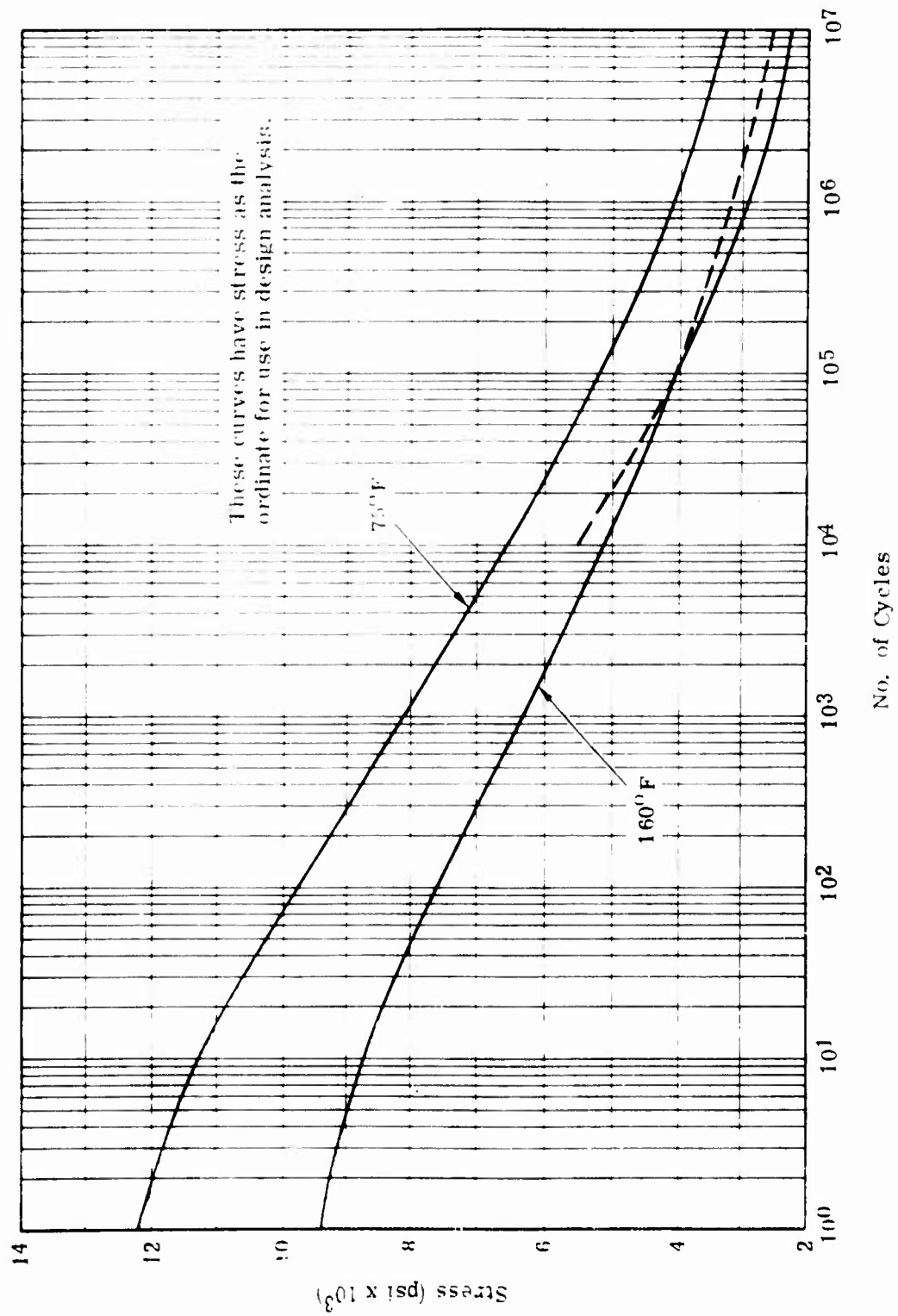


Figure 8. Fatigue Design Curves (A-Basis) for the Composite.

Requirement: Determine the damage length of a composite ballistically impacted under the following conditions:

- Composite thickness 0.375 in.
- Ultimate preload 15 pct
- Impact temperature 160°F

Approach: Select the proper combination of values from Table VIII to develop the effective damage length criteria. These criteria are listed in Table XIII.

TABLE XIII. DEVELOPMENT OF EFFECTIVE DAMAGE LENGTH CRITERIA			
Temp (°F)	Ult Preload (pct)	Thickness (in.)	Damage Length (in.)
70	25	0.375	1.979
70	15	0.125	1.516
70	25	0.125	1.562
160	25	0.125	1.674

Calculation: The damage length can now be calculated by applying these values to the formula given in the following equation:

$$\begin{aligned}
 \text{damage length} &= \text{DL for } t = 0.375 \left(\frac{15\%}{25\%} \right) \left(\frac{160^\circ\text{F}}{75^\circ\text{F}} \right) \\
 &= 1.979 \left(\frac{1.516}{1.562} \right) \left(\frac{1.674}{1.562} \right) \\
 &= 2.06 \text{ in.}
 \end{aligned}$$

where DL = damage length, in.

t = composite thickness, in.

Therefore, a 0.375-inch-thick composite will lose effectively 2.06 inches of material due to ballistic impact damage. Any component design must provide for this much material plus that which is additionally required to carry the post-damage loads with adequate margins of safety.

By using the calculated effective damage length as a starting point, the required additional material to sustain the required load for any thickness

of material can be calculated. This type of information can be plotted in the form of the design curves shown in Figure 9.

The critical design factors for the flight control components are listed below.

- Ballistic damage impacts from tumbled caliber .30 ball M2 projectiles
- Impacts at a temperature of 160°F
- Component ultimate preload of 15 percent

To determine the damage length of a nominal 0.125-inch-thick composite under these conditions, select the proper combination of values from Table VIII. The damage length is calculated by taking the value for damage length of a specimen 0.125 inch thick and at a test temperature of 160°F and modifying it for the specified preload. The calculation for effective damage length (EDL) is given in the following equation:

$$\begin{aligned} \text{EDL} &= \text{DL} (t = 0.125 \text{ at } 160^{\circ}\text{F and } 25\% \text{ PL}) \frac{\text{DL} (15\%)}{\text{DL} (25\%)} \\ &= 1.674 \left(\frac{1.516}{1.562} \right) \\ &= 1.622 \text{ in.} \end{aligned}$$

To provide sufficient material to withstand such a damage length and still have load-carrying ability, a minimum web width of 2.00 inches was used in the design of the components.

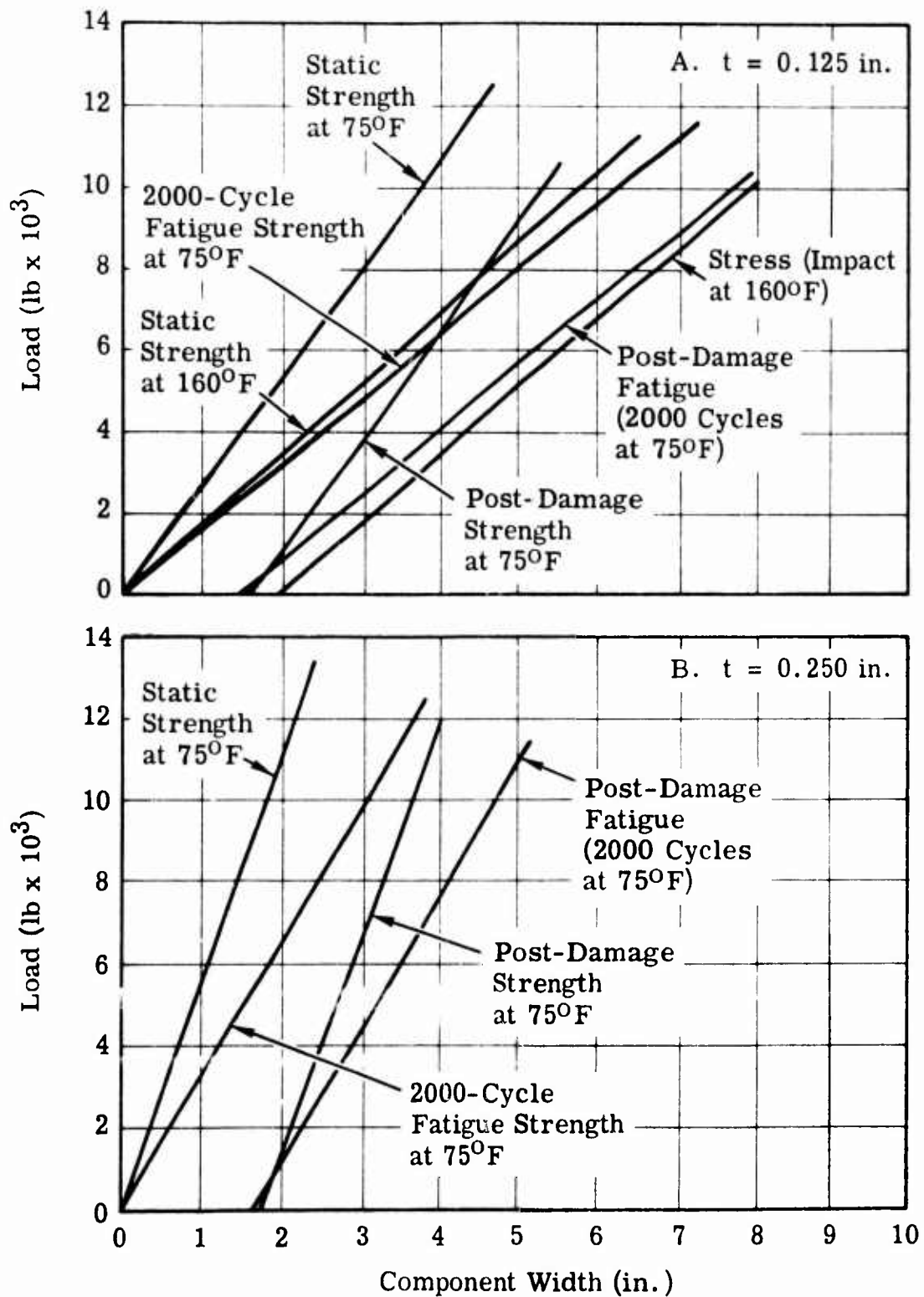


Figure 9. Typical Design Curves for Ballistic-Damage-Tolerant Components.

COMPONENT DESIGN

DESIGN CONCEPTS

Once the design allowables for both static loads and cyclic loads have been established, the design of components using the selected short-fiber composite can be undertaken. The following criteria can be used in the design of the components:

- Keep the design simple.
- Consider moldability factors.
- Provide multiple load paths.
- Minimize weight.
- Strength factors
- Fatigue life

The purpose of the simplicity in design is to avoid as far as practical the detrimental effects of complex molded shapes in achieving consistent properties. Multiple load paths are necessary to provide ballistic-damage-tolerant parts. However, it is necessary to provide parts with adequate margins of safety and minimum weight consistent with good design practice.

Figure 10 shows some of the typical components that can be designed and molded using short-fiber composites. There are various other components that may also be considered candidates, which would be obvious to the experienced designer. Figure 11 shows specific design details that must be adhered to for assurance of proper moldability and structural capability of the components.

The program conducted by Goodyear Aerospace Corporation under U.S. Army Contract DAAJ02-70-C-0062 to develop ballistic-damage-tolerant components using compression-molded, short-fiber, reinforced-plastic composites is documented in the Phase II Summary Report² for that program. The design effort is described in this section of the design guide. The tooling, fabrication, testing, and evaluation efforts are described in subsequent sections of the design guide.

TYPICAL COMPONENT DESIGNS

Components currently used in the flight control systems of U.S. Army helicopters are designed and manufactured using standard aircraft metal concepts and technology. To develop the ballistic-damage-tolerant design concept, components typical of the standard metal design were evaluated in composite form. The following three flight control system components were selected for evaluation:

- Forged aluminum bell crank for the aft control system (Sta 440 - idler) of the Boeing CH-47C helicopter

- Forged aluminum bell crank for the output control system (aft pylon upper left-hand bell crank) of the Boeing CH-47C helicopter
- Cast magnesium quadrant assembly for the aft rotor control system of the Bell UH-1B/D helicopter

These metal components were redesigned as molded composite components using the composite consisting of 1/2-inch-long, 470-finished S-2 fiber glass in a 438 epoxy resin matrix.

The metal components in the helicopter flight control systems function within a prescribed set of dimensional, structural, and environmental conditions that are fully described in a subsequent paragraph under "Design Criteria." The redesigned molded composite components are required to function within this envelope and must be capable of withstanding ballistic impact in the most critical structural load path of the component under the most severe environmental conditions without disabling failure. The redesigned molded components are also required to be directly interchangeable with the existing metal components. However, in new aircraft designs, the flight control components would not be confined to the interchangeable dimensional constraints that redesigned components must adhere to for proper fit and function as in existing aircraft.

Other factors that were considered during the conceptual design and analysis are listed below.

- **Producibility** - The ability to manufacture the molded components using state-of-the-art technology with good repeatability must be considered as a design goal.
- **Reduced Weight** - As a design goal, the weight of the molded components should be equal to or lower than that of the metal components.
- **Cost** - The cost of manufacturing the molded components should be competitive with the cost of manufacturing the metal components.
- **Reliability** - The molded components must perform their prescribed functions without the need for replacement or excessive maintenance.

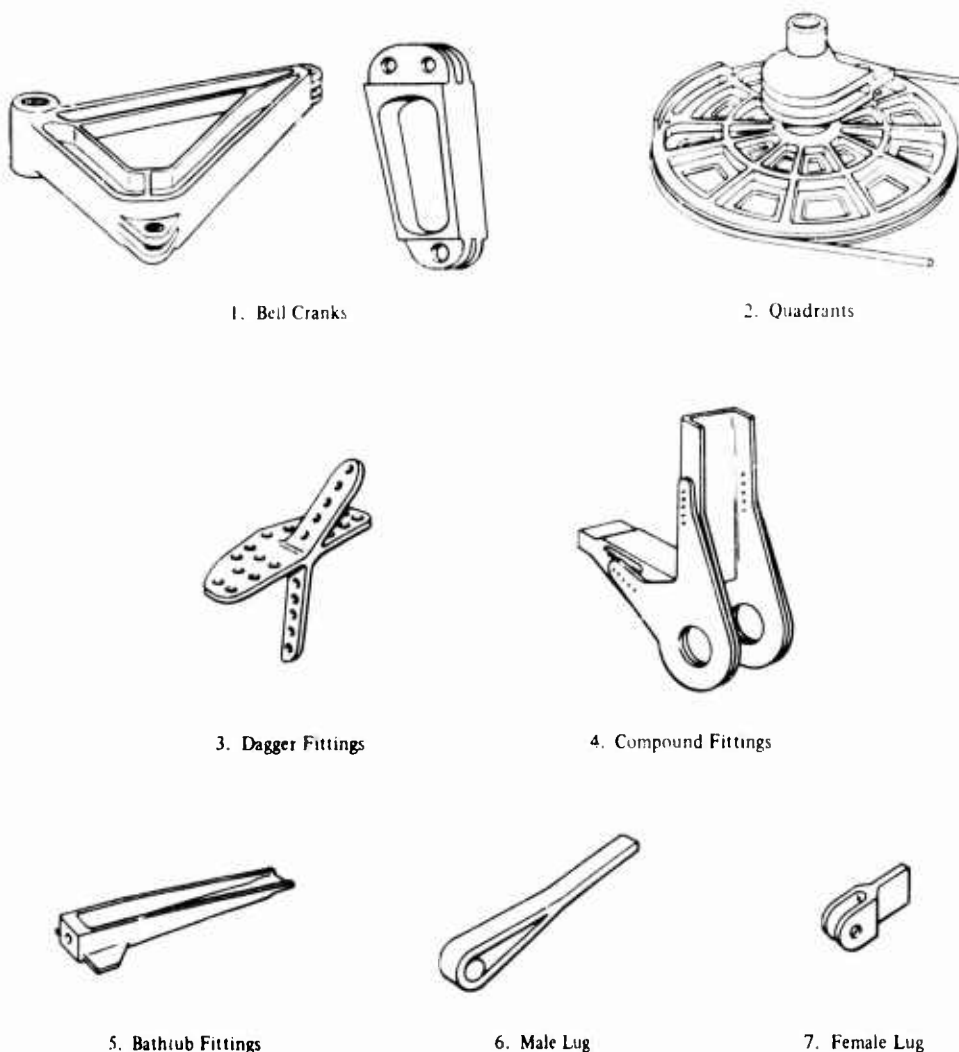


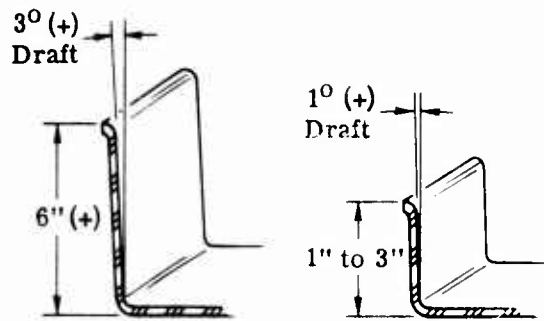
Figure 10. Typical Components Molded of a Short-Fiber Composite Material.

DESIGN CRITERIA

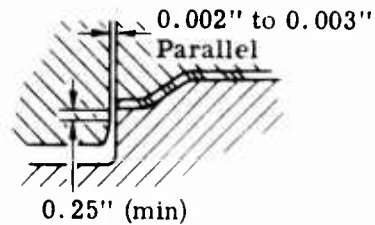
The loading conditions for the components (maximum design, operational cyclic, and cyclic fatigue loads) are shown in Figure 12. The maximum design loads shown in Figure 12 are the baseline or limit loads used in the original metal component analyses.^{3,4,10} Thus these loads represent the maximum applied loads that would be imposed on the components while in service. The operational cyclic loads are the maximum loads that the components would sustain in the flight operational mode. The cyclic fatigue loads are the repetitive loads sustained during the long-time, in-service life of the components (damaged or undamaged) under any conditions of operation. In the case of the CH-47C components, the operational and fatigue cyclic loading conditions are the same.

1. **Draft.** Draft angles on all surfaces parallel to the direction of the press platen must have the following draft:

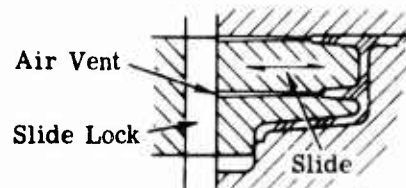
Dimensions (in.)	Draft (deg)
1 to 3	1
3 to 6	3
> 6	> 5



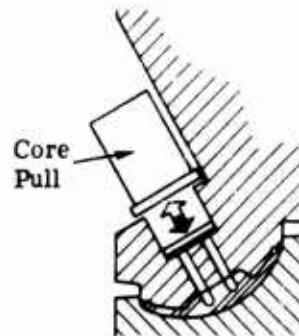
2. **Mold Cavity and Punch Telescope.** The mold cavity and punch shall telescope a minimum of 0.25 inch with a maximum gap of 0.003 inch to assure good seal and minimum flash.



3. **Slides.** Slides are used to mold external undercuts and should be located at the periphery of the mold part. Slides are mechanically or hydraulically actuated.



4. **Cores.** Cores can be molded into the component and should be located near the periphery. Cores are incorporated to remove excess material or to mold holes. Core pulls are mechanically or hydraulically actuated.



5. **Ejectors.** Ejectors are used to facilitate part removal. Ejector pins should be placed over vertical bosses or flanges or over heavy material sections, but never over a thin, flat surface.

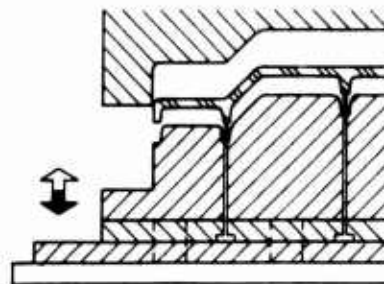
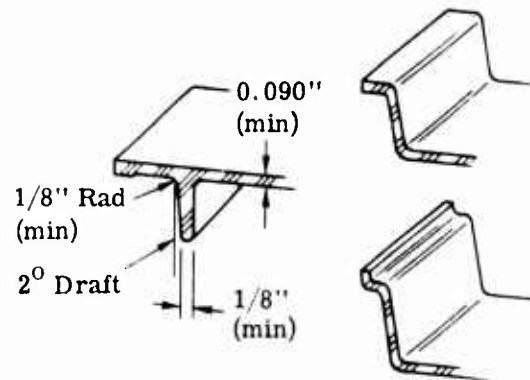
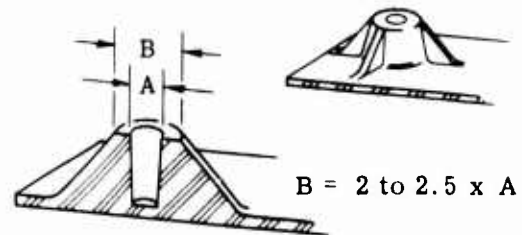


Figure 11. Specific Design Details for Components Molded of a Short-Fiber Glass-Epoxy Composite Material (Sheet 1 of 2).

6. Ribs and Flanges. Ribs and flanges should be a minimum of 0.090 inch thick when flat or perpendicular to die action and a minimum of 1/8 inch thick when vertical or parallel to die action. Minimum draft should be 2 degrees. Minimum radius is 1/8 inch.



7. Bosses. The same general rule for ribs should be followed for bosses. Holes should be molded in to reduce mass. The shoulder width of the boss should be no larger than the diameter of the boss.



8. Inserts. A variety of studs or cavity inserts (threaded or unthreaded) can be molded into the components.



9. Thickness Variation. Thickness variations are to be avoided as they lead to fiber crippling and loss of strength. Thicknesses up to 1 inch can be molded, but care in fabrication must be exercised to ensure fiber randomness and continuity.

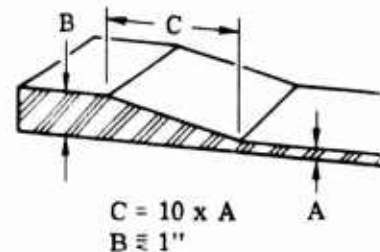
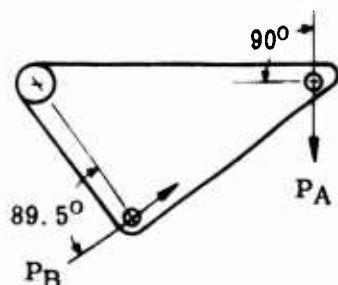


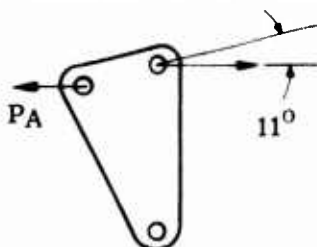
Figure 11. Specific Design Details for Components Molded of a Short-Fiber Glass-Epoxy Composite Material (Sheet 2 of 2).

A. CH-47C Aft Pylon Upper Bell Crank



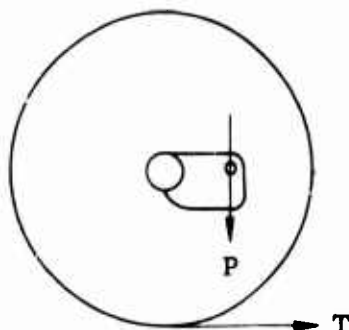
Load Area	Type of Load (lb)		
	Max Design	Operational Cyclic	Cyclic Fatigue
P _A	±2070	±310	±310
P _B	±4010	±602	±602

B. CH-47C Idler Bell Crank



Load Area	Type of Load (lb)		
	Max Design	Operational Cyclic	Cyclic Fatigue
P _A	±2760	±420	±420

C. UH-1B/D Quadrant Assembly



Load Area	Type of Load (lb)		
	Max Design	Operational Cyclic	Cyclic Fatigue
P	±883	±883	±175
T	±353	±353	±70

Figure 12. Loading Conditions for the Ballistic-Damage-Tolerant Components.

The disparity between the maximum design loads and the operational cyclic loads on the CH-47C components is due to high static loads imposed on these components when the helicopter is parked and the main rotor blades are stationary. The static load is the load applied to the control system when the rotor blades are shut down. At the time of system shutdown, the load is transmitted from an extreme position of the rotor blades to the upper control system hydraulic actuators. After the control system hydraulic actuators bleed down, the load is passed down into the lower control system and then is transmitted through the control system components.

Static loads are not present in the operational mode, where the loads are obtained from pilot effort and from the lower boost actuator in roll, pitch, yaw, and thrust.⁵

The quadrant assembly component will normally experience only the 175-pound load at P; however, the high load of 883 pounds can be imposed on the component if both pilots' effort is applied to a jammed control system. It was concluded that this event may be experienced in a ballistic threat environment; therefore, the post-damage operational cyclic loads for the quadrant assembly were established at the higher level.

The structural design criteria based on the loads given in Figure 12 are as follows:

1. The components must be capable of sustaining, without failure, a cyclic fatigue load for a maximum of 10×10^6 cycles within a temperature range of -80° to 160°F under the most adverse environmental conditions.
2. The components must be capable of sustaining the maximum design load after being subjected to a cyclic fatigue load of at least 5×10^6 cycles under the most adverse environmental conditions.
3. After ballistic impact, the components must be capable of sustaining an operational cyclic load of 2000 cycles within a temperature range of -80° to 160°F . Prior to ballistic impact, these components shall have sustained a cyclic fatigue load of 5×10^6 cycles.

DESIGN CONFIGURATIONS

In the component designs, primary consideration was given to the ballistic-damage tolerance factors (extent of damage and residual strength after damage). Other factors such as the undamaged structural capability, similarity in fit and function to their metal counterparts, and environmental conditions were also given serious consideration.

A ballistic-damage-tolerant component must retain sufficient structural integrity, after impact and perforation, to withstand the operational cyclic load for a time period sufficient for safe return of the aircraft to a friendly base. Inasmuch as the ballistic impact eliminates or "wipes out" a portion of the structure, it is apparent that some minimum component size (on an area basis) is required to retain an adequate structural section. It follows then that a component size is indicated below which ballistic-damage tolerance cannot be achieved.

Cost and producibility were also carefully considered. Many unique designs incorporating multiple webs, changing sections, and cutouts can be visualized which might have superior ballistic-damage tolerance. However, such designs result in very high tooling and manufacturing costs and are not readily producible.

CH-47C Idler Bell Crank

This component was originally designed as an aluminum forging (Boeing Part No. J114C2516). Based on the design curves, the loading requirements shown in Figure 12, and the fit and function installation requirements, a web width of 2 inches was selected. A web thickness of 0.125 inch appeared to be structurally marginal. Therefore, a web thickness of 0.150 inch was chosen as the best trade-off for adequate structure and weight control. After systematically eliminating several multiple-load-path redundant structures of the waffle design, because of high tooling and/or fabrication costs and high weight penalties, an H-beam design was adopted. This design provided a satisfactory alternate load path after ballistic impact from any direction along with reasonable producibility and weight factors. Since the redesigned molded component must be directly interchangeable with the existing metal component, no attempt was made to achieve ballistic-damage tolerance at the attachment points. Therefore, the existing metal bushings, sleeves, and bearings were incorporated in the design of the molded component without modification. This constraint, however, would not apply to components designed for new aircraft systems where ballistic-damage tolerance at attachment points of mechanical linkage would be considered. The metal parts were attached to the molded component by using an adhesive bonding process. A press-fit attachment method is used in the metal components. It was found that the press-fit method of attaching the metal parts to the plastic caused cracking around the holes. One solution to this problem is to have a relatively loose fit and an adequate adhesive bond line. An alternate solution would be to mold-in the hardware at the time of molding. This can be accomplished by using appropriately designed tools. The design of the molded idler bell crank is shown in Figure 13.

CH-47C Aft Pylon Upper Bell Crank

This component was also originally designed as an aluminum forging (Boeing Part No. J114C2514). The general structural and dimensional envelope requirements for this component are the same as those for the idler bell crank except that the primary structural loads are transmitted

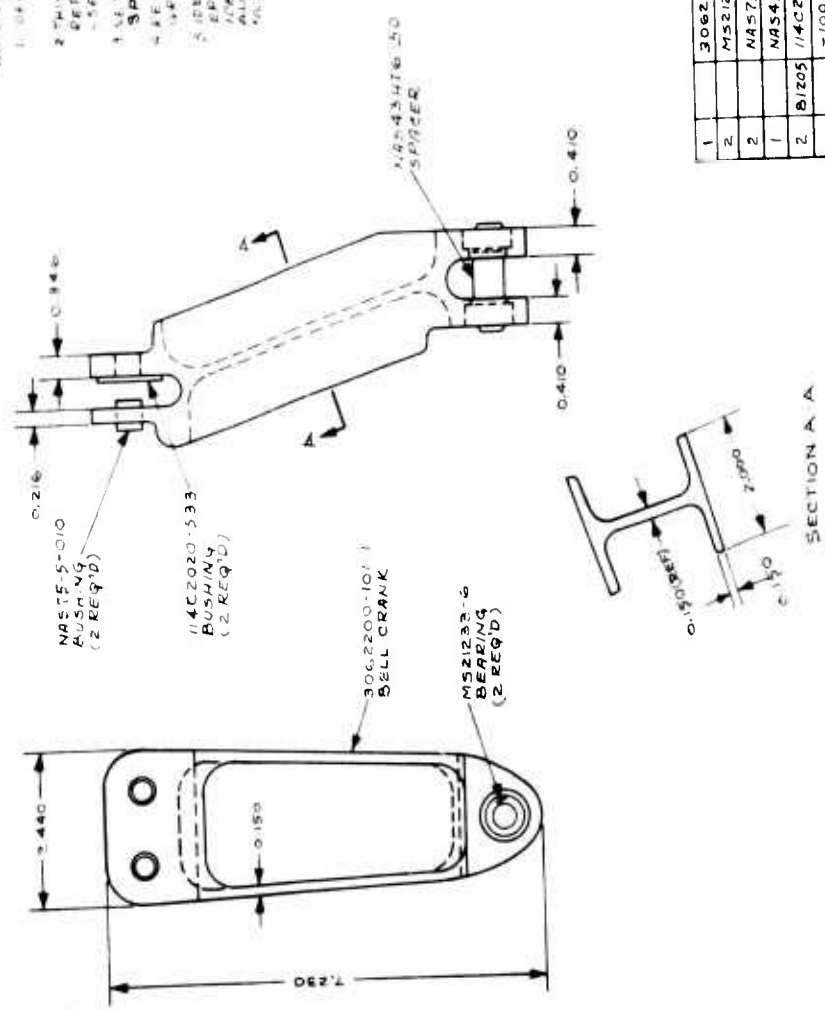
NOTE: ALL PARTS, UNLESS OTHERWISE SPECIFIED, TO BE MANUFACTURED TO MIL-STD-1302.

THIS PART IS BALLISTICALLY TOLERANT EXPERIMENTAL REPLACEMENT FOR BOEING PART NUMBER J4C2516 USED ON AIRCRAFT CH-47C.

1. 1/4" HOLE IN REAR OF BUSHING WITH MATERIALS AND PROCESS SPEC GER-15863.

2. REMOVE SLASH BY HAND SANDING WITH 180 GRIT SAND PAPER OR EQUIVALENT.

3. IDENTIFY BY NUMBER, STAMPING WITH WHITE EPOXY INK AND USING 1/8" INCH MICRODOTTER. IDENTIFY WITH 1/8" TO 1/4" INCH INCH MICRODOTTER. AND REPAIR WITH 1/8" TO 1/4" INCH INCH MICRODOTTER. IDENTIFY WITH 1/8" TO 1/4" INCH INCH MICRODOTTER.



ITEM NO.	CODE IDENT NO.	PART OR IDENTIFYING NO.	NOMENCLATURE OR DESCRIPTION	MATERIAL AND SIZE	ZONE
1		3062200-101-1	BELL CRANK		5
2		MS21233-6	BEARING		4
3		NAS15-5-010	BUSHING		3
4		NAS434TG-50	SPACER		2
5		J4C2020-533	BUSHING	BOEING AIRCRAFT	1
6		100	BELL CRANK ASSY		1
7					1
8					1
9					1

Figure 13. Design of CH-47C Ballistic-Damage-Tolerant Idler Bell Crank.

from lug to lug through the body of the component. In the idler bell crank, only the two attachment holes in the lug area carry the primary loads. To provide adequate structure for ballistic-damage tolerance, a structural web width of 2 inches and a web thickness of 0.150 inch are required. Both the maximum design load, undamaged at 160°F, and the operational loads, damaged at 160°F, are critical on this component. The H-beam design was used for this component to provide redundant structural sections. The H-beam was tailored to join the three attachment points, thus providing an alternate load path for an impact on any one of the primary load members. The existing metal bushings, bearings, and sleeves were incorporated in the design of the molded component without modification. The metal parts were attached to the molded component by using the adhesive bonding process. To achieve the static structural strength required, it was necessary to increase the overall thickness of the attachment lugs on the impact side from 0.125 inch to 0.219 inch. The design of the molded aft bell crank is shown in Figure 14.

UH-1B/D Quadrant Assembly

This component presented a somewhat different design problem from those of the bell cranks because the loads are relatively low, the part is comparatively large, and the existing magnesium casting is lightweight. The cable attachment to this component renders any impact in the cable track intolerable. The critical impacts on this component are as follows:

- Impacts near or between the cable attachment points, which could result in cable detachment
- Impacts in the actuator lug, which is attached to the shaft
- Impacts through the central portion of the center shaft at the pivot bushings or attachment bolt

Another design problem is maintaining stability in the sheave and preventing buckling of the sheave at high loads and high temperature.

From the producibility standpoint, it would not be possible to compression-mold this component in one piece unless a very complex multi-piece compression die with sliding portions were designed, which would be very costly. Therefore, the component was designed in two pieces, split across the center hub, to simplify the tooling problem. If the component were produced in very large quantities, the more complex tool and therefore the one-piece design could be considered practical.

To solve the problem of ballistic impacts in the cable attachment area, which could result in cable detachment, a bridge was designed between the two cable attachment points. The bridge would allow the use of the standard dimpled washer and ball-cable-end fitting, yet provide a structural attachment above and between these attachment points. Thus an impact in the area below the cable end would result in a load transfer to the bridge.

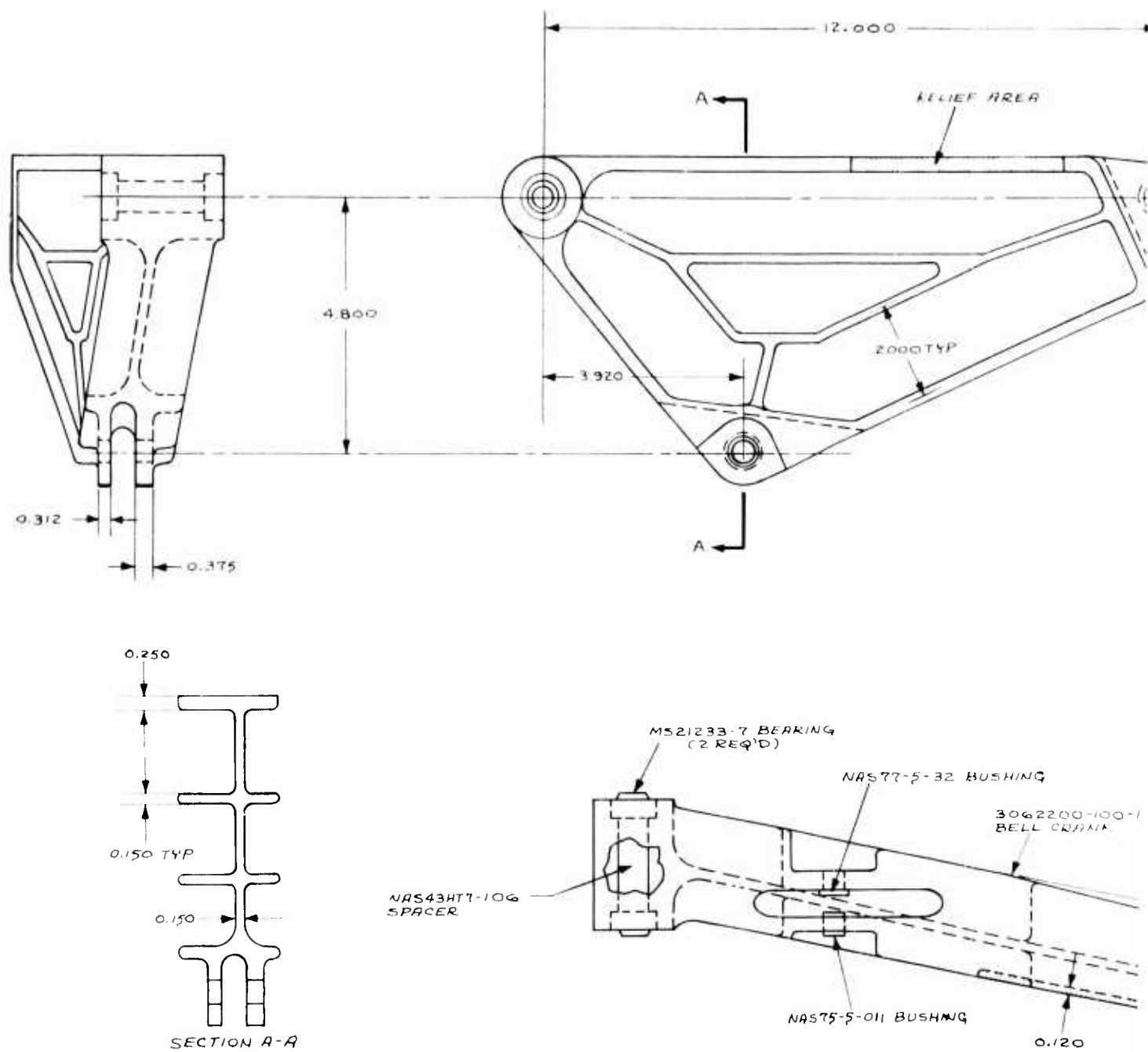
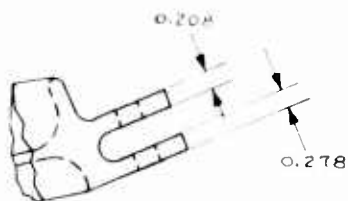
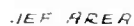


Figure 14. Design of CH-47C Ballistic-Damage-Tolerant Aft Pylon Upper Bell Crank.



1. IDENTIFY PART IN ACCORDANCE WITH MIL-STD-130.

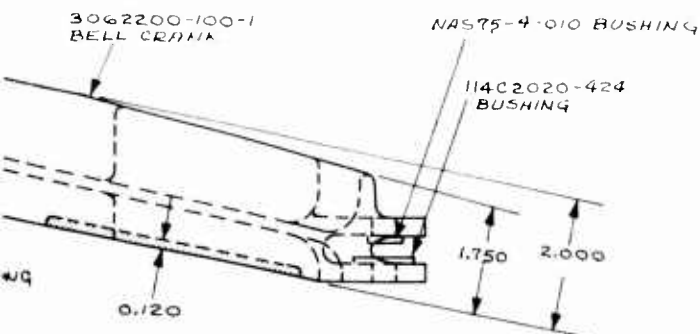
2 THIS PART IS A BALLISTICALLY TOLERANT EXPERIMENTAL
REPLACEMENT FOR BOEING PART NUMBER J114C2514
USED ON AIRCRAFT CH 47C.

3 NET-MOLD IN ACCORDANCE WITH MATERIALS AND PROCESS SPEC
GER-15863.

4. REMOVE FLASH BY HAND SANDING WITH 180 GRIT EMERY CLOTH OR EQUIVALENT.

5 IDENTIFY BY RUBBER STAMPING WITH WHITE EPOXY INK AND USING 1/8 INCH HIGH CHARACTERS. IDENTIFICATION TO INCLUDE THIS DWG. NUMBER AND REV LETTER, CURE DATE, AND SERIAL NUMBER (001, 002, ETC).

2 BUSHING



1		3062200-100-1	BELL CRANK			8
2		MS21233-7	BEARING			7
1		NAS77-5-32	BUSHING			6
1		NAS75-5-011	BUSHING			5
1		NAS75-4-010	BUSHING			4
1		NAS43HT7-106	SPACER			3
1	81205	114C2020-424	BUSHING	BOEING AIRCRAFT		2
		-100	BELL CRANK ASSY			1
QTY REQD	CODE IDENT NO.	PART OR IDENTIFYING NO	NOMENCLATURE OR DESCRIPTION	MATERIAL AND SIZE	ZONE	ITEM OR FINL NO.
PARTS LIST						

To solve the actuator-lug ballistic impact problem, the size of the lug was increased fourfold and a multiple load path was designed to carry the load in the event that an impact from any direction would destroy the primary load path.

Weight control was partly handled by incorporating lightening holes between the rib sections of the sheave.

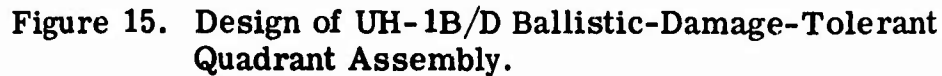
The load transfer between the crank and the sheave was accomplished by the castellation of both pieces at the hub joint and a structural epoxy adhesive bond. The existing metal bushings and bearing were incorporated in the design without modification. The metal parts were attached to the molded component by using the adhesive bonding process. The design of the molded quadrant assembly is shown in Figure 15.

During the structural design analysis and preliminary load testing of the quadrant assembly, a design deficiency was revealed in the bonded hub joint. The required maximum design-proof load capability of the component is 883 pounds (see Figure 12). The failure load of the component as designed was 1433 pounds at ambient temperature. This was felt to be an inadequate margin to sustain the elevated temperature and cyclic load tests. The location of the failure was between the castellations in the hub of the sheave part. The failure was characterized as an interlaminar shear type of failure in the randomly oriented X-Y plane material between the castellations.

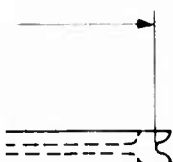
To increase the shear capability of the hub shaft, a 0.060-inch-thick-wall aluminum tube was designed to be bonded between the crank and the sheave in the hub area at the time the assembly is made. It was calculated that incorporation of this modification would increase the load capability of the component to 2040 pounds at 160°F.

STRUCTURAL DESIGN ANALYSIS

The ballistic-damage-tolerant component designs were structurally analyzed in both the undamaged and ballistically damaged conditions. The areas of high stress in the undamaged components under operational design loads are shown in Figure 16. High-stress areas in the ballistically damaged components are shown in Figure 17. The minimum margins of safety that were determined from the structural design analysis of the three components are summarized in Table XIV. Ultimate loads were used as the static loads in the analysis.



0.380 ALL AROUND TYP



1. THIS PART IS A BALLISTICALLY TOLERANT EXPERIMENTAL REPLACEMENT FOR BELL AIRCRAFT PART NUMBER 204-001-779-5 USED ON AIRCRAFT UH-1B/D.

2. CEMENT 3062200-108-1 TUBE INTO 3062200-103-1 SHEAVE
THEN CEMENT 3062200-104-1 CRANK TO BOTH TUBE AND SHEAVE.
USE AEROSPACE ADHESIVE EA-907 (HYSOL DIV. OF DEXTER CORP).
APPLY AND CURE PER MANUFACTURER'S DIRECTIONS.

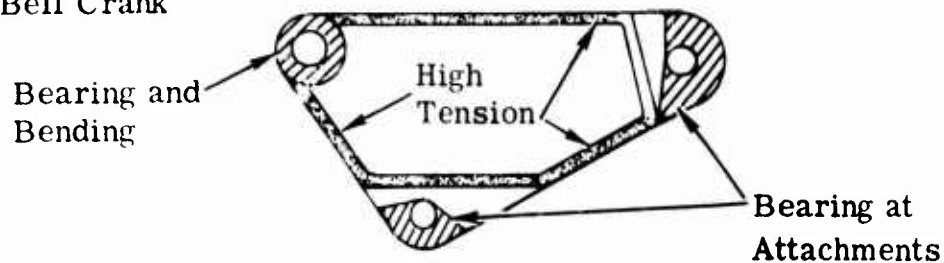
4. NET-MOLD IN ACCORDANCE WITH MATERIALS AND PROCESS SPEC GER-15863.

6. BREAK ALL SHARP EDGES 0.020R.

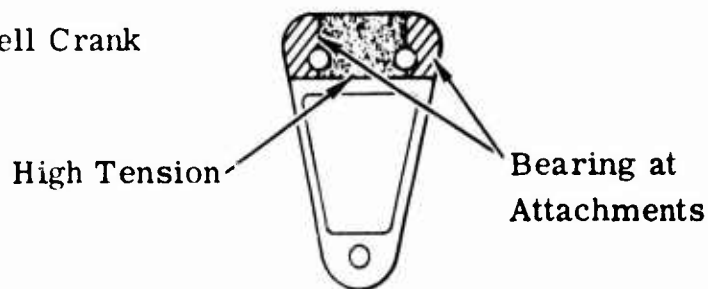
7. IDENTIFY BY RUBBER STAMPING WITH WHITE EPOXY INK AND USING 1/8 INCH HIGH CHARACTERS. IDENTIFICATION TO INCLUDE THIS DWG NUMBER AND REV LTR, CURE DATE AND SERIAL NUMBER (001, 002, ETC).

1		3062200-108-1	TUBE			7
1		M524643-4	BEARING			6
2	97499	22-009-15-37-22	BUSHING	BELL AIRCRAFT CORP		5
1	97499	205-001-719-1	BUSHING	BELL AIRCRAFT CORP		4
1		3062200-104-1	CRANK			3
1		3062200-103-1	SHEAVE			2
		-100	QUADRANT ASSY			1
	CODE IDENT N°	PART OR IDENTIFYING NO	NOMENCLATURE OR DESCRIPTION	MATERIAL AND SIZE	ZONE	ITEM OR FIND NO.
PARTS LIST						

A. Aft Bell Crank



B. Idler Bell Crank



C. Quadrant Assembly

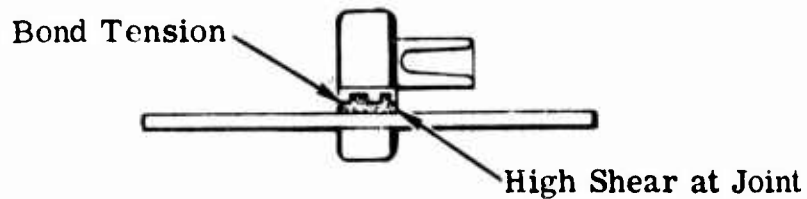
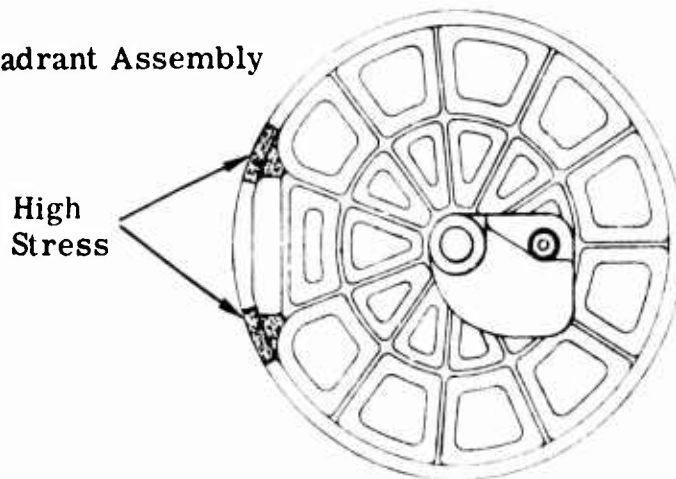


Figure 16. Areas of High Stress in Undamaged Components.

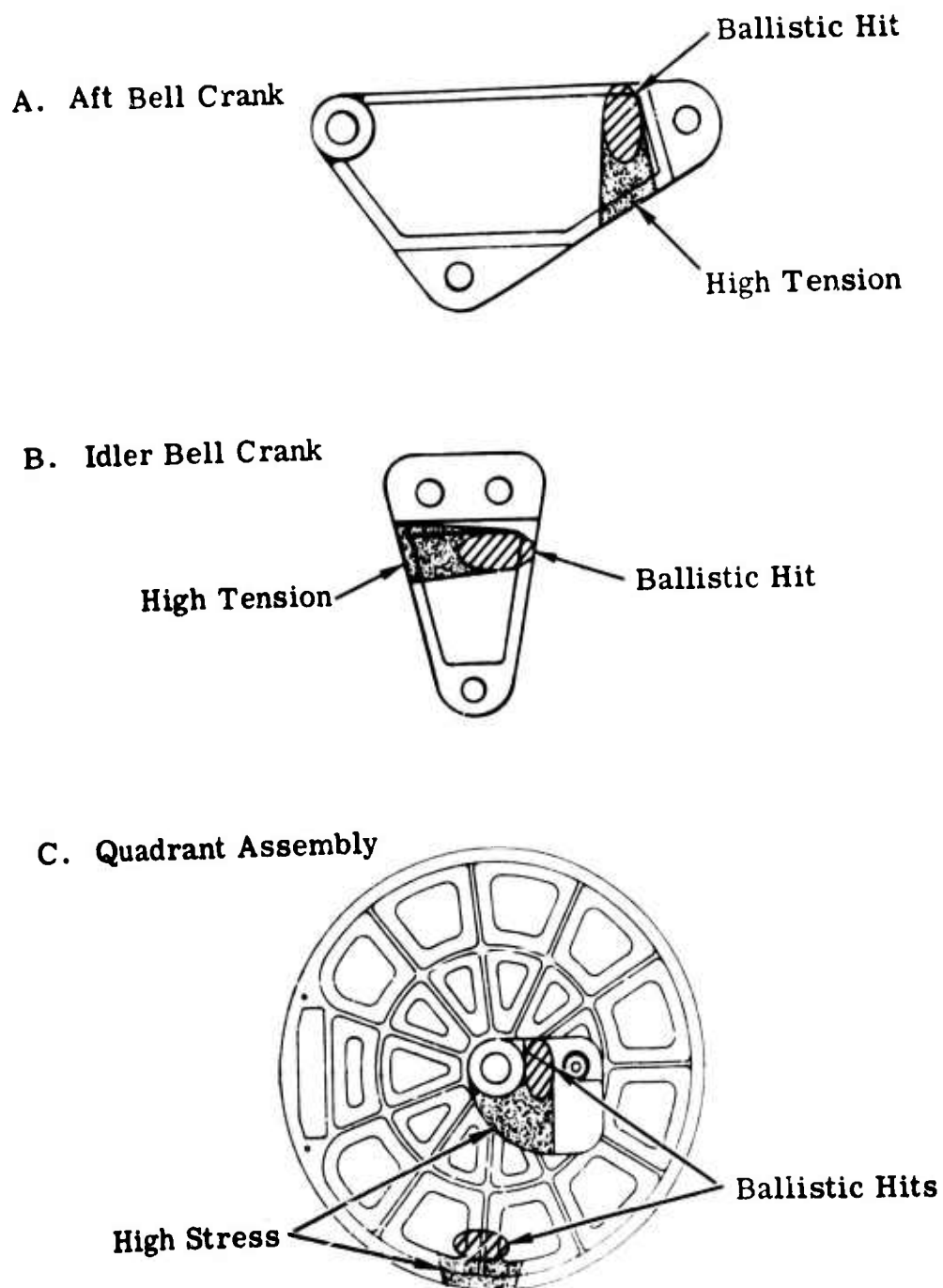


Figure 17. Areas of High Stress in Ballistically Damaged Components.

**TABLE XIV. SUMMARY OF STRUCTURAL DESIGN ANALYSIS -
CALCULATED MINIMUM MARGINS OF SAFETY**

Component	Element	Analysis	Margin of Safety
Aft Bell Crank	Rail tension	Static load	+0.03
	Rail tension	Ballistic damage	+0.12
Idler Bell Crank	Lug tension	Static load	+0.11
	H-beam tension	Ballistic damage	+0.79
Quadrant Assembly	Bond tension	Static load	+0.11
	Hub shaft shear	Static load	+0.00 ^a
	Hub shaft shear	Static load	+0.06 ^b
	Rim flexure	Ballistic damage	+0.01
^a As originally designed.			
^b After incorporation of the internally bonded, 0.060-inch-thick-wall aluminum tube.			

It should be noted that the attachment hard points on the components are considered to be more vulnerable than any other portion of the components. The attachment points include the rod-end bolted attachments of the bell cranks and the cable attachment point and groove in the quadrant assembly sheave. Since the ballistic-damage-tolerant components must be directly interchangeable with the existing metal components, no attempt was made to provide for ballistic-damage-tolerant attachments. Therefore, the existing metal bushings, bearings, bolts, and interfacing linkages, which may not be ballistic-damage-tolerant parts, were used without modification.

The ballistic impact location selected for the bell cranks was the point at which the projectile passes through the primary load path and impacts within the molded composite material of the component. In the case of the quadrant assembly, two impact locations were planned - one in the primary load path of the crank and the other in the sheave spoke.

WEIGHT COMPARISON

The weights of the three ballistic-damage-tolerant components are compared with the weights of their metal counterparts in Table XV.

TABLE XV. COMPONENT WEIGHT COMPARISONS		
Component	Component Weight (lb)	
	Metal	Composite
Aft Bell Crank	2.50	2.75
Idler Bell Crank	0.86	0.72
Quadrant Assembly	2.35	3.85

TOOLING AND FABRICATION

GENERAL

The complexity of the tooling designs depends on the complexity of the components and the quantity of components to be molded. If the component designs are complex, the compression-molding dies may require elaborate component-removal devices. Such tools should be machined from steel in multiple pieces with hydraulic- or pneumatic-actuated transverse punches to mold undercuts and back drafts. These types of tools are expensive and are used for relatively high-volume production (>1000 units). However, if the quantities of components to be molded are modest (10 to 500 units), lower-cost tooling can be utilized. Low-cost tooling approaches that can be considered include Kirksite tooling, nickel vaporform tools (chemical vapor deposition of nickel), and mild steel dies not incorporating costly items such as hardened shear edges, heat treatment, or component-removal devices.

Matched-die tooling was used for manufacturing the redesigned components. The compression-molding dies were machined from mild steel. The dies were used to mold the chopped-fiber glass-epoxy molding compound to the shape and size of the design configurations developed. These tools proved to be adequate for component fabrication in the quantities required (15 to 25 units). The compression-molded components were typical of mass-produced components, not necessarily inferior or superior in any respect.

The short-fiber molding materials used for component fabrication were produced using commercially available fiber glass rovings and epoxy resin systems. The process specification for fabrication and quality control of the composite materials is available as a Government Specification.⁶ The molding compound is similar to many commercially available materials and can be procured to the process specification requirements from several vendors.

The fabrication processes emphasize component reliability by using the minimum-flow preform technique. This technique requires that the proper amount of chopped short-fiber molding material be prepositioned in the approximate location that will be retained in the molded component. The material after positioning is compacted at ambient temperature under a pressure of 40 psi. This operation can be accomplished in the compression-molding tool prior to heat-up and final molding or in a separate, auxiliary, wooden or plastic tool. Details of this process are given in subsequent paragraphs of this section. The fabricated components should

be typical of mass-produced components and should not necessarily represent laboratory-controlled specimens.

IDLER BELL CRANK TOOLING

The design of this tool is shown in Figure 18. Basically, it is a three-piece tool with dual punch dies (upper and lower) and a shell type of cavity that can be moved up and down the punches. The cavity die action forms a seal against the brass shear edges of the punches, providing the back-pressure required for compression molding. To effect component removal, the cavity is stripped away from the lower punch, and the component is retained in the cavity. The component is then removed from the cavity by placing a spacer between the upper punch and the component and moving the punch downward. Figure 19 illustrates the step-by-step procedure for removing the component from the tool.

The tool is indexed through a set of four guide pins mounted at the corners of the tool. The tool is constructed of mild steel with a surface finish of 0.125 root mean square (RMS). The small size of the tool allows it to be surface heated by press-mounted steam platens, eliminating the need for internal die coring. The matched-die steel tooling for the idler bell crank is shown in Figure 20.

AFT BELL CRANK TOOLING

The design of this tool is shown in Figure 21. The design and construction features of the aft bell crank tooling are the same as those of the idler bell crank tooling. However, the tooling for the aft bell crank is more complex because of its larger size and multiple load path structure. The tooling die action employed in the component molding and removal operations is the same for both bell cranks. The aft bell crank is also surface heated by press-mounted steam platens. The matched-die steel tooling for the aft bell crank is shown in Figure 22.

QUADRANT ASSEMBLY TOOLING

The quadrant assembly is molded in two separate pieces, a sheave and a crank. Two separate tools were designed and fabricated.

The design of the quadrant sheave tool is shown in Figure 23. Although the tooling design is conventional, this tool is representative of a more complex tool. It has a large surface area and a great length of shear edge. Mild steel was used in the construction of the tool, which consists

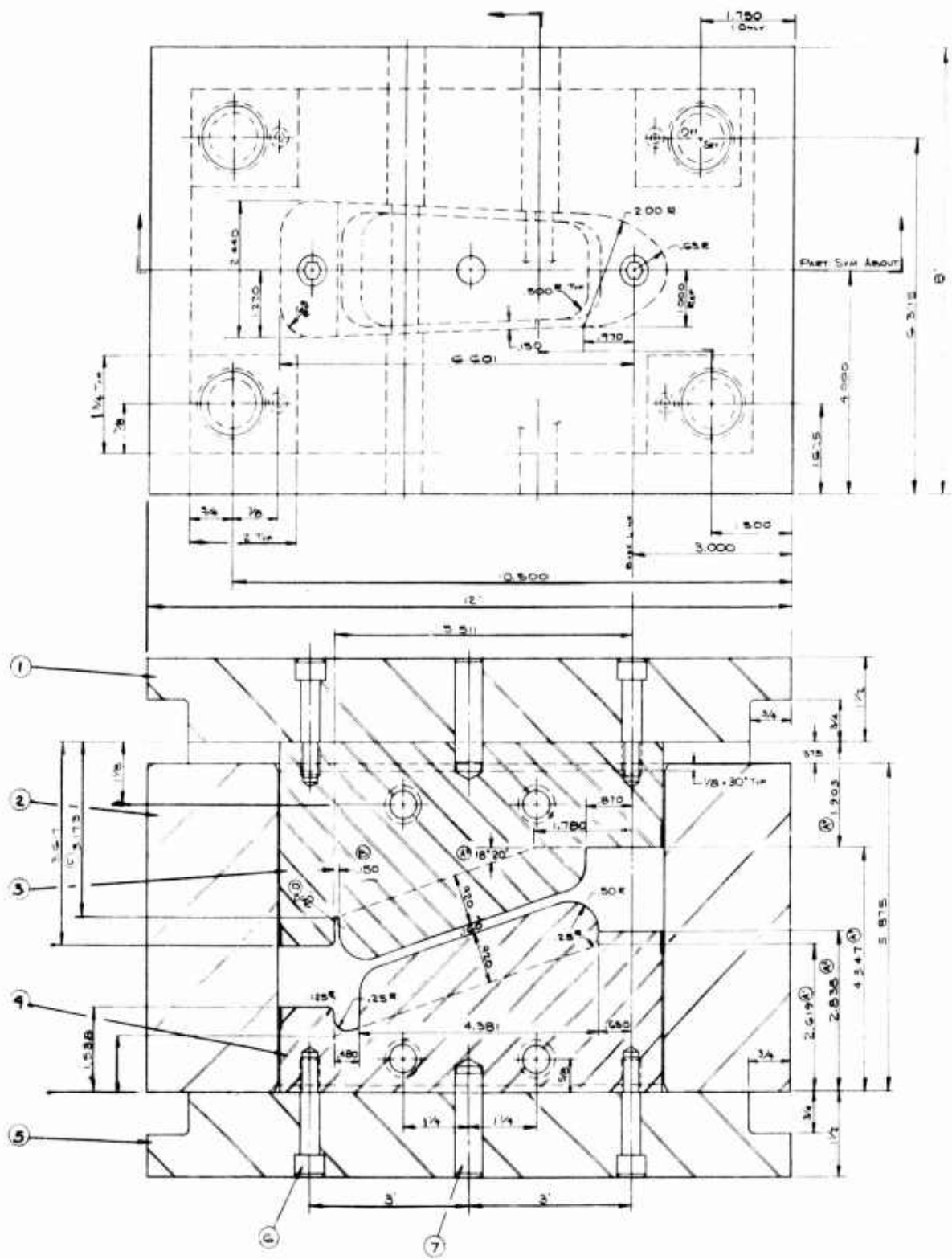
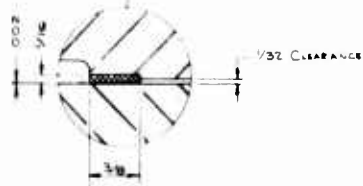
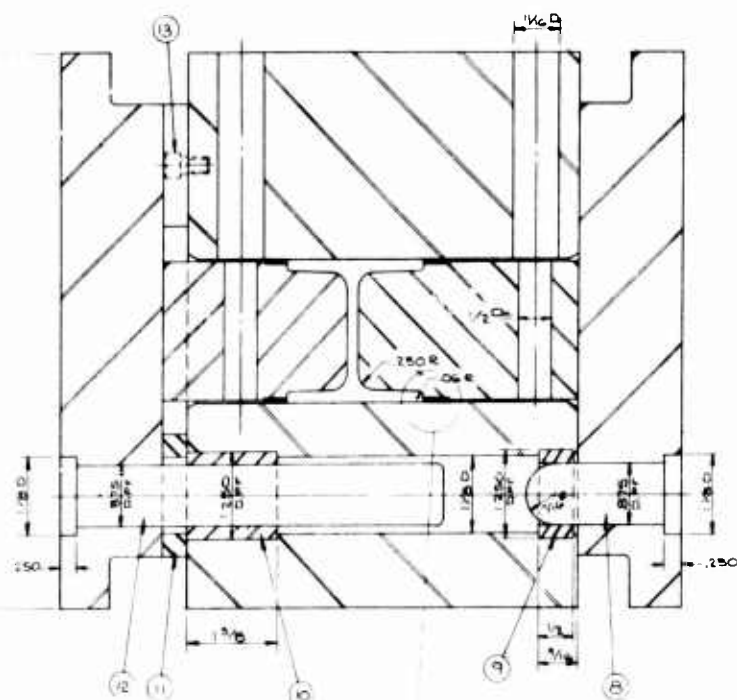


Figure 18. Design of Compression-Molding Tool for Idler Bell Crank.

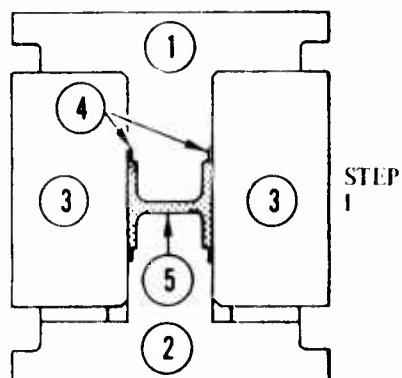


2° TYP DRAFT

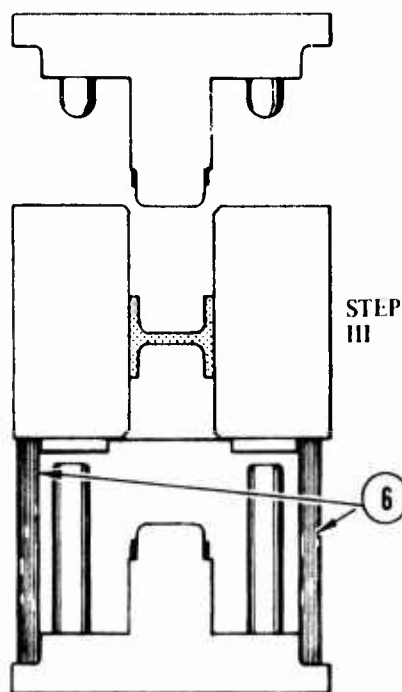
TEM	REQD	SIZE	MAT.
1	1	$3\frac{1}{2} \times 8\frac{3}{4} \times 2\frac{3}{4}$	M.S.
2	1	$6 \times 8\frac{3}{4} \times 12\frac{3}{4}$	M.S.
3	1	$2\frac{3}{4} \times 4\frac{1}{4} \times 7\frac{3}{4}$	M.S.
4	1	$2\frac{3}{4} \times 3\frac{3}{4} \times 7\frac{3}{4}$	M.S.
5	1	$1\frac{1}{2} \times 8\frac{3}{4} \times 2\frac{3}{4}$	M.S.
6	4	$\frac{3}{16} 16 T10 \times 3\frac{1}{4}$	SHCS.
7	2	$\frac{1}{2} Dia \times 2$	Down
8	4	$= 5100$	DME
9	4	$1\frac{1}{4} 00 \times 7\frac{1}{2} Dia \times 1\frac{1}{2}$	STEEL
10	4	$= 5502$	DME
11	4	$3\frac{1}{2} \times 1\frac{3}{4} \times 2\frac{1}{2}$	CRS.
12	4	$= 5107$	DME
13	4	$\frac{1}{4} 20 T10 \times 5\frac{1}{4}$	SHCS.

ell Crank.

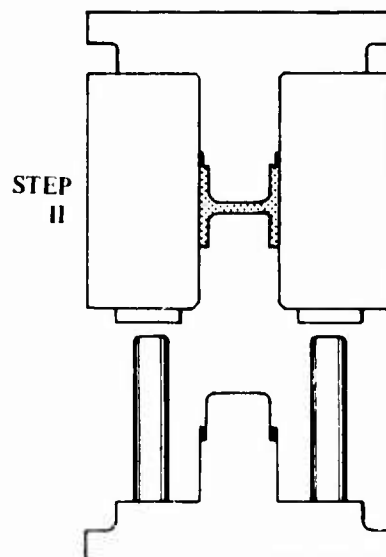
2



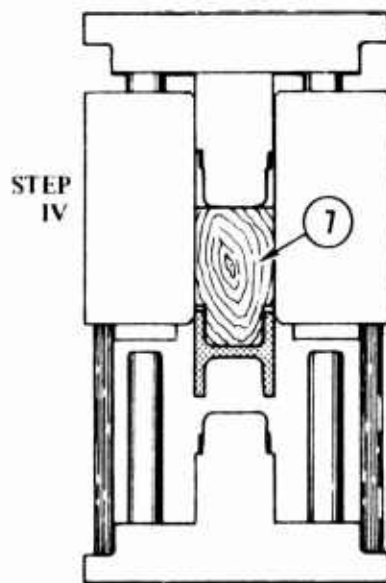
Component in Tool
(Closed Position).



Both Punches Removed.
Component Retained
Within Cavity.



Tool in Open Position.
Component Retained in
Upper Punch and Cavity.



Component Removed From
Tool by Removal Block.

- | | |
|----------------------|----------------------------|
| 1. Upper Punch Die | 5. Molded Component |
| 2. Lower Punch Die | 6. Cavity Support Ring |
| 3. Cavity Shell | 7. Component Removal Block |
| 4. Brass Shear Edges | |

Figure 19. Procedure for Removing Component
From Three-Piece Tool.

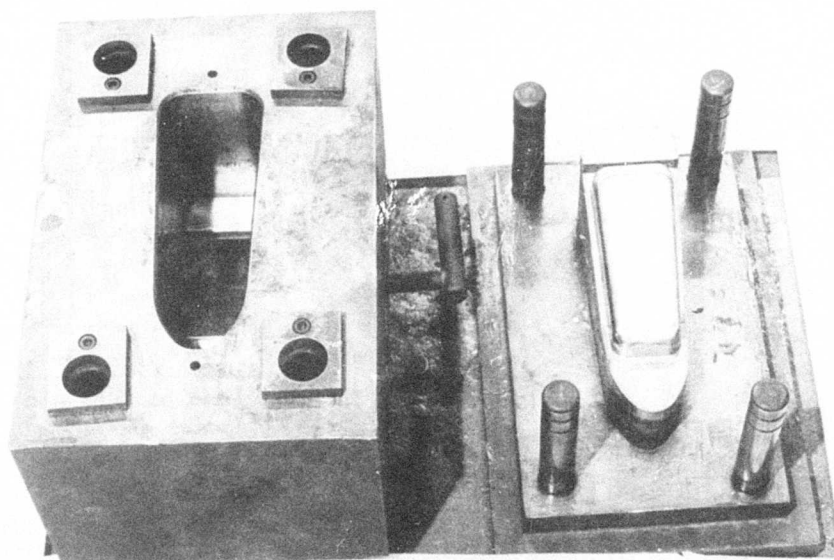


Figure 20. Matched-Die Steel Tooling for Idler Bell Crank.

of a cavity die and a punch die with brass shear edges. To effect component removal, a pin-ejection system was built into the cavity die. The ejection system is actuated through chains attached to the upper (punch) die. At the conclusion of the compression-molding cycle, the ejector plate moves upward and nine pins push the component out of the lower (cavity) die. Both the cavity and the punch are heated by steam coring. The matched-die steel tooling for the quadrant sheave is shown in Figure 24.

The design of the quadrant crank tool is shown in Figure 25. It is basically a straight compression-molding tool. The only problem that required a tooling design innovation was removal of the component from the tool. When this type of tool is used for molding, the component can become entrapped in the cavity die and can be very difficult to remove. Therefore, a groove was machined in the punch die, transverse to the die action, which had the effect of locking the molded component on the punch die. The molded component can then be removed from the punch

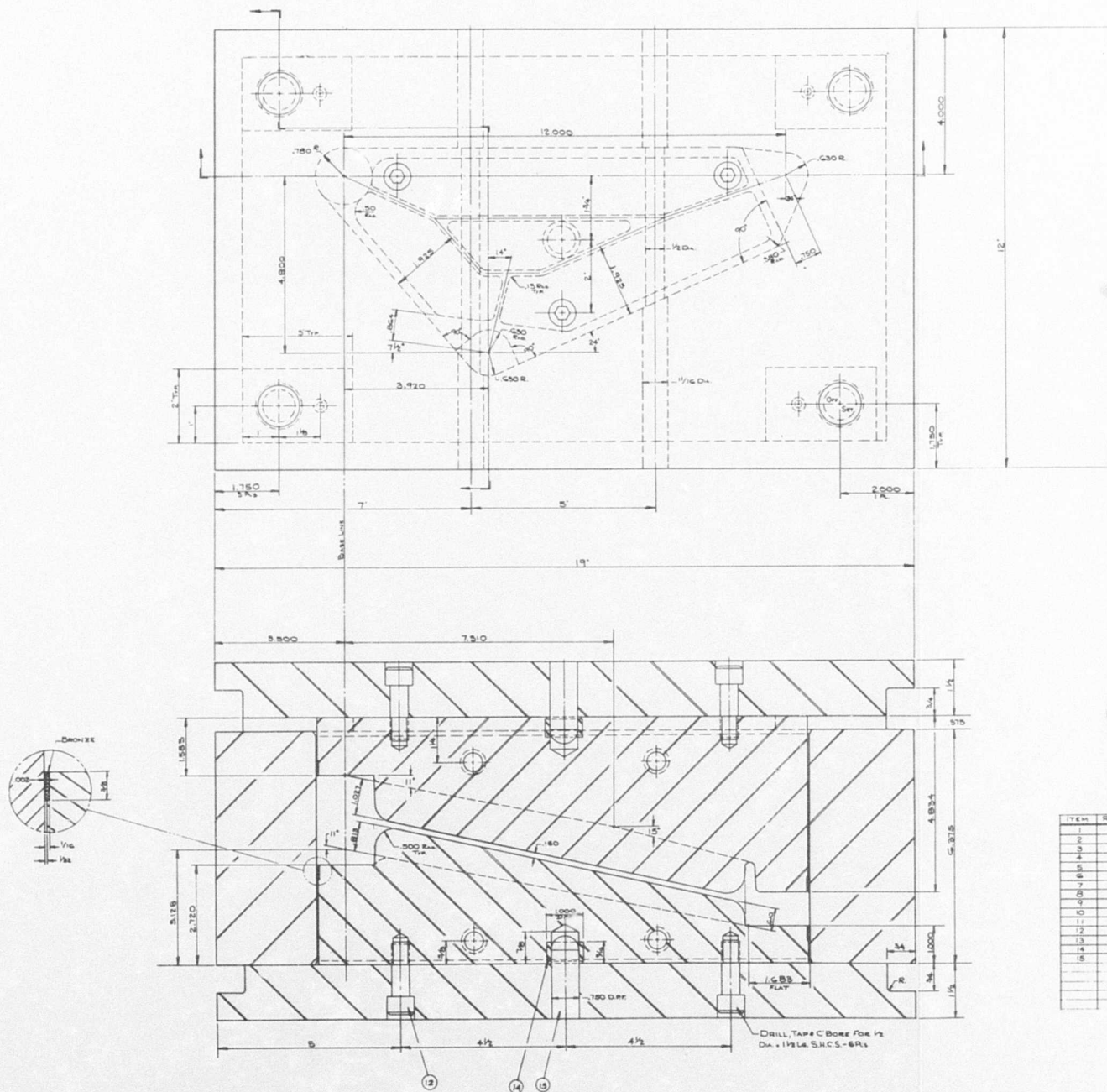
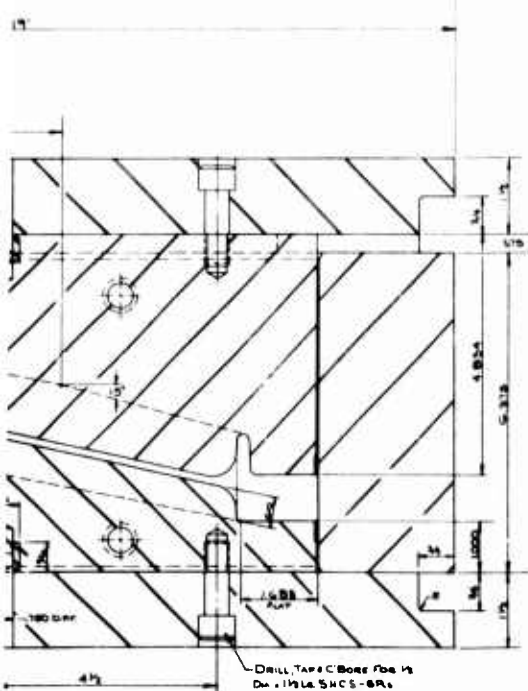


Figure 21. Design of Compression-Molding Tool for Aft Bell Crank.



TEM	TRIP	SEE	MAN
1	1	150 - 12.40 - 1.40	M.S
2	4	17.10 - 12.40 - 1.10	M.S
3	1	2 - 6.40 - 3.30	M.S
4	1	6.4 - 12.40 - 1.40	M.S
5	1	1 - 6.40 - 3.30	M.S
6	1	100 - 12.40 - 1.40	M.S
7	4	100 - 12.40 - 3.10	Don't know
8	4	0.100	D.M.E
9	4	0.803	D.M.E
10	4	0.8 - 3.4	C.B.S
11	4	1 - 12.40 - 1.40	S.H.C.S
12	6	100 - 12.40 - 2.40	C.B.S
13	2	100 - 12.40 - 1.40	Don't know
14	5		

ool for Aft Bell Crank.

2

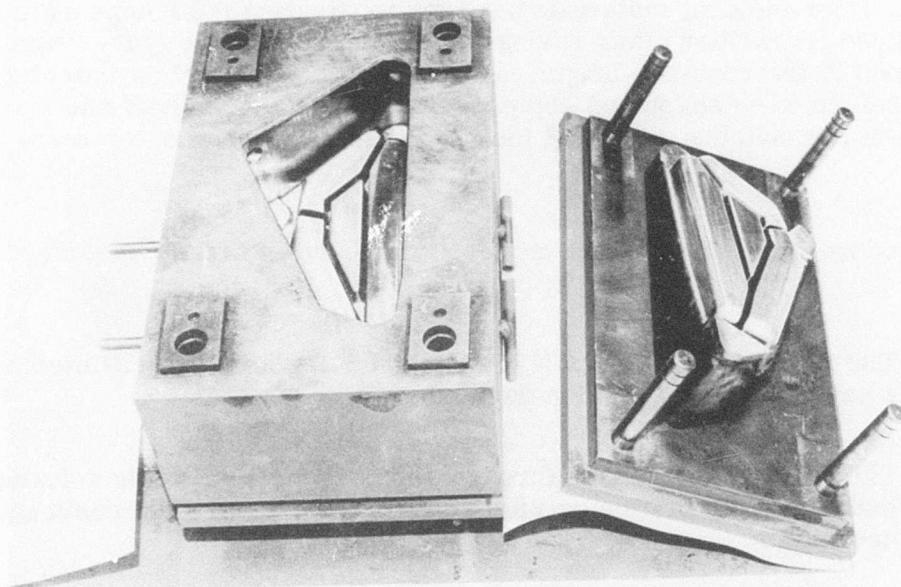


Figure 22. Matched-Die Steel Tooling for Aft Bell Crank.

die by moving the component parallel along the groove (perpendicular to the die action) until the component clears the groove. The matched-die steel tooling for the quadrant crank is shown in Figure 26.

FABRICATION OF COMPONENTS

The detailed procedures for fabricating the molded ballistic-damage-tolerant components are defined in the process specification.⁶ The following discussion briefly describes the materials and techniques used in fabricating the components, along with some of the problems that may be encountered in the fabrication processes and the solutions to these problems.

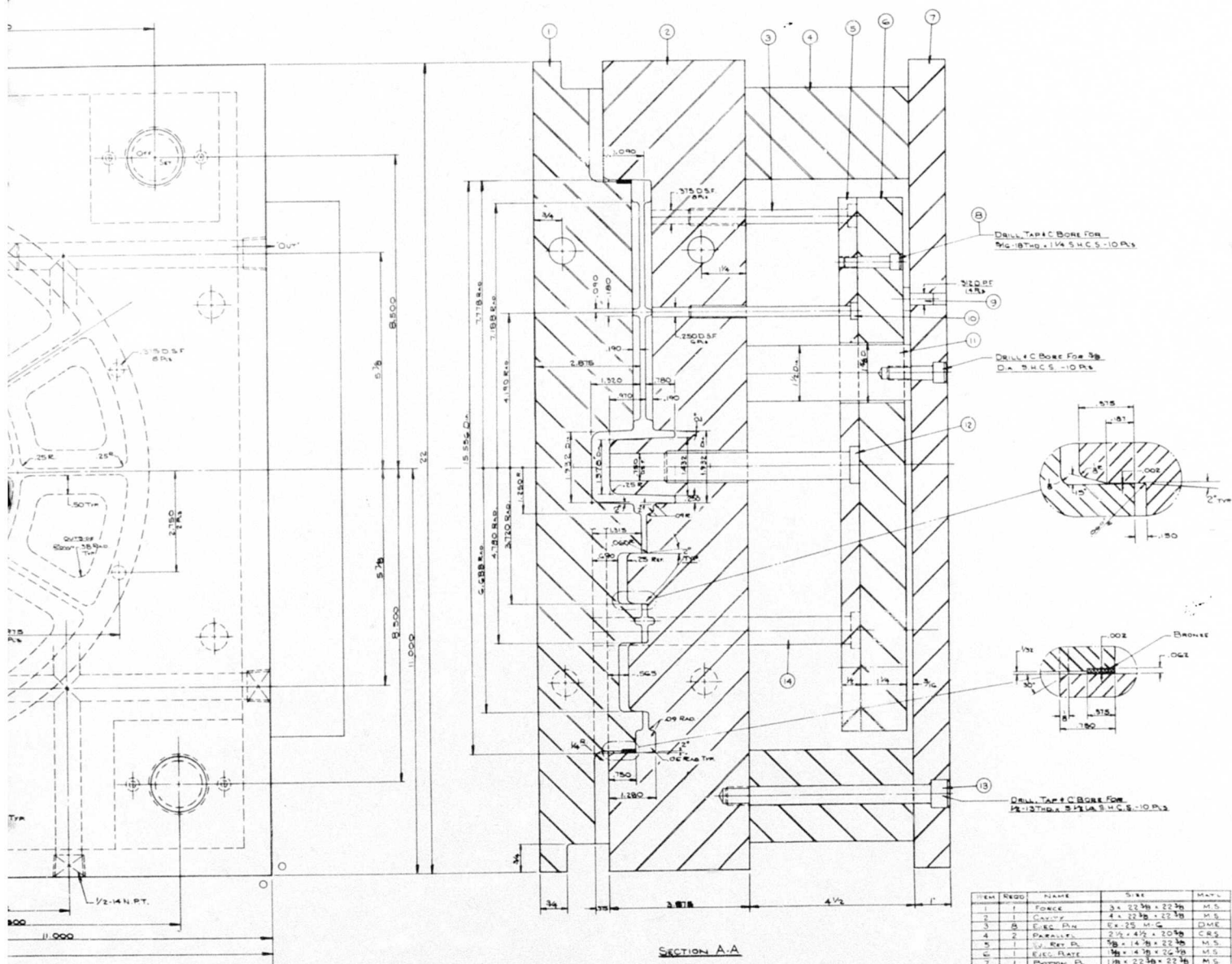
Preparation of Chopped Fiber Glass-Epoxy Molding Material

The short-fiber molding materials used for fabricating the components are produced from fiber glass rovings impregnated with an epoxy resin and chopped to the required length. A weighed quantity of this material is then preformed to shape and compression-molded under heat and pressure in the matched-die steel tooling to fabricate each of the components.

The procedure for preparing the molding compound is briefly described below.

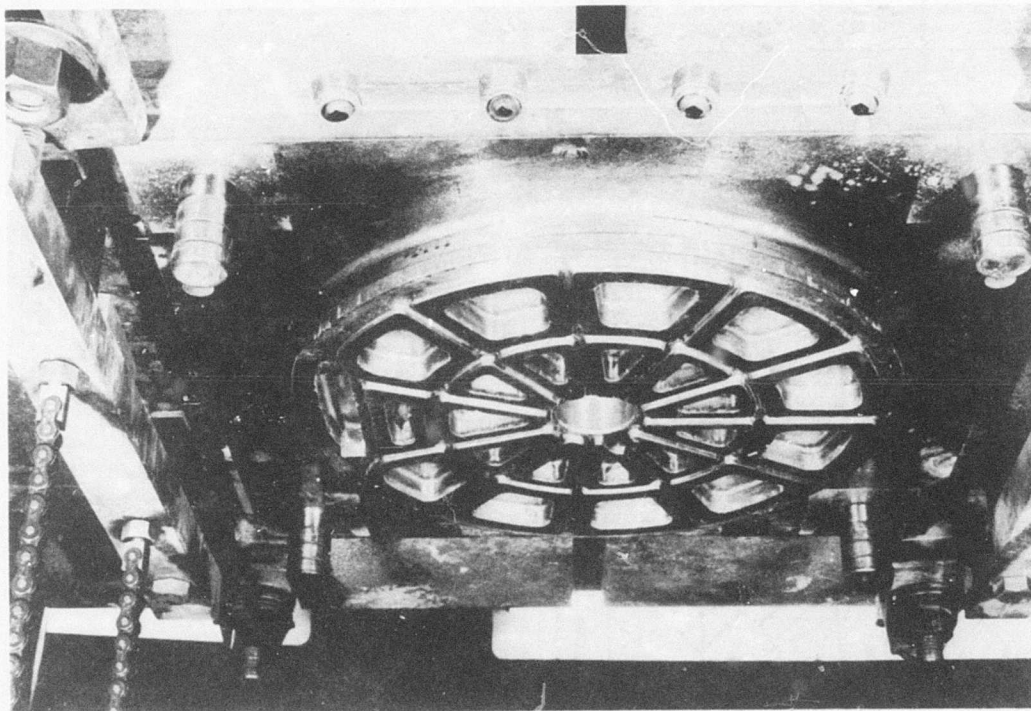
1. The fiber glass rovings (470-finished S-2 glass) are mounted on a payout reel and tension device.
2. The rovings are passed through an epoxy-novalac resin solution tank and a nip orifice or metering rolls for controlled resin impregnation.
3. The wet impregnated rovings are passed through hot-air-circulating ovens for solvent removal and resin staging.
4. The staged impregnated rovings are cooled and way-wound on a paper core.
5. The core-wound material is aged under controlled temperature and humidity conditions until the prescribed resin flow and gel time properties are achieved.
6. The impregnated rovings are unwound, chopped to 1/2-inch lengths, and stored at 0°F.

Schematic diagrams of typical vertical tower fiber glass roving impregnation equipment and rotary roving cutting equipment are shown in Figures 27 and 28, respectively. Multiple-roving inputs are used in this equipment to increase productivity. Figure 29 shows a Turner Model M-600 roving cutter and the setup used for chopping the roving to the required length.

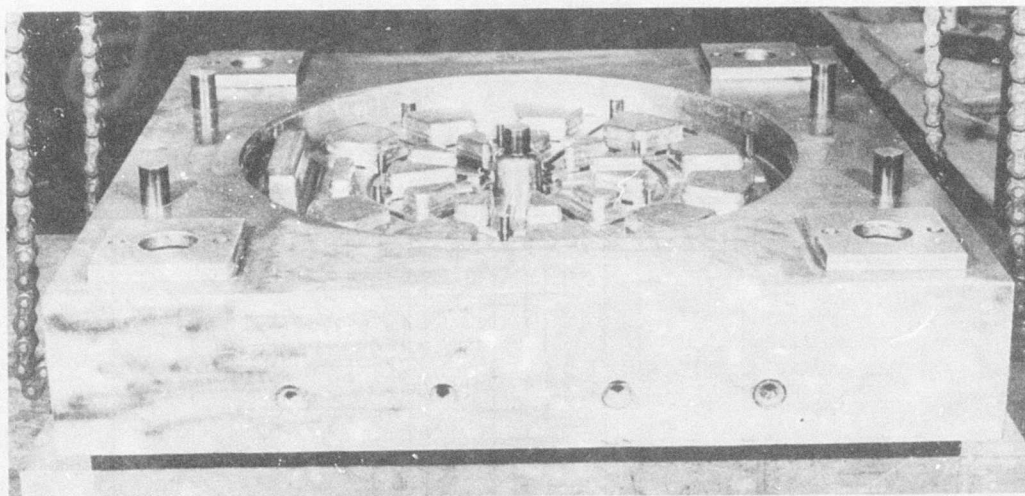


SECTION A-A

ITEM	REQD	NAME	SIZE	MAT'L
1	1	FORGE	34 x 22 3/8 x 22 3/8	M.S.
2	1	CAST IRON	4 x 22 3/8 x 22 3/8	M.S.
3	2	DRILL PIN	2 1/2 x 4 1/2 x 20 3/8	C.S.
4	2	DRILL PIN	2 1/2 x 4 1/2 x 20 3/8	C.S.
5	1	DRILL PIN	2 1/2 x 4 1/2 x 20 3/8	C.S.
6	1	DRILL PIN	2 1/2 x 4 1/2 x 20 3/8	C.S.
7	1	DRILL PIN	2 1/2 x 4 1/2 x 20 3/8	C.S.
8	1	DRILL PIN	2 1/2 x 4 1/2 x 20 3/8	C.S.
9	1	DRILL PIN	2 1/2 x 4 1/2 x 20 3/8	C.S.
10	1	DRILL PIN	2 1/2 x 4 1/2 x 20 3/8	C.S.
11	1	DRILL PIN	2 1/2 x 4 1/2 x 20 3/8	C.S.
12	1	DRILL PIN	2 1/2 x 4 1/2 x 20 3/8	C.S.
13	1	DRILL PIN	2 1/2 x 4 1/2 x 20 3/8	C.S.
14	1	DRILL PIN	2 1/2 x 4 1/2 x 20 3/8	C.S.
15	1	DRILL PIN	2 1/2 x 4 1/2 x 20 3/8	C.S.
16	1	DRILL PIN	2 1/2 x 4 1/2 x 20 3/8	C.S.
17	1	DRILL PIN	2 1/2 x 4 1/2 x 20 3/8	C.S.
18	1	DRILL PIN	2 1/2 x 4 1/2 x 20 3/8	C.S.
19	1	DRILL PIN	2 1/2 x 4 1/2 x 20 3/8	C.S.
20	1	DRILL PIN	2 1/2 x 4 1/2 x 20 3/8	C.S.
21	1	DRILL PIN	2 1/2 x 4 1/2 x 20 3/8	C.S.
22	1	DRILL PIN	2 1/2 x 4 1/2 x 20 3/8	C.S.
23	1	DRILL PIN	2 1/2 x 4 1/2 x 20 3/8	C.S.
24	1	DRILL PIN	2 1/2 x 4 1/2 x 20 3/8	C.S.



A. Upper (Punch) Die



B. Lower (Cavity) Die

Figure 24. Matched-Die Steel Tooling for Quadrant Sheave.

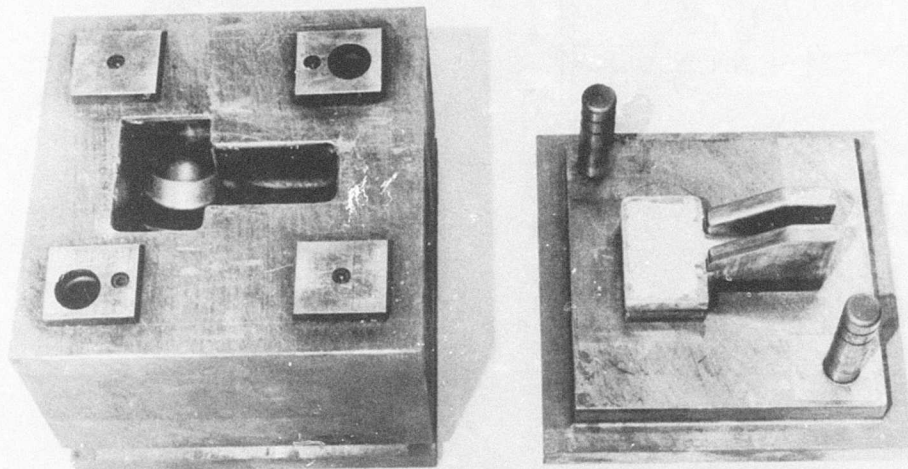


Figure 26. Matched-Die Steel Tooling for Quadrant Crank.

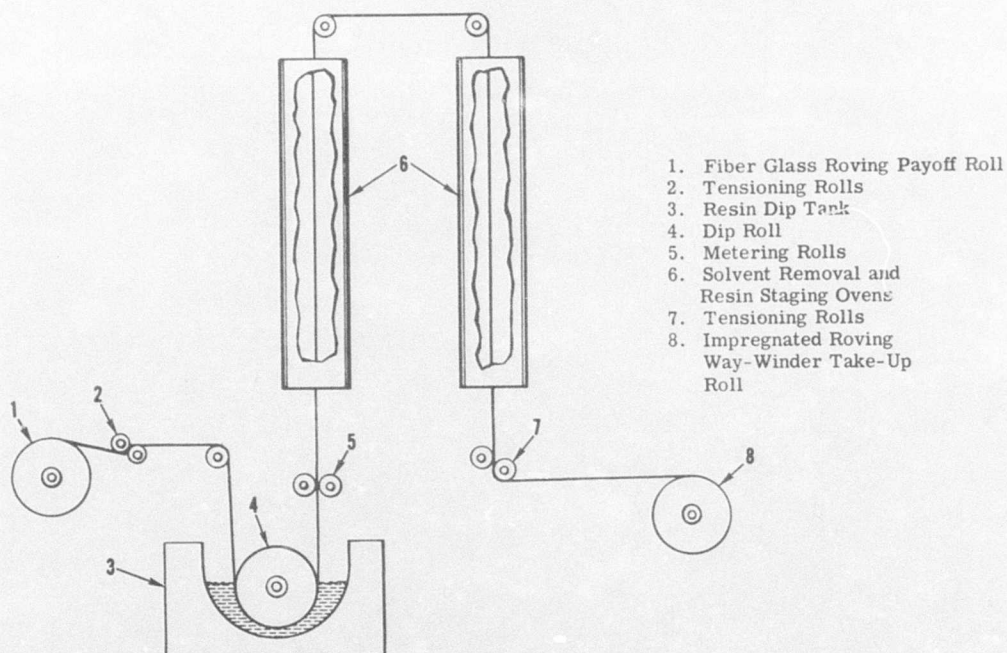
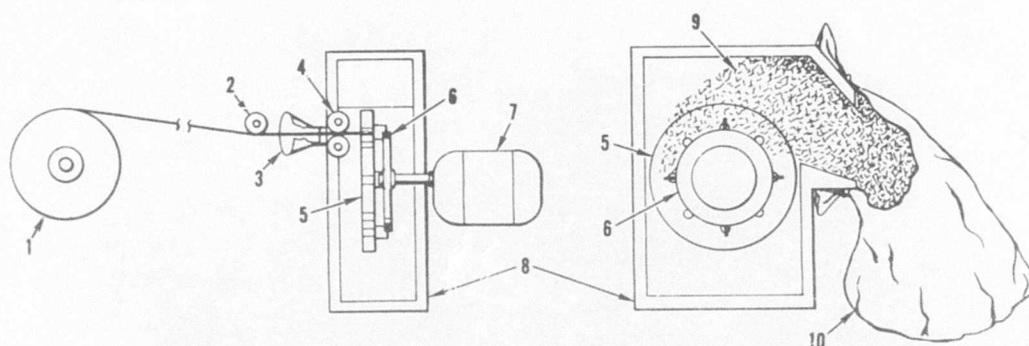


Figure 27. Schematic Diagram of Typical Fiber Glass Roving Impregnation Equipment.



- | | |
|-----------------------------------|----------------------------|
| 1. Impregnated Roving Payoff Roll | 6. Rotary Cutter Wheel |
| 2. Idler Roll | 7. Synchronous Drive Motor |
| 3. Inlet Orifice | 8. Housing |
| 4. Drive Rolls | 9. Chopped Fibers |
| 5. Steel Shear Plate | 10. Collection Bag |

Figure 28. Schematic Diagram of Typical Rotary Roving Cutting Equipment.

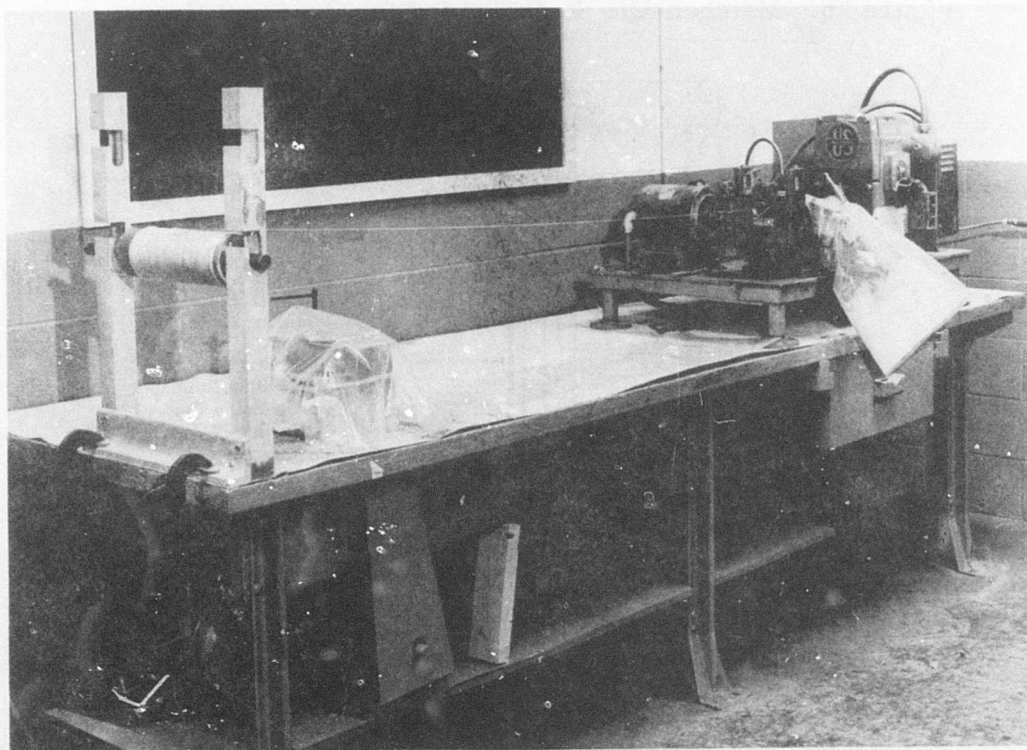


Figure 29. Turner Model M-600 Roving Chopper.

Fabrication of Idler Bell Crank

The following procedure was used for fabrication of the idler bell crank:

1. The molding material was prepared by mixing 4 grams of green tracer fibers with 385 grams of the chopped-fiber molding compound. The tracer fibers are used to indicate the fiber orientation after molding and thus are a quality control procedure.⁶
2. The material was divided into five portions of proportionate weight and preformed to shape as required by the process specification.
3. The preforms were charged into the compression-molding tool and cured for 20 minutes at 1000 psi and 300°F.
4. The molded component was removed from the tool and deflashed.
5. The slots were machined and the holes were drilled to drawing requirements.
6. The metal bushings, sleeves, and bearings were bonded in place with an epoxy adhesive.
7. The finished component was inspected for conformance to drawing requirements.

Figure 30 shows the idler bell crank at various stages in the fabrication process.

Fabrication of Aft Bell Crank

The basic fabrication procedure for the aft bell crank is the same as that for the idler bell crank, except that 13 grams of green tracer fibers were mixed with 1330 grams of the chopped-fiber molding compound. This material was then divided into ten preform portions of proportionate weight and a quantity of bulk material, which were charged into the compression-molding tool. All other conditions remained the same.

Fabrication of Quadrant Assembly

This assembly was molded in two parts, a crank and a sheave, which were bonded together to make the assembly.

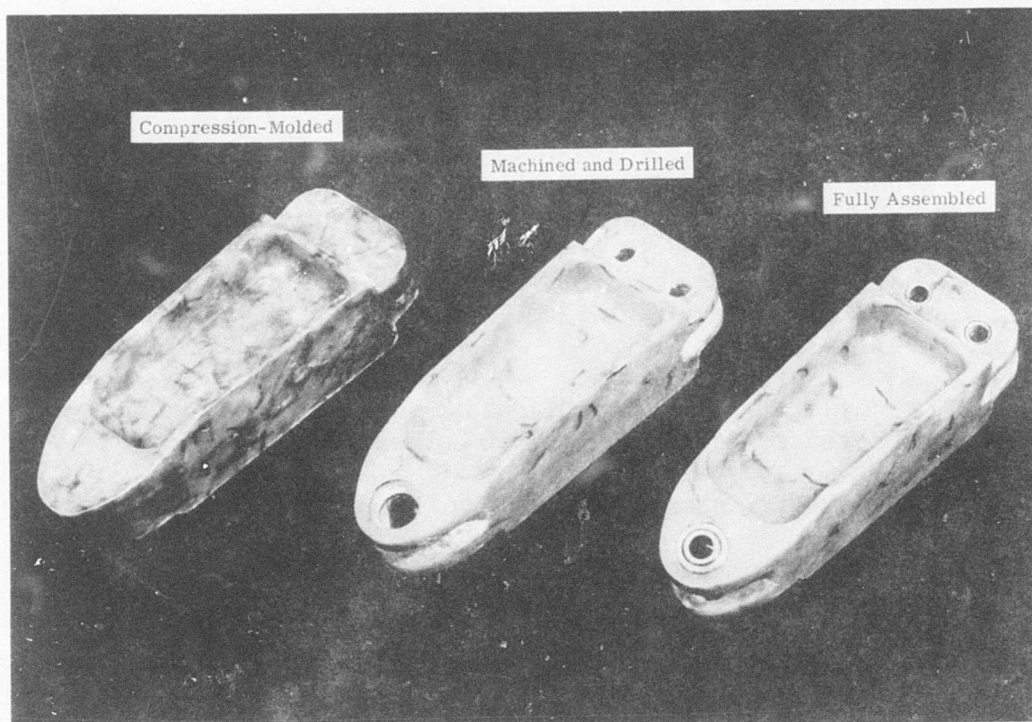


Figure 30. Various Fabrication Stages of Idler Bell Crank.

The basic fabrication procedure for the quadrant crank is the same as that for the idler bell crank, except that 7 grams of green tracer fibers were mixed with 698 grams of the chopped-fiber molding compound. This material was then divided into four preform portions of proportionate weight and preformed to shape for charging into the compression-molding tool.

The quadrant sheave was the most difficult part to fabricate because the matched-die steel tooling used for fabricating this part is the most complex tool used. The molding material was prepared by mixing 13 grams of green tracer fibers with 1345 grams of the chopped-fiber molding compound. This material was divided into ten preform portions of proportionate weight, which were preformed in the unheated compression-molding tool. Figure 31 shows the preform material in the unheated tool.

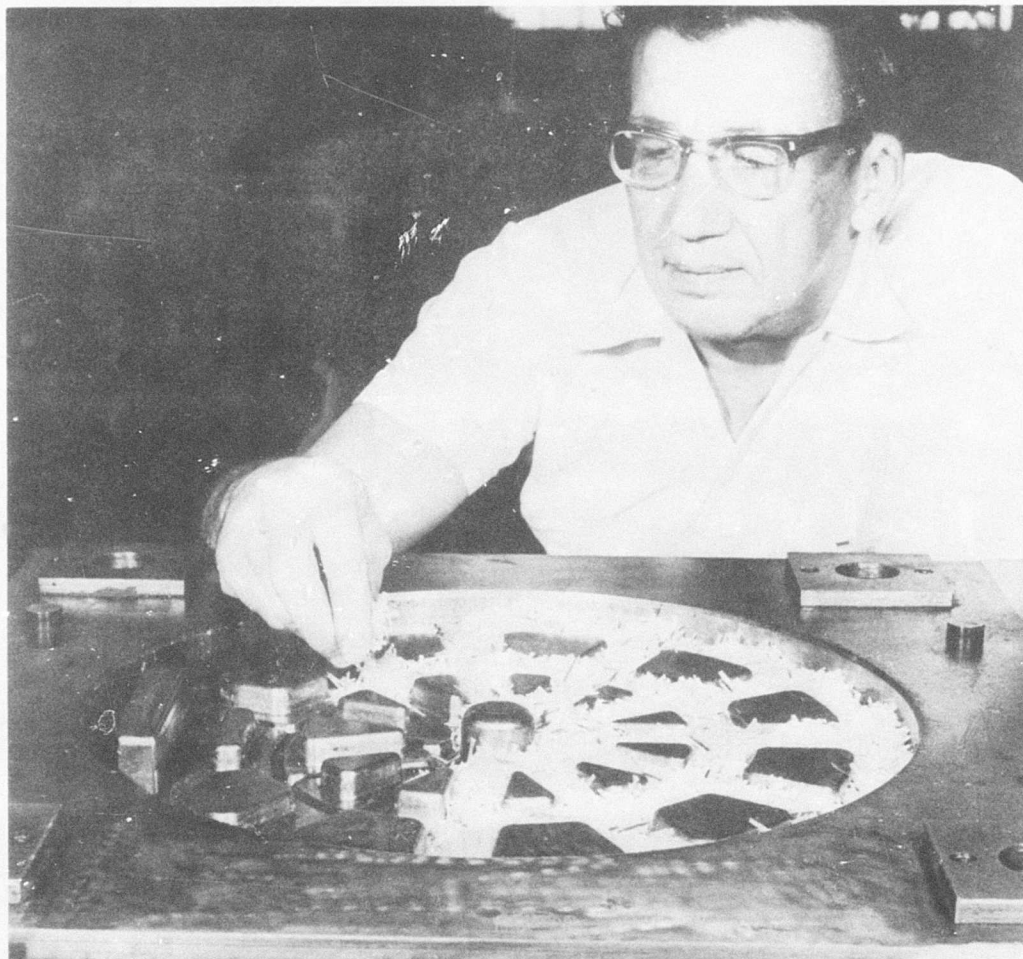


Figure 31. Preforming Chopped-Fiber Molding Material for Quadrant Sheave.

The completed preform ready for compression-molding is shown in Figure 32. Figure 33 shows the molded quadrant sheave on the knock-out pins in the tool. The completed quadrant sheave removed from the compression-molding tool is shown in Figure 34.

After molding, the castellations were machined and the holes were drilled. Then the two parts were assembled with an aluminum tube bonded into the hub. An epoxy adhesive was used for the bond, which was cured for 2 hours at 190°F.

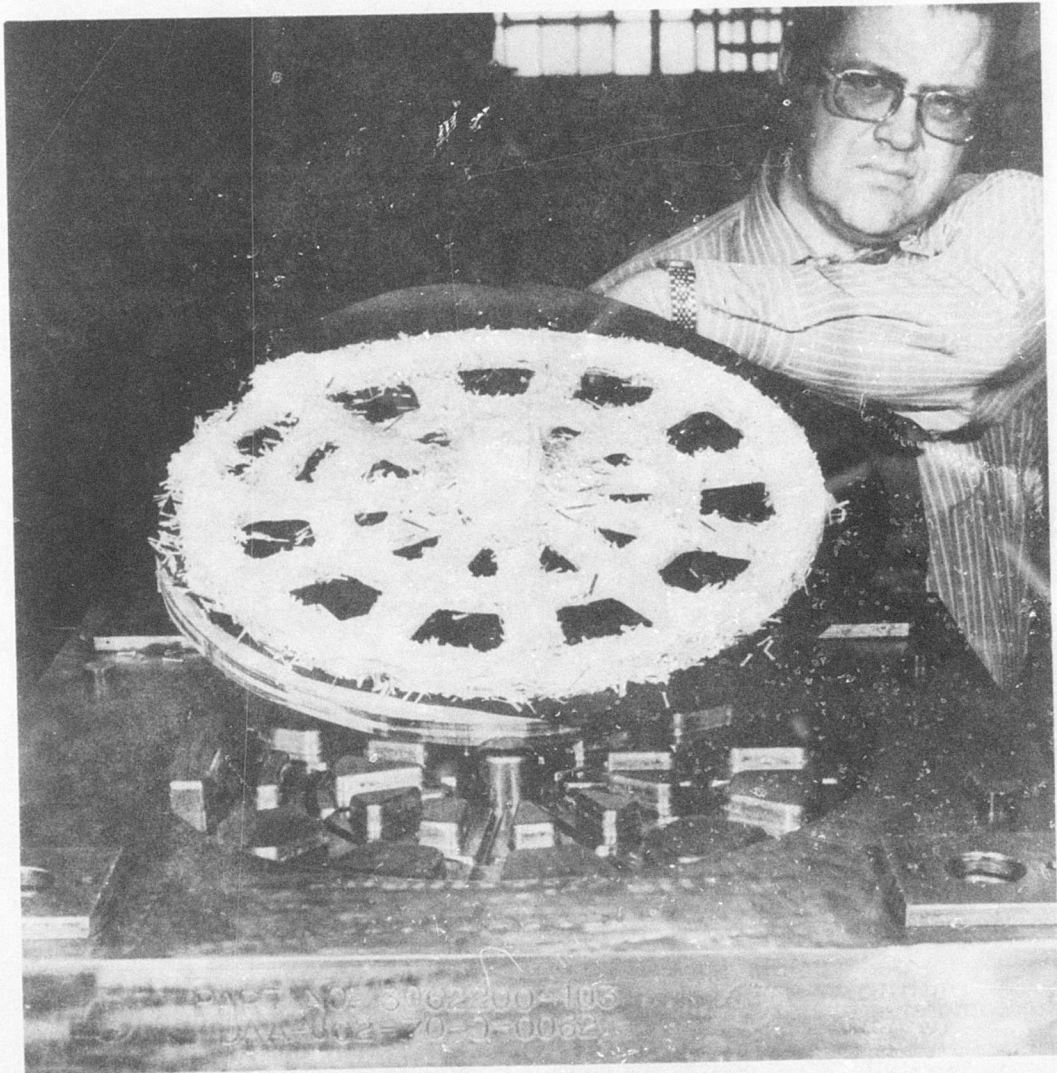


Figure 32. Completed Preform for Quadrant Sheave.

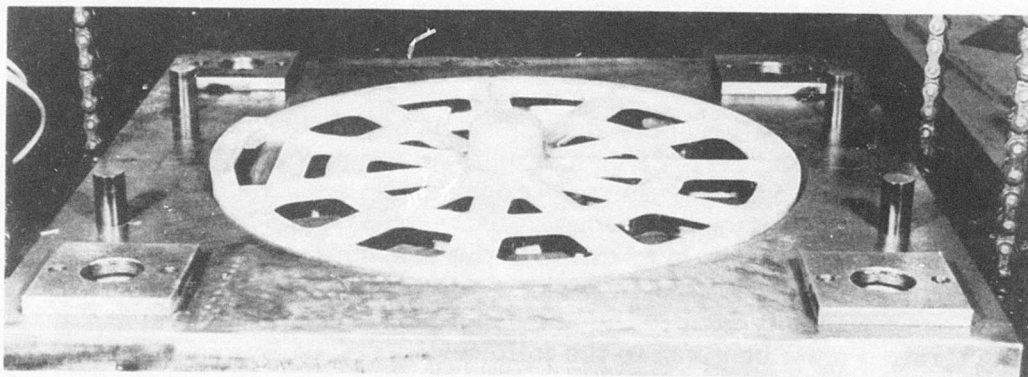


Figure 33. Molded Quadrant Sheave on Knock-Out Pins in Tool.

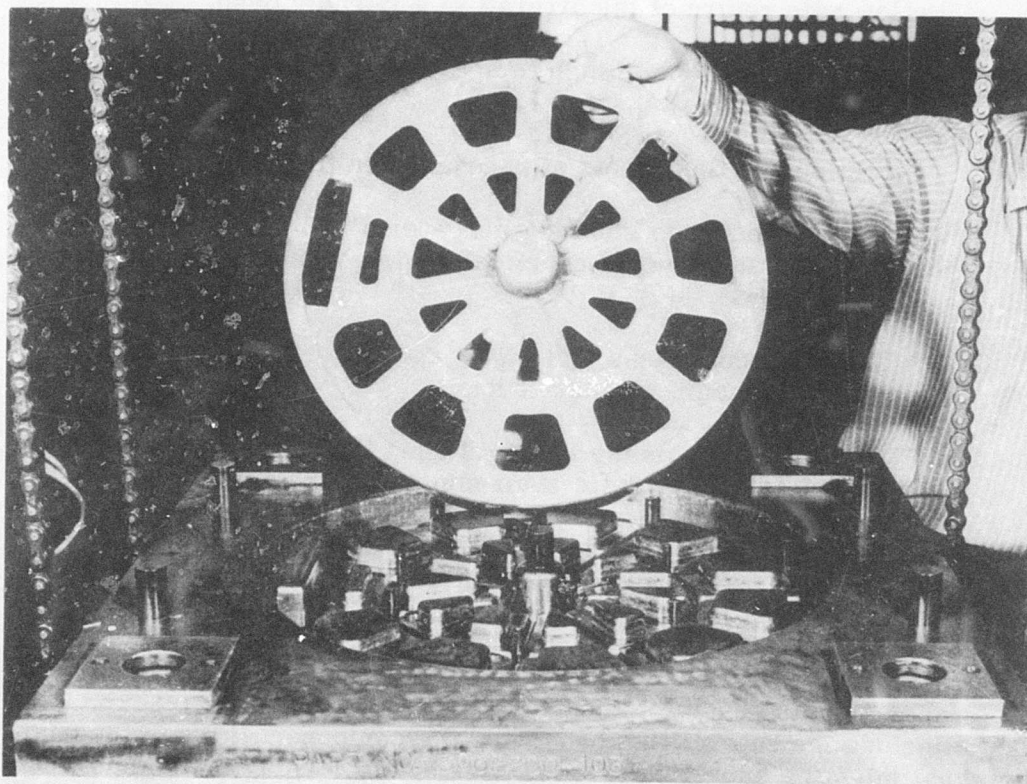


Figure 34. Completed Quadrant Sheave Removed From Tool.

TESTING AND EVALUATION

TEST AND EVALUATION CRITERIA

Although the design allowables and approaches developed are considered to be predictable and reliable design criteria for producing structurally adequate ballistic-damage-tolerant components, testing and evaluation of specific design conditions are considered necessary. The primary purpose of the test program is to evaluate the response of the redesigned components to the various structural, ballistic threat, and environmental conditions that are typical to the service aircraft or vehicle. Specific consideration must be given to the following:

1. Cyclic fatigue at operational loads both before and after ballistic damage. Post-damage loading should be based on the mission profile, the threat to be encountered and at what time frame in the profile, and the time and extent of loading after damage to allow safe return of the aircraft to a friendly base.
2. Thermal conditions of high temperature, low temperature, and thermal shock.
3. Vibration and the effects of resonance on the component.
4. Climatic conditions including long-term high humidity, salt spray, and any unusual chemical environments (fuel, oil, cleaning compounds, etc).
5. Any loading conditions that might cause torque loads, with high transverse shear, or impact loads.
6. Fire resistance, or the length of time the component can survive in an oxidizing-pyrolytic environment before failure.

Some of the climatic conditions to which the components have been exposed with negligible effects include ultraviolet or solar radiation, sand and dust, and fungus.

The component testing should be conducted using a test fixture that simulates, as nearly as possible, the aircraft installation. The test fixture should include the capabilities of moving the component through the positions that might be experienced in service and of loading the components both statically and cyclically in the extreme positions. Because of the cyclic loading requirements and the need to provide for ballistic impact

without damage to the fixture, it may not be possible to use a single test fixture for static, cyclic, and/or ballistic impact testing.

For the ballistic threat evaluation, multiple hits should be considered; however, this is a function of component size and ballistic environment. The probability of a multiple hit in a small area (10 to 30 in.²) is very small; however, as the projected surface area of the component is increased, the probability of a multiple hit is increased significantly. The position of the component in the vehicle must also be considered to determine the most likely path of the projectile and the limits of that path.

Adequate verification of the structural integrity of short-fiber moldable composite components is accomplished by a comprehensive test and evaluation program that is structured to include these baseline considerations. The testing effort and the test results for the three redesigned flight control components² are described in detail in this section of the design guide.

DESCRIPTION OF THE TEST PROGRAM

The functional reliability of the three redesigned flight control components was evaluated by subjecting the molded components to various environmental (climatic and temperature extremes), ballistic impact, and structural tests. Eight sets of components were tested. The tests were categorized as shown in Figure 35, which is a sequential presentation of the test program. Within each category, the tests were conducted sequentially on each of the components. One each of the three flight control components was subjected to each category of testing except in the Category 1 tests, where two sets of components were used. One set of components was subjected to caliber .30 ballistic impacts, and the other set was subjected to caliber .50 ballistic impacts.

The test program was planned so that each component was subjected to the maximum design-proof load (MDPL) for a 1-minute duration to ensure structural capability before any subsequent test was conducted and after each individual test to verify that the test condition did not degrade the structural capability below the design load level.

Before initiation of the actual test program, the components were subjected to two preliminary-type tests: (1) fit checks and (2) preliminary proof loading.

TEST FIXTURES AND EQUIPMENT

The structural tests were conducted using two basic test fixtures. The high-cyclic loading fatigue tests were conducted using a Sonntag SF-10-U fatigue test machine for the cyclic load application. Three interrelated test fixtures were used with this equipment as illustrated in Figure 36. All other structural tests were conducted in the universal ballistic test fixture. This test fixture was used to apply the MDPL, the preload prior to ballistic impact, the cyclic load after impact and during crack propagation, and the failure load. The loads were supplied through a hydraulic cylinder that applies either static or operational cyclic loads to each of the components. Figure 37 shows the components mounted in the test fixture.

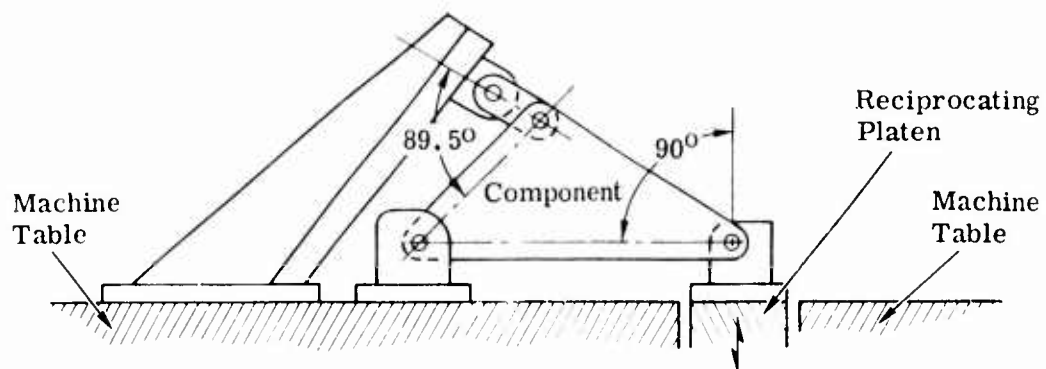
The vibration tests were conducted on an MP Electronics Model C210 vibrator. The components were rigged through a gimbal device to a base plate on the equipment to simulate aircraft installation. The gimbal was then oriented so that the components could be vibrated in the three axes as required. These fixtures are described in a subsequent paragraph under "Category 4 Tests."

COMPONENT FIT CHECKS

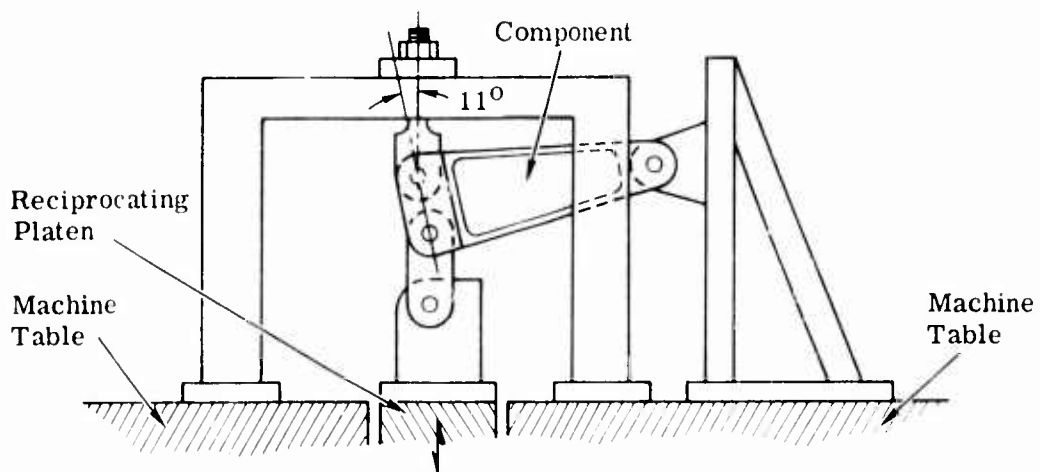
Before initiation of the actual test program, the molded components were subjected to fit check tests on the respective flight control systems. Figure 38 shows a comparison of the three ballistic-damage-tolerant components with their metal counterparts.

Idler Bell Crank

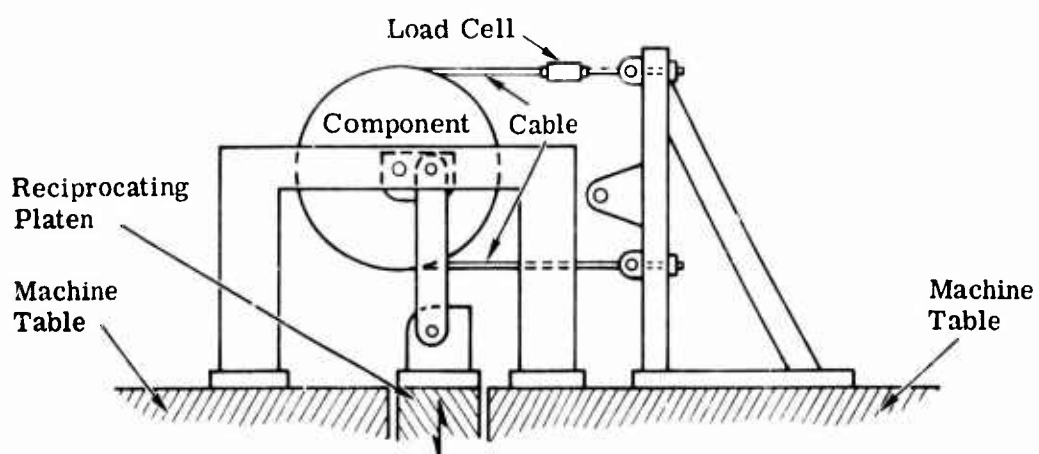
Two idler bell cranks were installed in a CH-47C training unit. The components fit well with the mating attachment points and linkages. However, when the control system was worked to the limits of its travel, the lower edge of the H-beam section of the component was found to interfere slightly with the adjacent metal structure. A 0.37-inch-deep relief area was cut into the 0.150-inch legs of the H-section of the components to correct this condition. This modification was incorporated in the design of all components to be evaluated. Figure 39 shows two idler bell cranks installed in the CH-47C training unit.



A. Test Setup for Aft Bell Crank

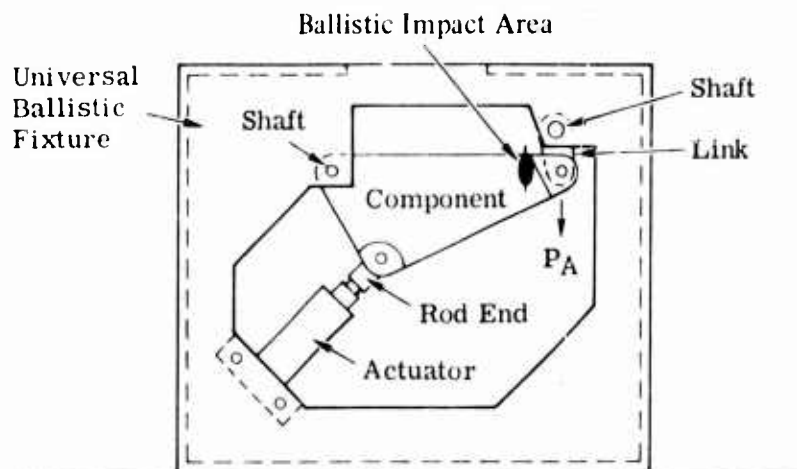


B. Test Setup for Idler Bell Crank

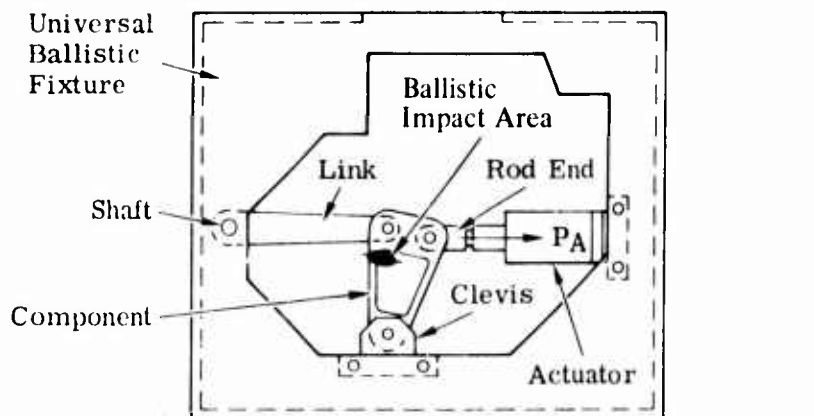


C. Test Setup for Quadrant Assembly

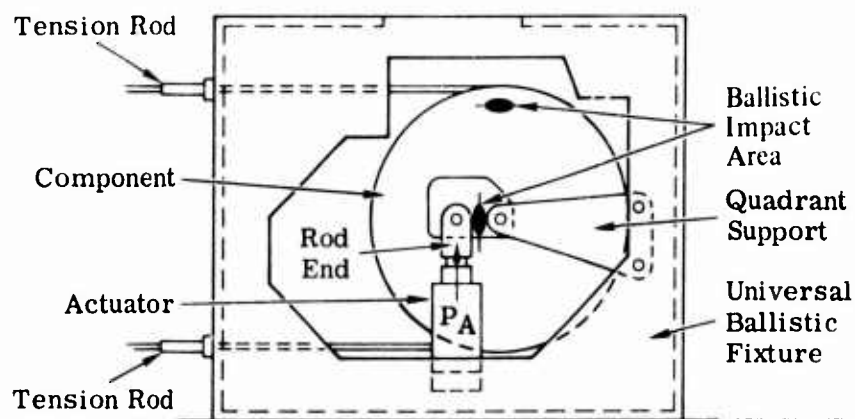
Figure 36. Fatigue Test Fixtures and Component Installations.



A. Aft Bell Crank

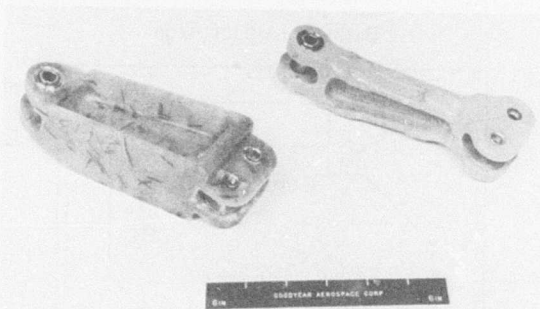


B. Idler Bell Crank



C. Quadrant Assembly

Figure 37. Universal Ballistic Test Fixture and Component Installations.



A. Idler Bell Cranks



B. Aft Bell Cranks



C. Quadrant Assemblies

Figure 38. Comparison of Ballistic-Damage-Tolerant Flight Control Components With Their Metal Counterparts.

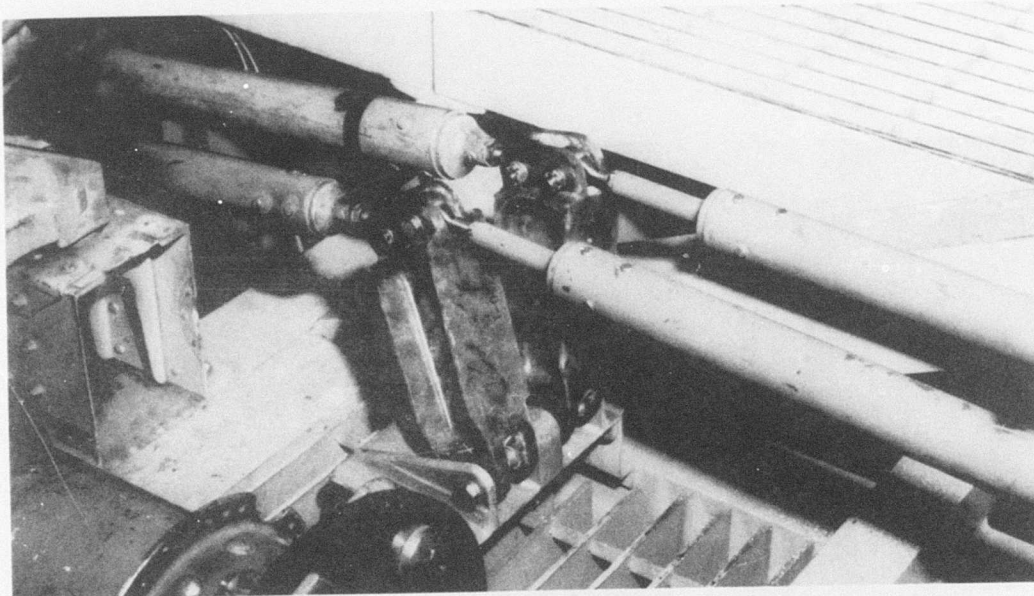


Figure 39. Two Molded Idler Bell Cranks Installed in CH-47C Training Unit.

Aft Bell Crank

One of the aft bell cranks was installed in a CH-47C training unit. The component fit well with the mating linkages and attachment points. However, when the control system was worked to the limits of its travel, the bell crank rubbed against a portion of the metal structure. The metal bell crank showed a similar interference, and a field-fix was made on this component. A 4-inch-long, 0.12-inch-deep slot along the interfering edge was incorporated in the design of all components to correct the condition. Figure 40 shows the aft bell crank installed in the CH-47C training unit.

Quadrant Assembly

One of the quadrant assemblies was installed in the UH-1D aircraft. The fit with mating parts and linkages was good. Figure 41 shows the quadrant assembly installed in the UH-1D aircraft.

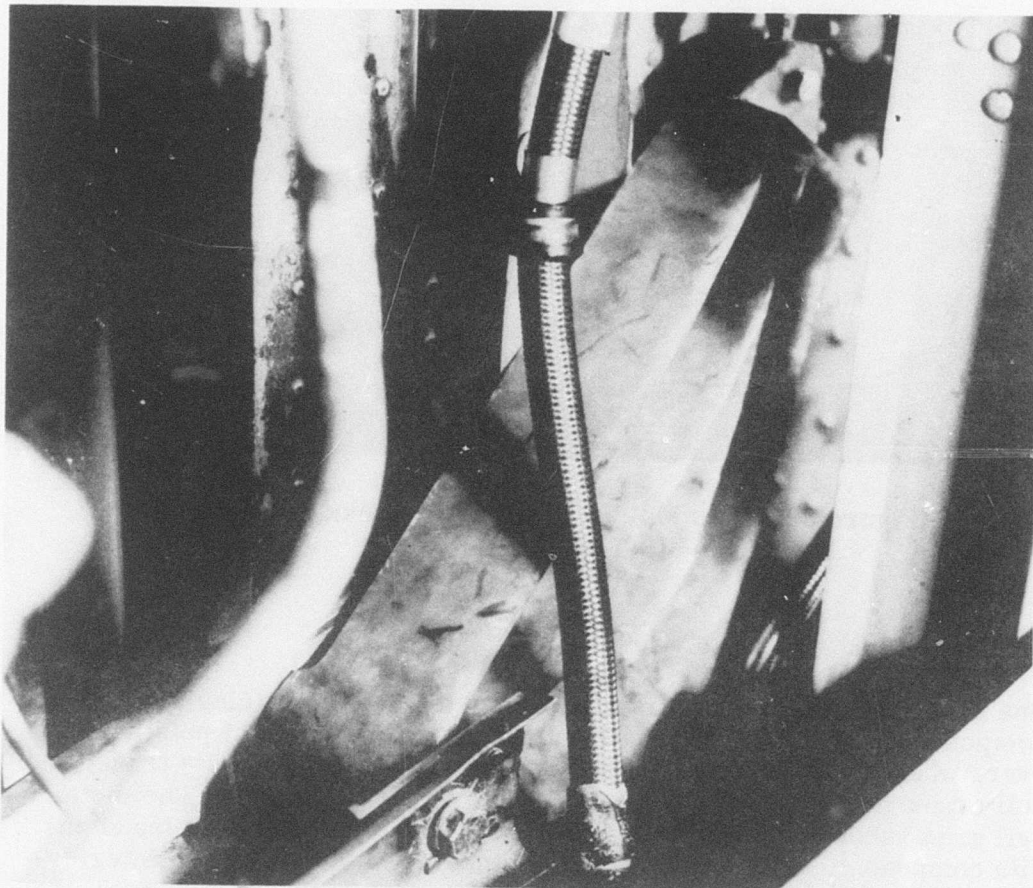


Figure 40. Molded Aft Bell Crank Installed in CH-47C Training Unit.

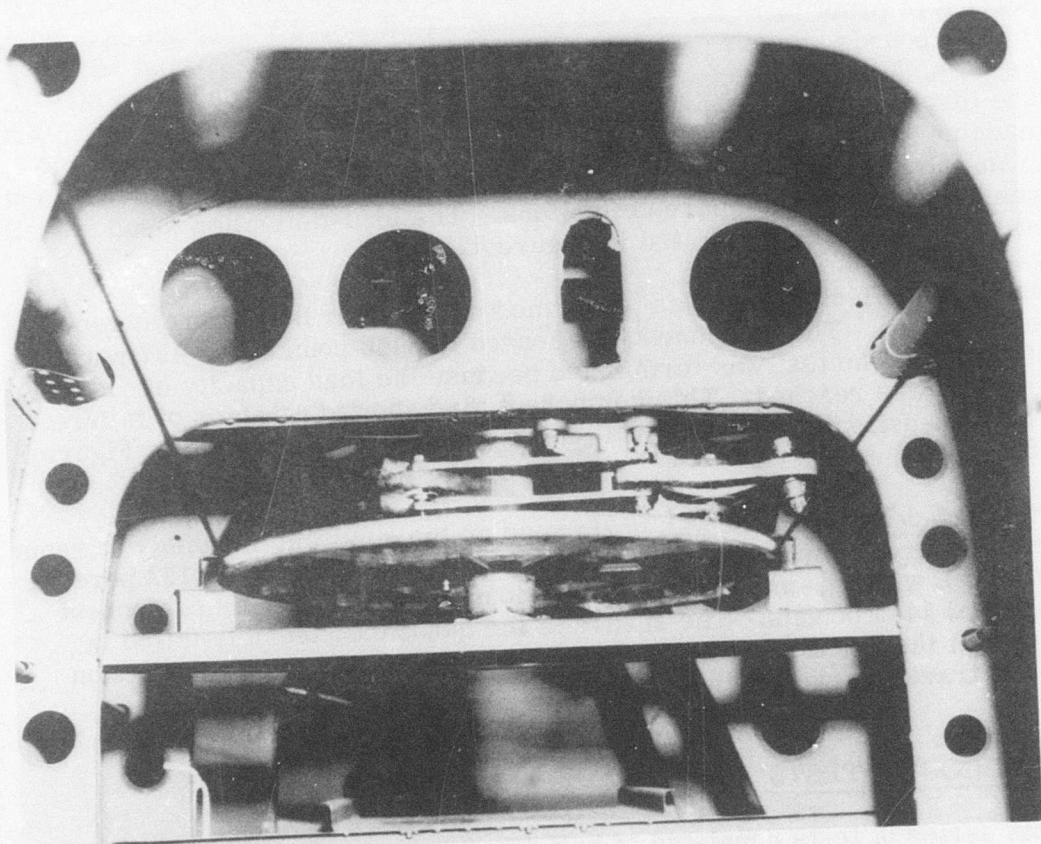


Figure 41. Molded Quadrant Assembly Installed in UH-1D Aircraft.

PRELIMINARY PROOF LOADING

Preliminary proof load tests were conducted on each of the three molded flight control system components to verify their structural integrity.

Three load-deflection tests were performed on the aft bell crank at room temperature. Test No. 1 loaded the component to 2315 pounds, or 112 percent of MDPL with a 2-minute hold at 2060 pounds (MDPL). After test No. 1, the component was cycled at the operational load of 310 pounds (15 percent of proof load) for 14,000 cycles. Test No. 2 loaded the specimen to 3582 pounds, or 173 percent of MDPL with a 1-minute hold at MDPL. Test No. 3 loaded the specimen to 4470 pounds, or 216 percent of MDPL. The test was terminated because of travel restrictions on the Sonntag test machine. The component exhibited no sign of failure after this test program; however, the attachment bolts were deformed. A metal component was also tested to compare deflections. The load-deflection (head travel) curve for each test is plotted in Figure 42.

One load-deflection test was performed on the idler bell crank at room temperature. The component was loaded to 5440 pounds, or 197 percent of MDPL. The test was terminated because the load capacity of the test machine was reached. This component also showed no signs of failure. The load-deflection (head travel) curve for this test is plotted in Figure 43.

One load-deflection test was performed on the quadrant assembly at room temperature. The component was loaded to 1443 pounds, or 162 percent of MDPL with a 1-minute hold at 883 pounds (MDPL). This component failed at 1443 pounds. The sheave of the quadrant assembly failed in shear at the junction of the crank and the sheave. The load-deflection (head travel) curve for this test is plotted in Figure 44.

CATEGORY 1 TESTS

This series of tests consisted of half-life fatigue tests, caliber .30 and caliber .50 ballistic impact tests at 160°F, operational load tests at 2000 cycles, and failure load tests. Two sets of components were tested in Category 1.

Half-Life Fatigue Tests

During half-life fatigue testing, several problems were experienced in the

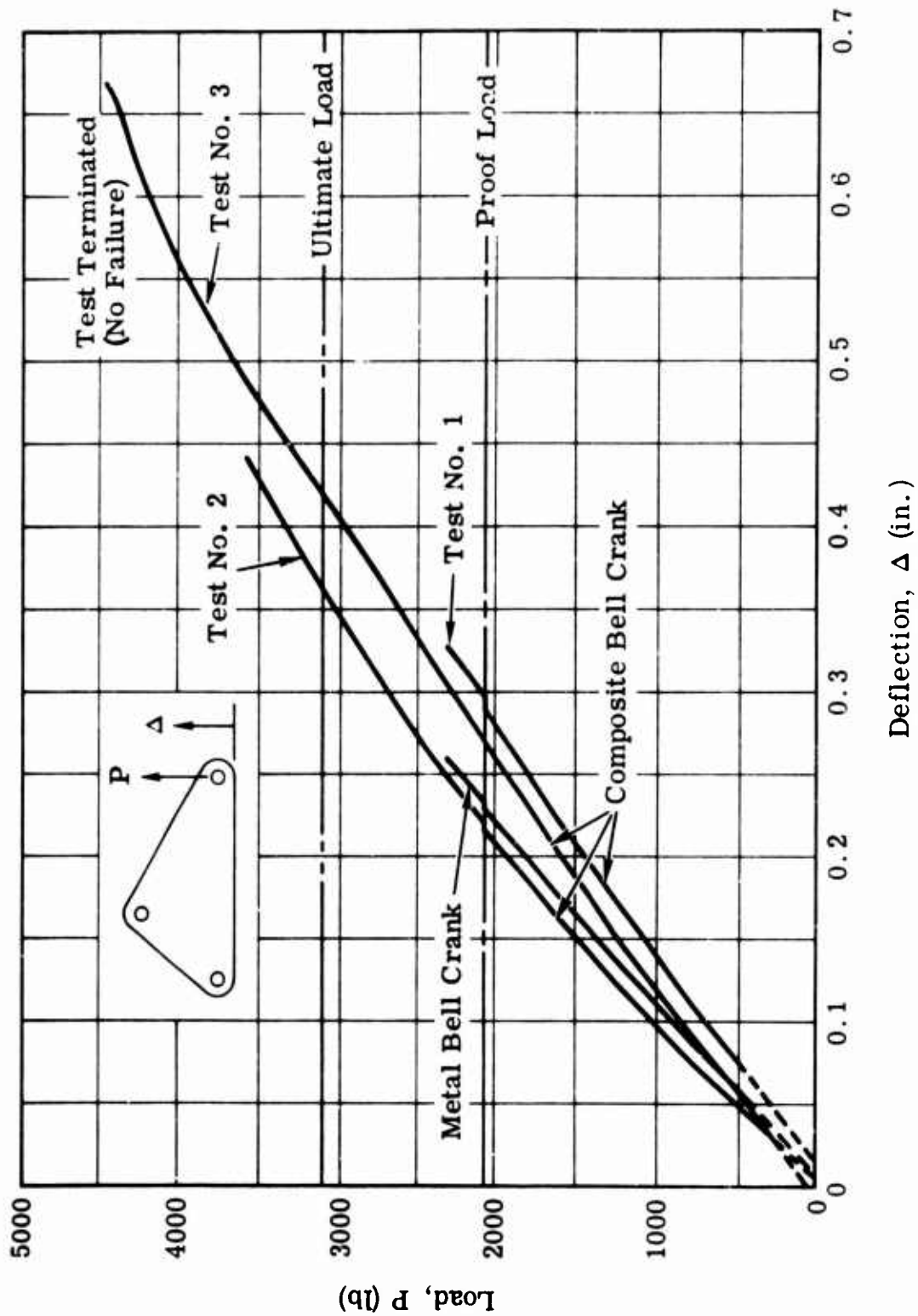


Figure 42. Load-Deflection Curves, Proof and Ultimate Loading - Aft Bell Crank.

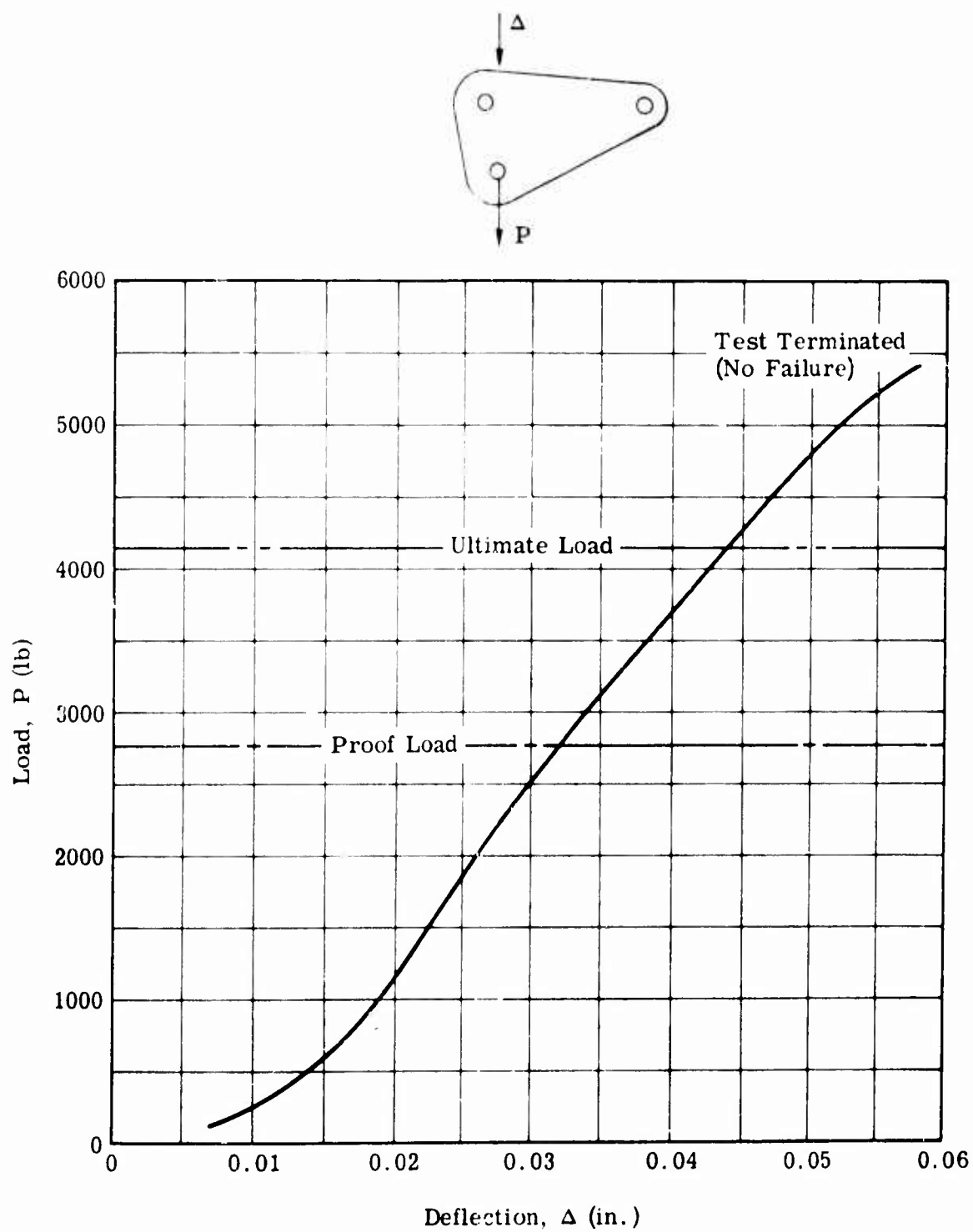


Figure 43. Load-Deflection Curve, Proof and Ultimate Loading - Idler Bell Crank.

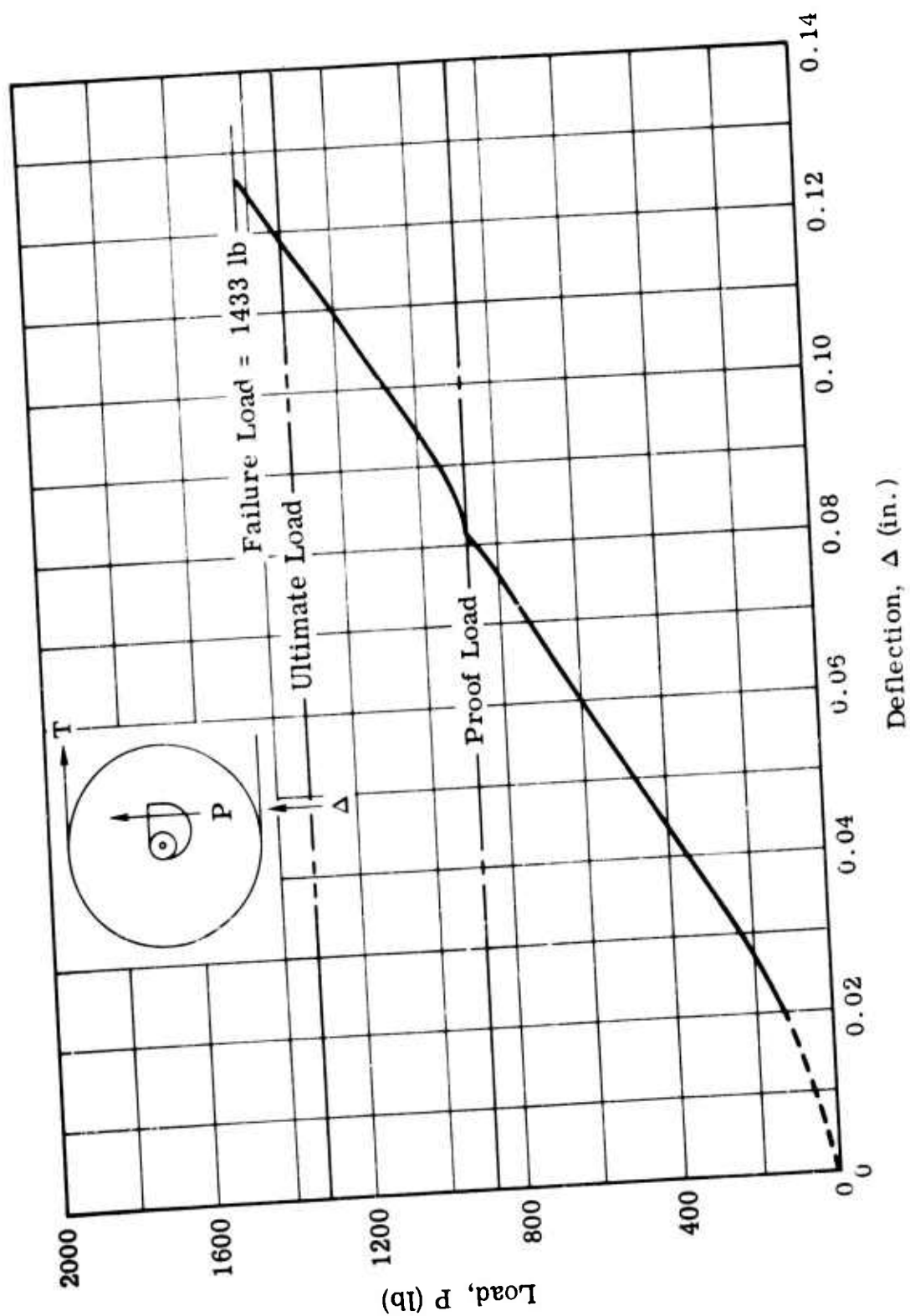


Figure 44. Load-Deflection Curve, Proof and Ultimate Loading - Quadrant Assembly.

areas where the metal parts were bonded to the molded components. During the course of the tests, the following incidences occurred:

1. The bushings bonded into the primary load lugs became unbonded and loose.
2. One of the 114C2020-533 metal bushings failed in shear at the intersection of the flange and the body of the bushing.
3. The bolt through the pivot bearing failed in shear.
4. One of the upper lug attachment bolts failed in shear.

These problems were found to be associated with the adhesive used to bond the metal bushings into the composite molding. Thus Hysol EA-901B was selected as the most satisfactory adhesive for bonding.

Other observations regarding half-life fatigue testing problems indicated an excessive amount of play between the link fitting and the bushings. The bushings were repositioned to obtain a close fit (0.002 to 0.003 inch) between the link fitting and the bushings. EA-901B adhesive was used for bonding the bushings. After incorporation of these modifications, the components were fatigue tested through 5×10^6 cycles without any further problems.

Maximum Design-Proof Loads

The maximum design-proof load (MDPL) was applied to each component before and after fatigue load cycling. During the first MDPL of the idler bell crank, some minor cracking was audible, but no visual change was noted. There was no change in the load application or rate of deflection, and there were no visible cracks. In subsequent MDPL testing of the components, no cracking of the idler bell crank or any other component was heard or seen. Figure 45 shows the fatigue test setup for the quadrant assembly.

Ballistic Impact Tests

The ballistic impact tests were conducted in a ballistic test range facility shown schematically in Figure 46. A universal ballistic test fixture was mounted on a positioning stand to provide up-and-down and right-and-left movement for proper location of the component during impact.

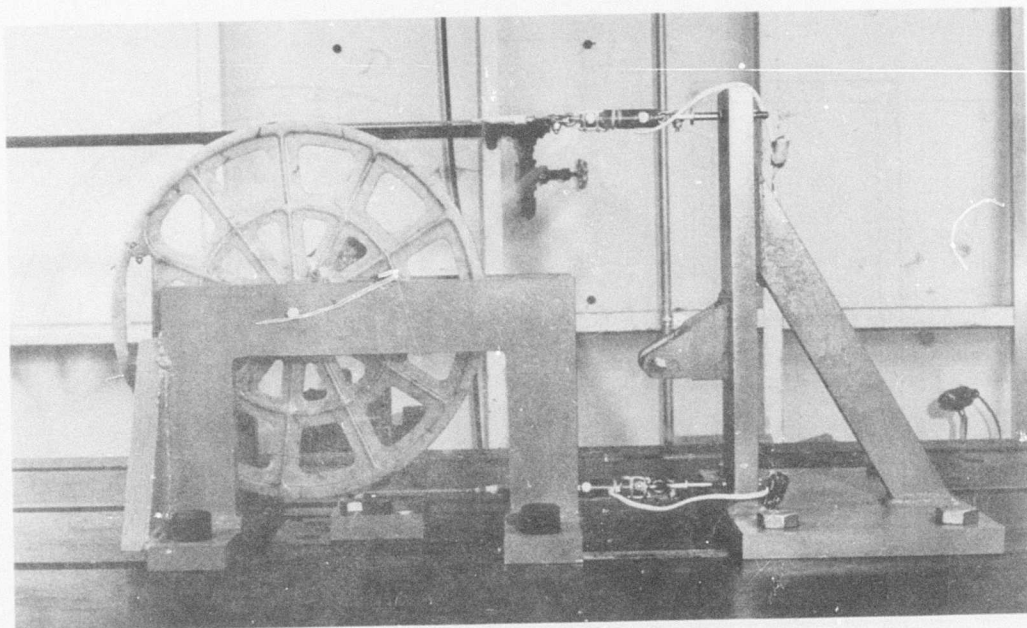


Figure 45. Fatigue Test Setup for Quadrant Assembly.

Two types of projectiles were used to perform the ballistic impact tests: (1) fully tumbled caliber .30 ball M2 projectiles and (2) untumbled caliber .50 AP M2 projectiles. The caliber .30 projectiles were fired from an M-98 Mauser gun barrel 30 inches long and 1.125 inches (minimum) in diameter with a caliber .30 smooth bore (0.306-inch-diameter). The gun barrel was modified by cutting the muzzle at 30 degrees at the center line of the bore. This modification provided the tumbling action required for the caliber .30 projectiles. The caliber .50 projectiles were fired from a standard caliber .50 aircraft machine-gun barrel.

The components were preheated to 160°F and allowed to stabilize before testing. The component to be tested was mounted in the test fixture. (A typical component installation is shown in Figure 47.) Component temperature was monitored at all times (see Figure 48). The prescribed preload, which is equivalent to the operational cyclic load given in Figure 12, was applied to the mounted component for 3 to 5 minutes prior to ballistic impact. High-intensity lights were used during high-speed motion-picture filming of the ballistic impact tests. Projectile firing was initiated when the component reached a minimum temperature of 160°F. It was found that the high-intensity lights overheated the components; therefore, the timing of the motion-picture filming sequences with the projectile firing was critical.

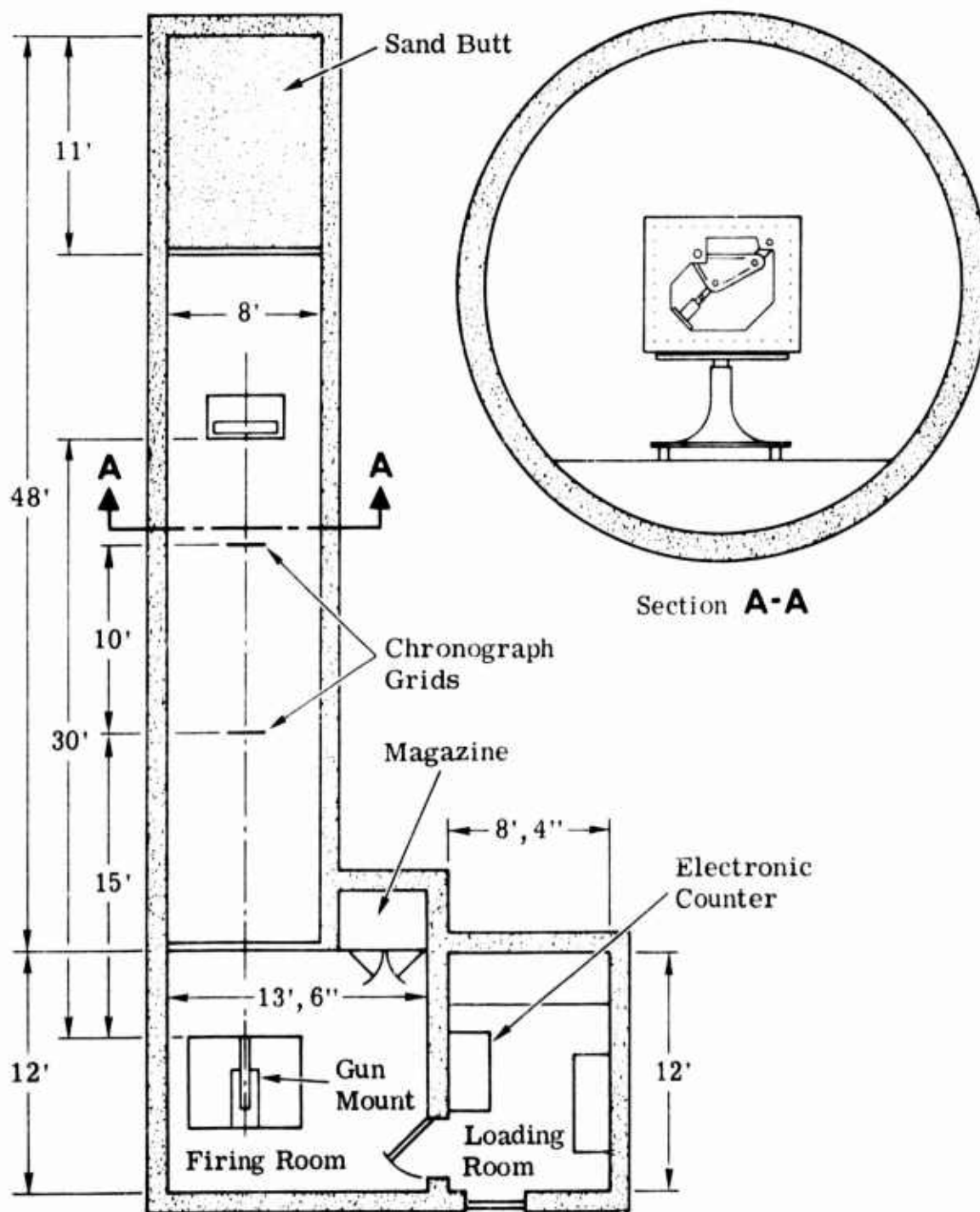


Figure 46. Schematic of Ballistic Test Range Facility.

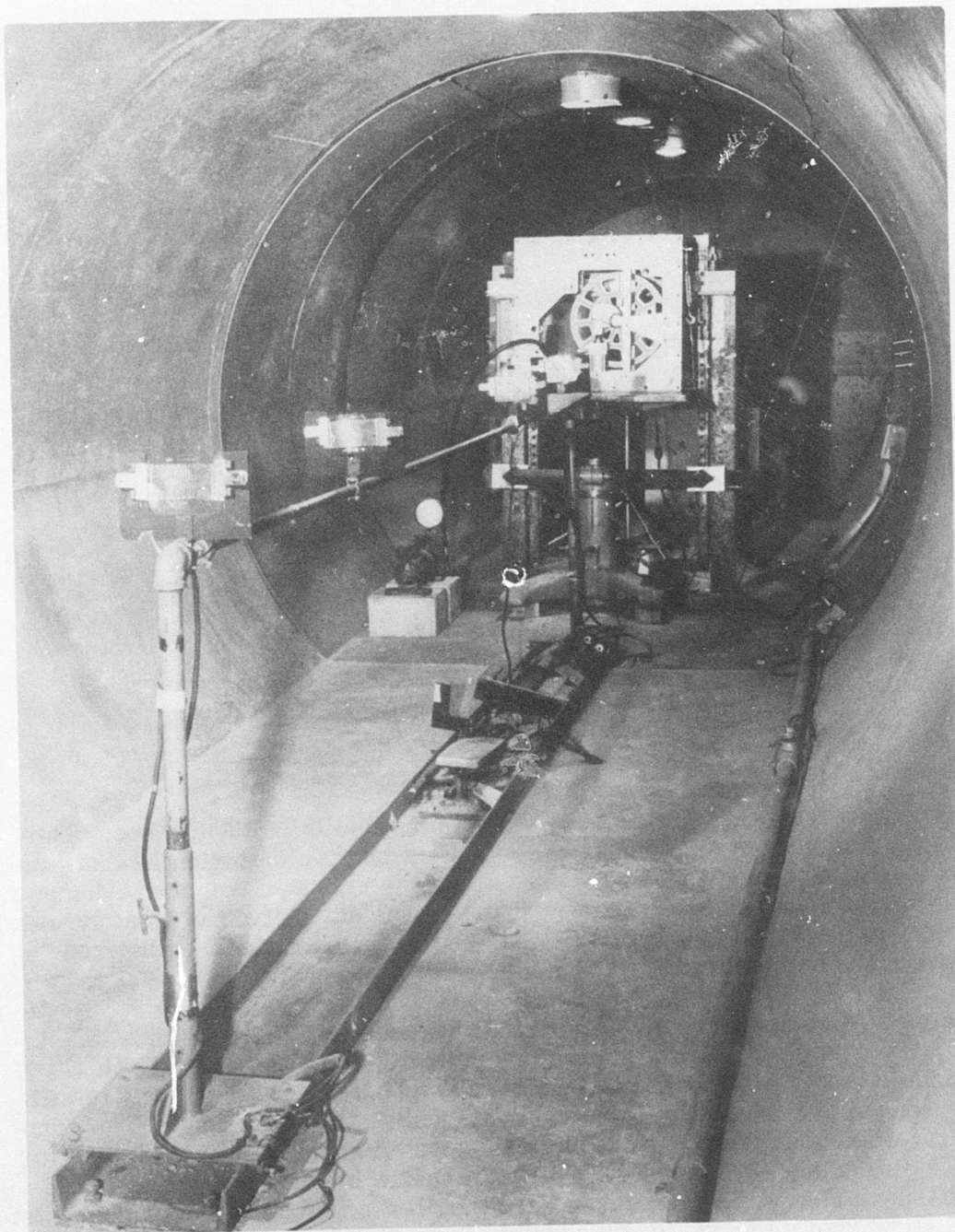


Figure 47. Quadrant Assembly Mounted in the Test Fixture at the Ballistic Test Range.

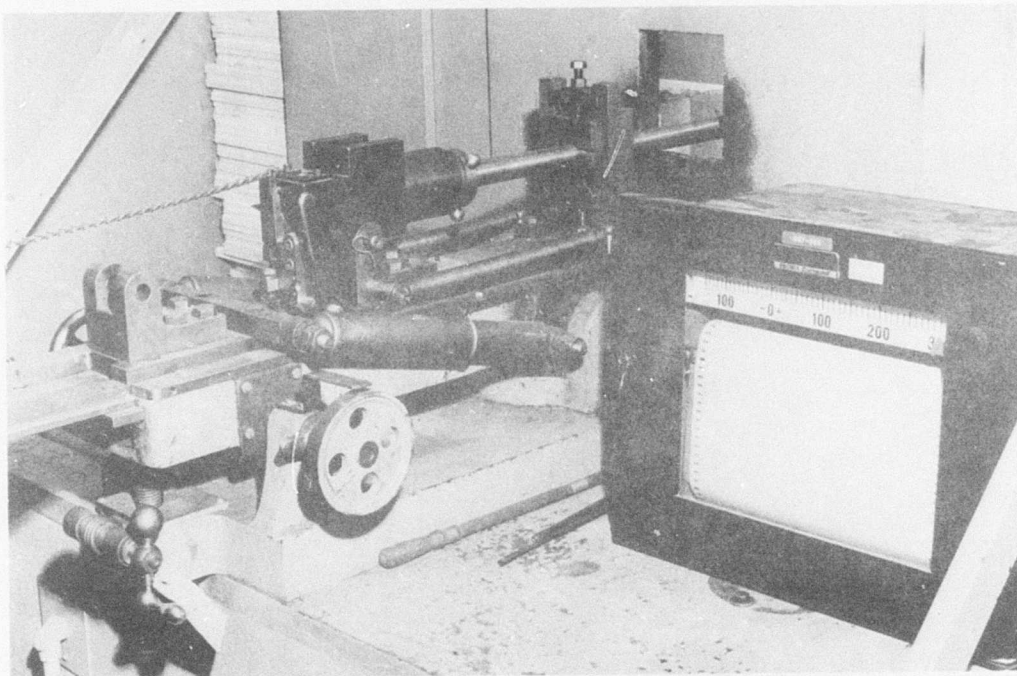
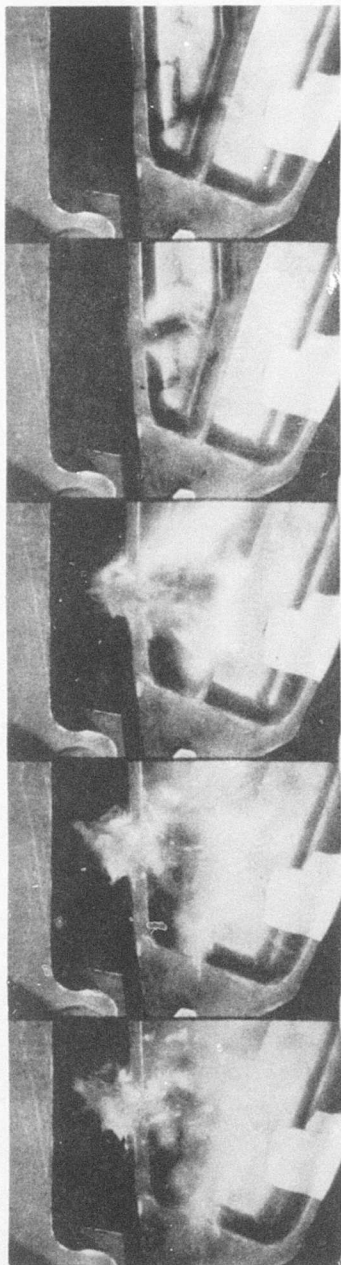


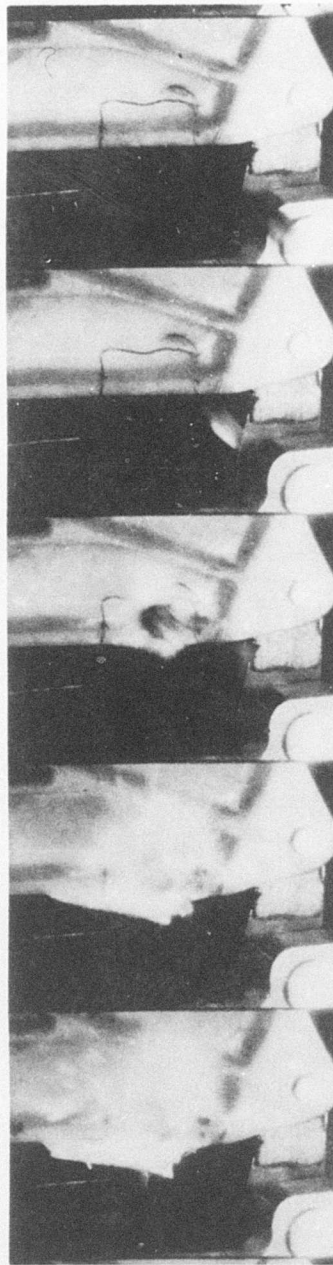
Figure 48. Temperature Recorder and Gun Mount
Used in Ballistic Testing.

The components were impacted at a nominal velocity of 1500 ft/sec. This velocity was chosen as a result of previous work, which indicated that projectile velocity does not significantly affect the extent of composite damage and that the residual load capacity of the composite increases directly with projectile velocity. The minimum velocity at which reliably positioned impacts can be achieved is 1500 ft/sec.

The molded components were impacted with caliber .30 or caliber .50 projectiles at a minimum temperature of 160°F and at a nominal velocity of 1500 ft/sec. After ballistic impact, the mounted component was tested functionally for the ability to move freely while still under load. The component was then removed from the loading fixture and inspected closely for extent of damage. Figures 49, 50, and 51 show several sequences of the high-speed motion pictures taken during ballistic impact of the components. Figure 52 shows the quadrant assembly immediately after caliber .30 impact under load.



A. Caliber .30 Impact

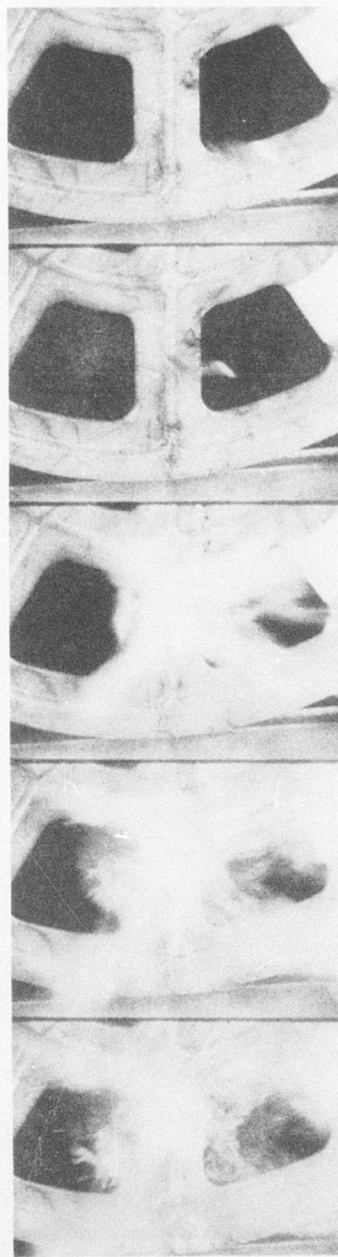


B. Caliber .50 Impact

Figure 49. High-Speed Motion-Picture Sequences, Caliber .30 and Caliber .50 Ballistic Impacts - Aft Bell Crank.

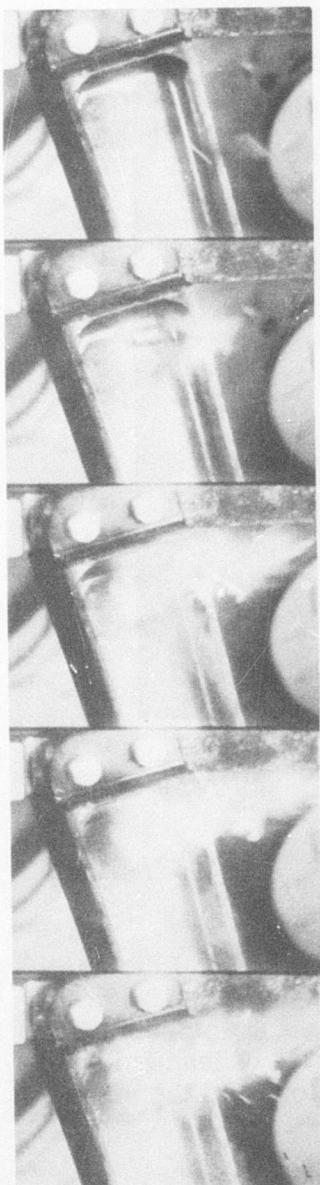


A. Impact in Crank Area

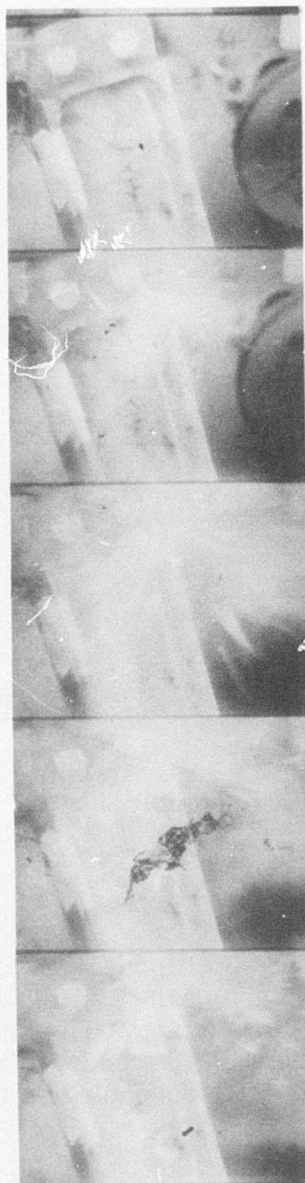


B. Impact in Sheave Spoke

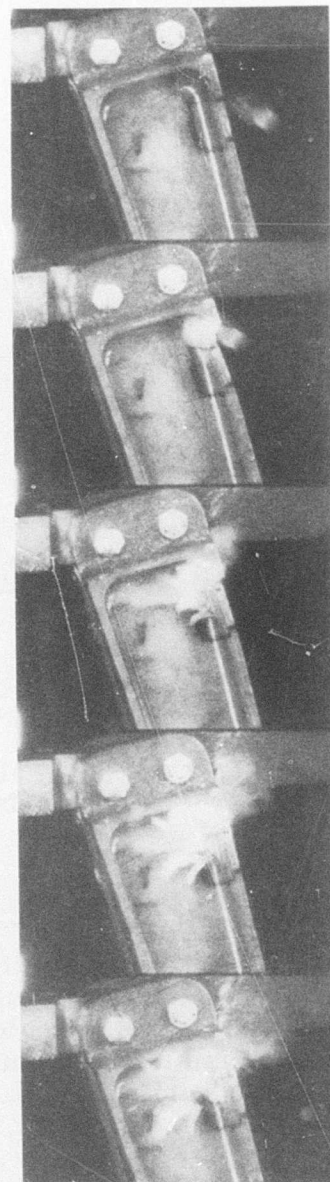
Figure 50. High-Speed Motion-Picture Sequences, Caliber .30
Ballistic Impacts - Quadrant Assembly.



A. Caliber .30 Impact



B. Caliber .30 Impact
(High Hit)



C. Caliber .50 Impact

Figure 51. High-Speed Motion-Picture Sequences, Caliber .30 and Caliber .50 Ballistic Impacts - Idler Bell Crank.

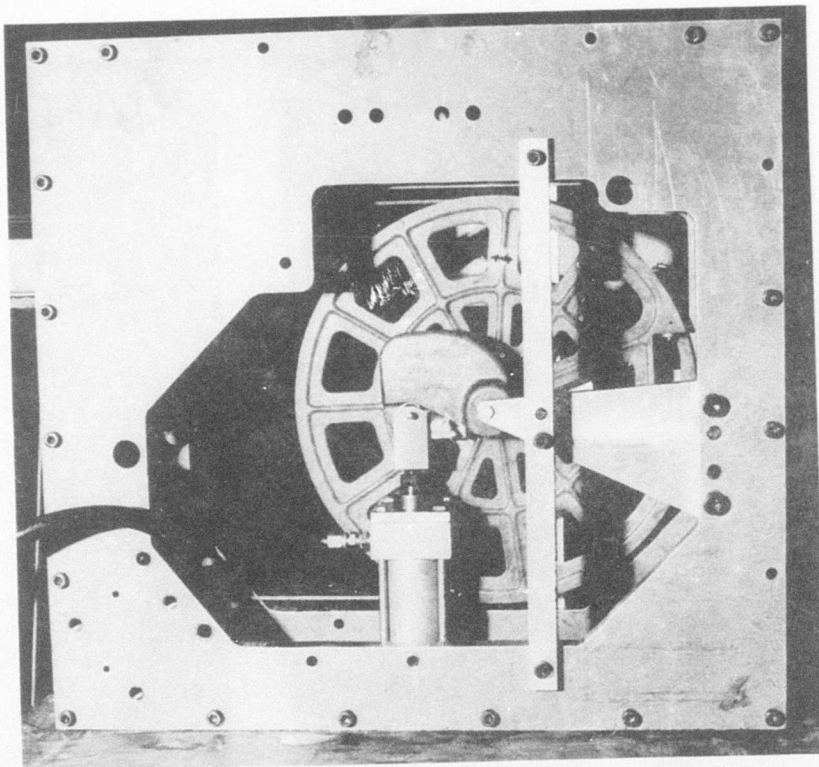


Figure 52. Caliber .30 Ballistic Impact Under Load - Quadrant Assembly.

Operational Cyclic Loading Tests

All component cycling after ballistic impact was accomplished in the universal ballistic test fixture. Each of the six impacted components was subjected to 2000 operational load cycles. The component was held under the required load for a minimum of 5 seconds. The rate of load build-up and decay varied from part to part, depending on the load and the size of the hydraulic cylinder.

Failure Load Tests

At the conclusion of the operational load cycling, the load was increased in the direction that applied maximum stress in the ballistically damaged area until failure of the component was achieved. The load applied at failure was recorded.

Summary

The Category 1 test data for the three components impacted with fully tumbled caliber .30 ball M2 projectiles and the six components impacted with untumbled caliber .50 AP M2 projectiles are Confidential. The classified data are presented in Volume II of this report.

CATEGORY 2 TESTS

Category 2 testing consisted of an environmental test series. High-temperature, temperature shock, low-temperature, and high-altitude (at low temperature) tests were conducted in accordance with the requirements of MIL-E-527C.⁷ The components were subjected to an MDPL test prior to the beginning of the test series. The aft bell crank and the quadrant assembly sustained the MDPL with no apparent change in condition. The idler bell crank exhibited a slight delamination around one of the linkage bushings. However, this delamination did not adversely affect the structural capability of the component. The environmental tests were conducted in the sequence shown in Table XVI.

TABLE XVI. SEQUENCE OF CATEGORY 2 TESTS		
Test No.	Test Description	Specification
1	High-Temperature Tests	MIL-E-5272C, para 4.1.2, procedure II
2	Temperature Shock Tests	MIL-E-5272C, para 4.3.1, procedure I
3	Low-Temperature Tests	MIL-E-5272C, para 4.2.2, procedure II
4	Altitude Tests	MIL-E-5272C, para 4.5.6, procedure VI, cond C

High-Temperature Tests

The components for high-temperature testing were conditioned for 48 hours at 160°F. After the 48-hour preconditioning period, the component to be tested was placed in the universal ballistic test fixture, and

the heated cover was attached. The component was thermally stabilized at 160°F, and the MDPL test was conducted. The component was allowed to cool to room temperature, and the MDPL test was repeated.

All components sustained the high-temperature test and the MDPL tests at 160°F and at ambient temperature without any significant changes in condition. A slight delamination occurred in the quadrant assembly at the castellations around the hub. However, this delamination did not adversely affect the structural capability of the component.

Temperature Shock Tests

The thermal shock tests were conducted by alternating the components between a +185°F chamber and a -40°F chamber for a 4-hour duration in each chamber until four cycles of tests were completed. The MDPL test was conducted at the conclusion of this test sequence, with the components stabilized at ambient temperature. There was no apparent change in the appearance or the structural condition of the components as a result of these tests.

Low-Temperature Tests

The low-temperature tests were conducted by exposing the components to -80°F for 72 hours and then raising the temperature to -65°F for an additional 24 hours. The MDPL test was conducted at -65°F. The components were allowed to stabilize at ambient temperature, and the MDPL test was repeated. None of the components showed any change in appearance or structural condition at the conclusion of these tests.

Altitude Tests

The altitude tests were conducted by stabilizing the components for 1 hour at -65°F and at a reduced pressure of 3.44 inches of Hg (equivalent to a 50,000-foot altitude). The MDPL test was conducted while the components were under these conditions. The components were allowed to stabilize at ambient temperature, and the MDPL test was repeated. None of the components showed any change in appearance or structural condition after these tests.

Summary

The Category 2 test results are summarized in Table XVII.

TABLE XVII. SUMMARY OF CATEGORY 2 TEST RESULTS

Test	Idler Bell Crank	Aft Bell Crank	Quadrant Assembly
MDPL at Amb Temp	Loaded to +2760 lb. Slight delamination around one of the linkage bushings.	Loaded to -4010 lb at P _B . No change in structural condition.	Loaded to -883 lb at P. No change in structural condition.
High-Temp Exposure 48 hr at 160°F	No change in appearance.	No change in appearance.	No change in appearance.
MDPL at 160°F	Loaded to +2760 lb. No change in structural condition.	Loaded to -4010 lb at P _B . No change in structural condition.	Loaded to -883 lb at P. Slight delamination at hub due to debonding.
MDPL at amb temp	Loaded to +2760 lb. No change in structural condition.	Loaded to -4010 lb at P _B . No change in structural condition.	Loaded to -883 lb at P. No change in structural condition.
Temp Shock Exposure 4 hr at 185°F & 4 hr at -40°F (four cycles)	No change in appearance.	No change in appearance.	No change in appearance.
MDPL at amb temp	Loaded to +2760 lb. No change in structural condition.	Loaded to -4010 lb at P _B . No change in structural condition.	Loaded to -883 lb at P. No change in structural condition.
Low-Temp Exposure 72 hr at -80°F	No change in appearance.	No change in appearance.	No change in appearance.
24 hr at -65°F	No change in appearance.	No change in appearance.	No change in appearance.
MDPL at -65°F	Loaded to +2760 lb. No change in structural condition.	Loaded to -4010 lb at P _B . No change in structural condition.	Loaded to -883 lb at P. No change in structural condition.
MDPL at amb temp	Loaded to +2760 lb. No change in structural condition.	Loaded to -4010 lb at P _B . No change in structural condition.	Loaded to -883 lb at P. No change in structural condition.
High-Alt Exposure (1 hr at -65°F & 3.44 in. Hg)			
MDPL during exposure	Loaded to +2760 lb. No change in structural condition.	Loaded to -4010 lb at P _B . No change in structural condition.	Loaded to -883 lb at P. No change in structural condition.
MDPL at amb temp	Loaded to +2760 lb. No change in structural condition.	Loaded to -4010 lb at P _B . No change in structural condition.	Loaded to -883 lb at P. No change in structural condition.

CATEGORY 3 TESTS

Category 3 testing consisted of an environmental test series including adverse environmental conditions of sand and dust, high humidity, fungus, and salt spray. The environmental tests were conducted in accordance with the requirements of MIL-E-5277C.⁷ At the conclusion of the adverse environment test series, the components were subjected to half-life fatigue tests and failure load tests. The components were subjected to an MDPL test prior to the beginning of the environmental test series. All components sustained the MDPL with no apparent change in condition. Table XVIII summarizes the sequence of testing and the applicable specifications.

TABLE XVIII. SEQUENCE OF CATEGORY 3 TESTS		
Test No.	Test Description	Specification
1	Sand and Dust Tests	MIL-E-5272C, para 4.11.1, procedure I
2	Humidity Tests	MIL-E-5272C, para 4.4.1, procedure I
3	Fungus-Resistance Tests	MIL-E-5272C, para 4.8.1, procedure I
4	Salt Spray Tests	MIL-E-5272C, para 4.6.1, procedure I
5	Half-Life Fatigue Tests	-
6	Failure Load Tests	-

Sand and Dust Tests

The components were subjected to 12 hours of exposure to sand and dust in a test chamber. Examination of the components after exposure to the sand and dust environment showed no indication of degradation. There was a slight retention of sand and dust on the surface of the components. The components sustained the MDPL test after exposure without any apparent change in condition.

Humidity Tests

The humidity tests consisted of exposing the components to temperature-humidity cycles at 160°F and 95 percent relative humidity for 6 to 8 hours and temperature-humidity cycles at ambient temperature (68° to 100°F) and 95 percent relative humidity for 16 to 18 hours. The cycles were repeated until 240 hours of exposure were completed. The components exhibited no apparent degradation as a result of the exposure and sustained the MDPL without structural degradation.

Fungus-Resistance Tests

The fungus-resistance tests were conducted by exposing the components to a collection of four types of fungus culture for a period of 28 days. The temperature during the exposure was 86°F ($\pm 3.6^\circ$) and the relative humidity was 95 percent. The test results showed no evidence of fungus growth on the components. All components sustained the MDPL after exposure without structural degradation.

Salt Spray Tests

The components were subjected to 168 hours of exposure to salt spray. At the conclusion of this exposure, the plastic composites showed no degradation. However, the metal fittings showed evidence of corrosion and rust. This did not affect the installation of the components in the test fixture for the MDPL tests. All components sustained the MDPL without any change in condition.

Half-Life Fatigue Tests

At the conclusion of the above environmental test series, the components were fatigue tested. All tests were completed without incident or failure. The plastic composites and the metal fittings showed no evidence of degradation. The MDPL tests conducted after fatigue testing were sustained by all components without any change in condition.

Failure Load Tests

To evaluate the ultimate or failure load capability, the components were incrementally loaded in the universal ballistic test fixture until failure

occurred. A load-deflection curve was plotted for each component. Figures 53, 54, and 55 show the load-deflection curves for the idler bell crank, the aft bell crank, and the quadrant assembly, respectively. Figure 56 shows the quadrant assembly after the failure load test.

Summary

The Category 3 test results are summarized in Table XIX.

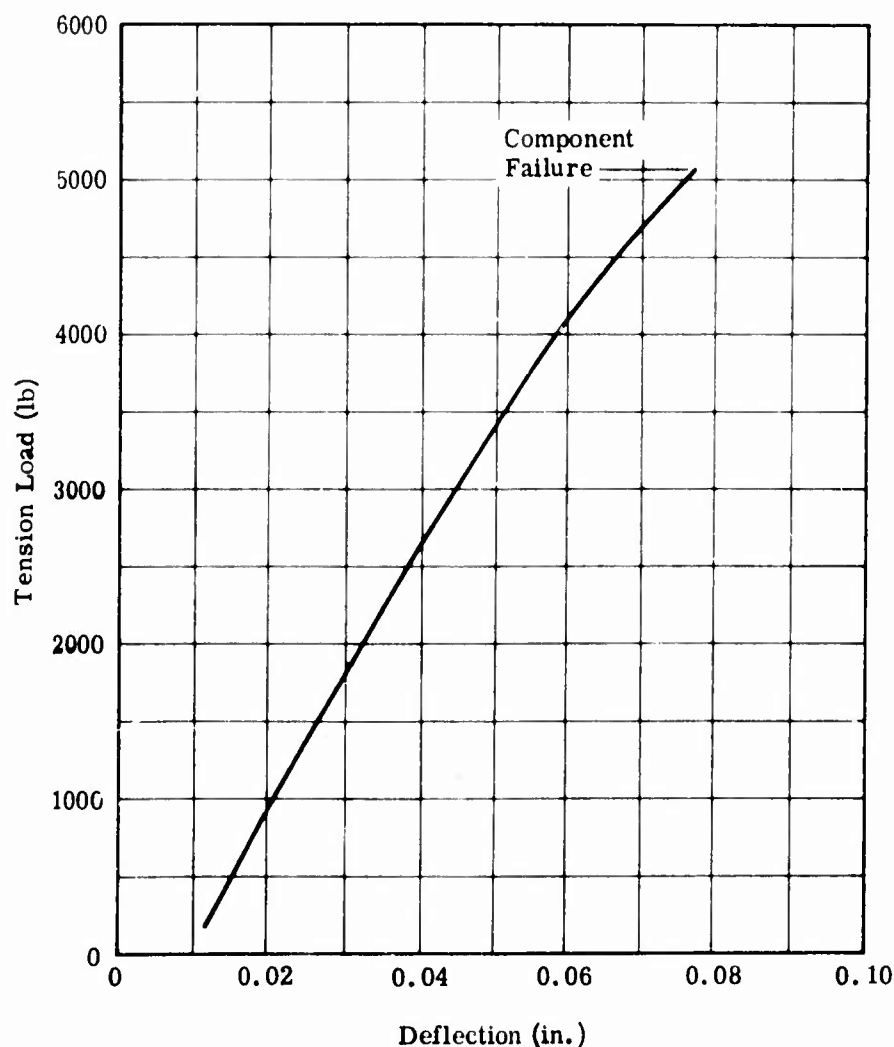


Figure 53. Load-Deflection Curve, Failure Loading - Idler Bell Crank.

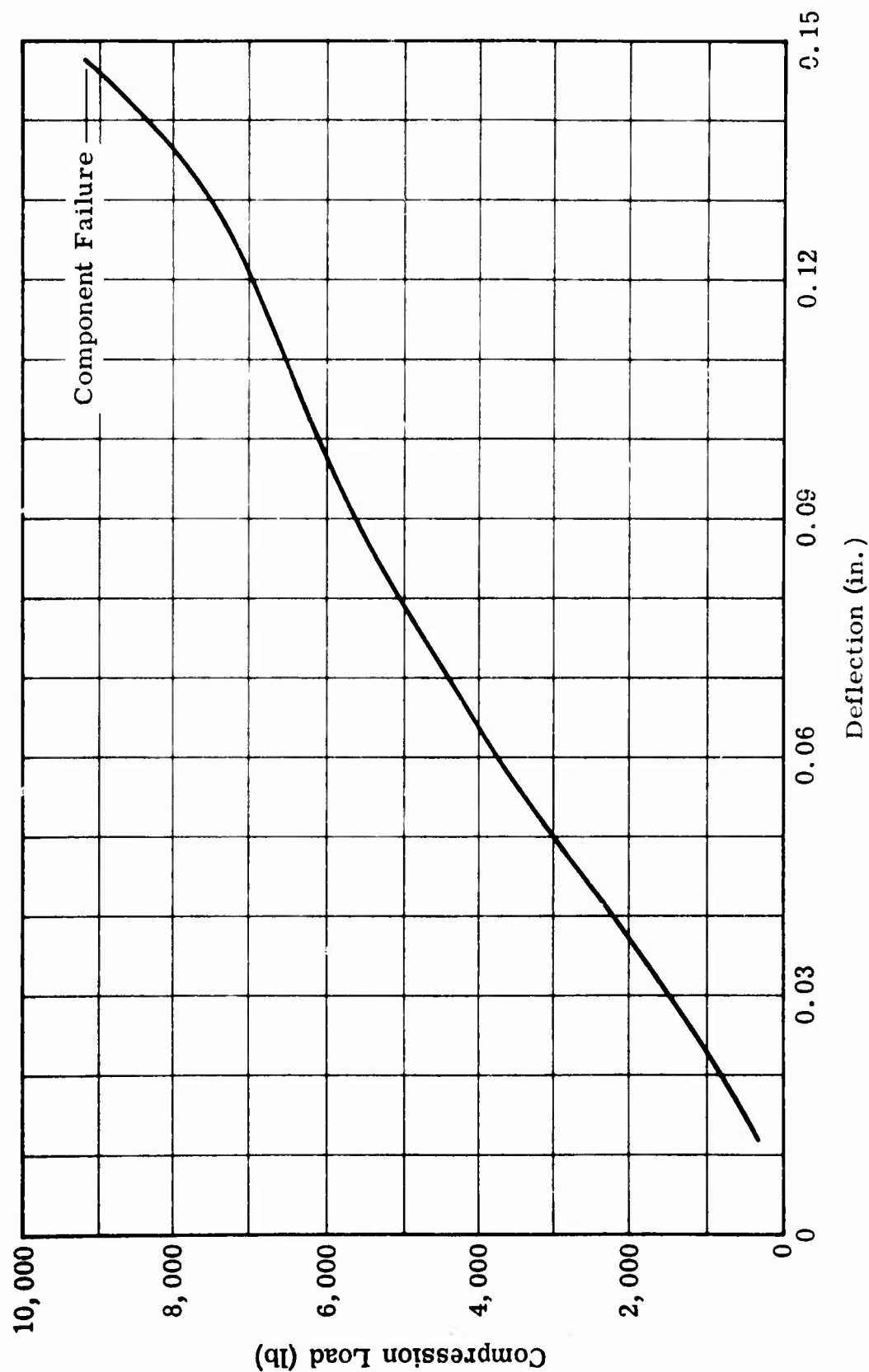


Figure 54. Load-Deflection Curve, Failure Loading - Aft Bell Crank.

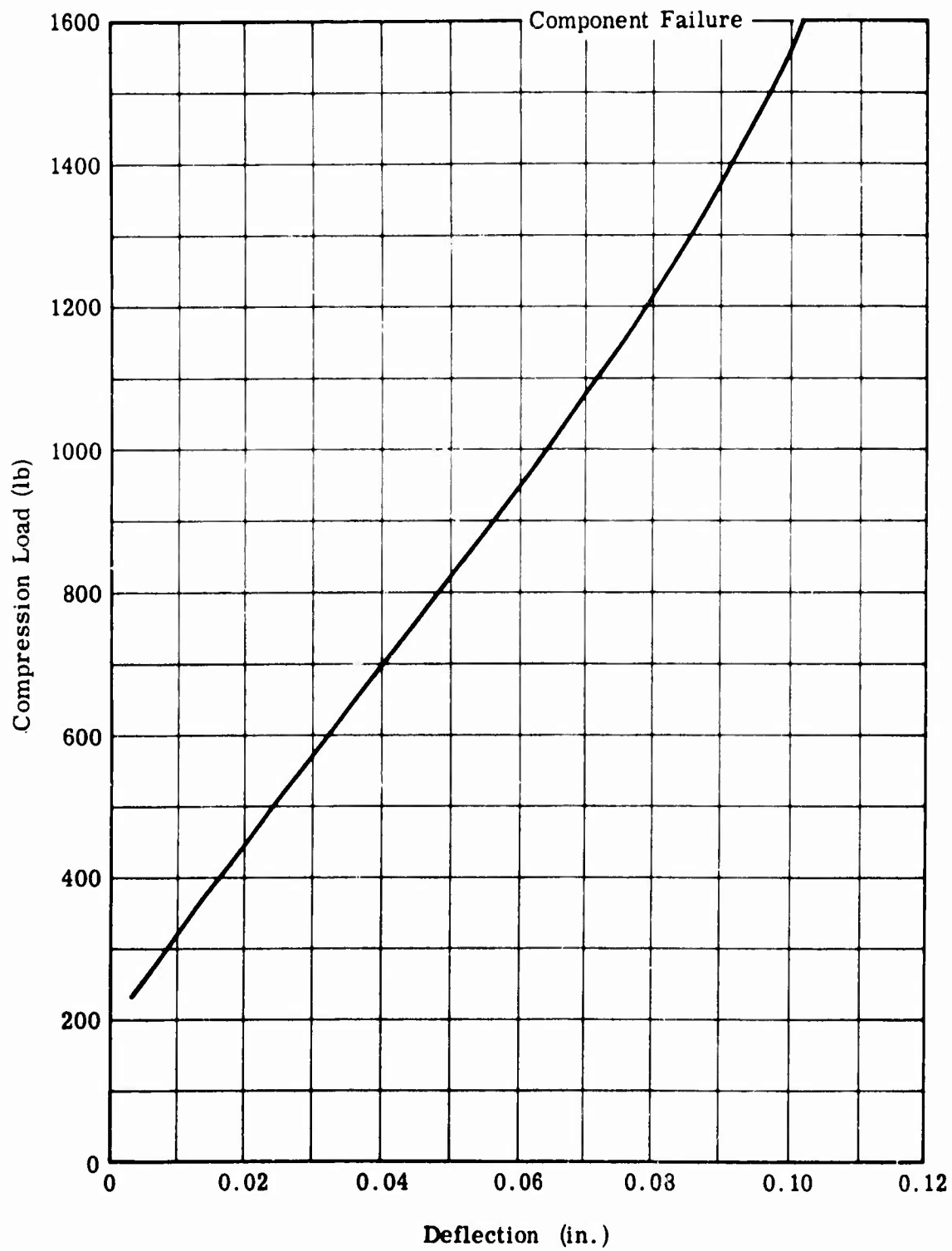


Figure 55. Load-Deflection Curve, Failure Loading - Quadrant Assembly.

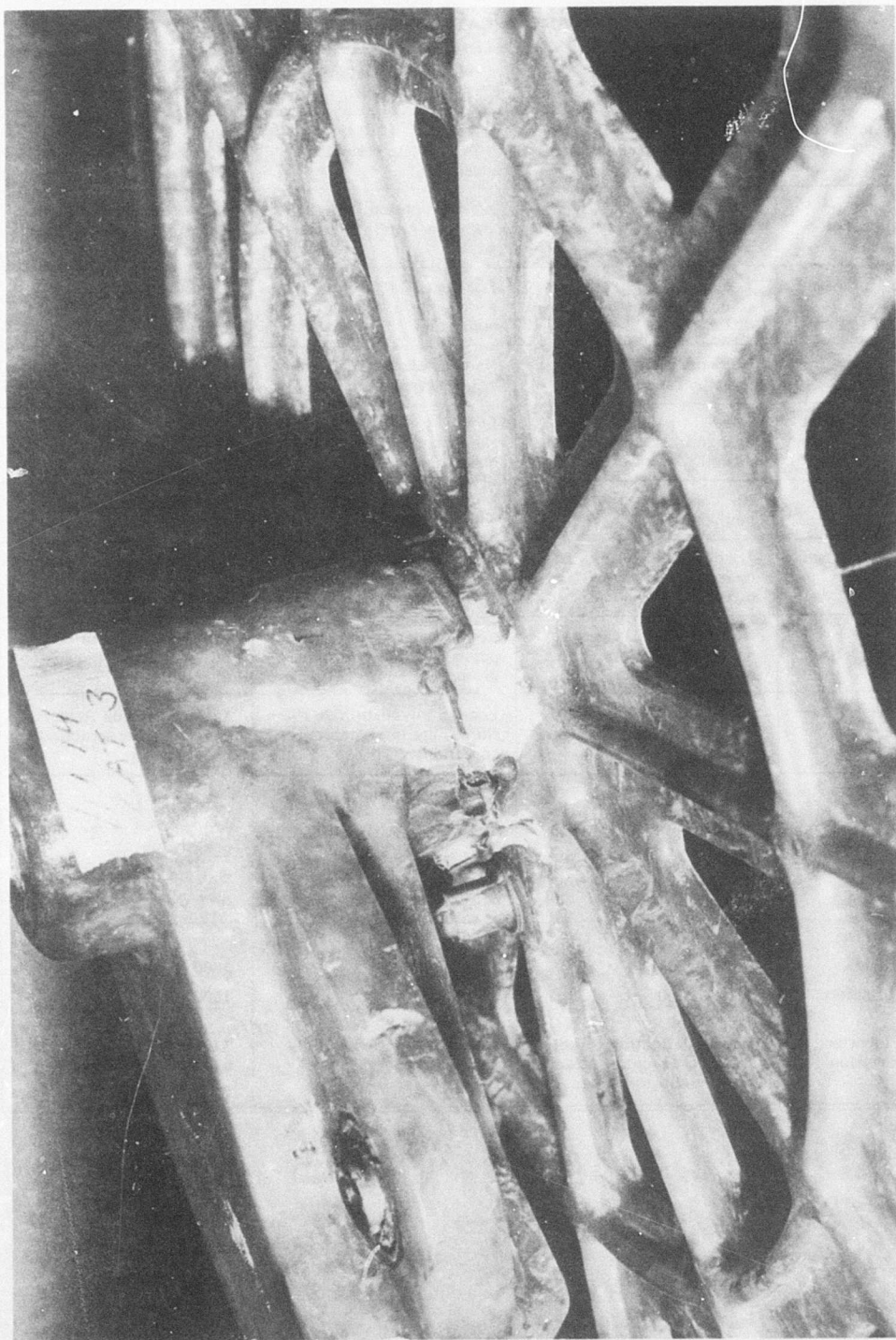


Figure 56. Quadrant Assembly After Category 3 Failure Load Test.

TABLE XIX. SUMMARY OF CATEGORY 3 TEST RESULTS

Test	Idler Bell Crank	Aft Bell Crank	Quadrant Assembly
MDPL at Amb Temp	Loaded to +2760 lb. No change in structural condition.	Loaded to -4010 lb at P _B . No change in structural condition.	Loaded to -883 lb at P. No change in structural condition.
Sand and Dust (12-hr exposure)	No degradation. Slight entrapment of sand and dust.	No degradation. Slight entrapment of sand and dust.	No degradation. Slight entrapment of sand and dust.
MDPL at Amb After Exposure	Loaded to +2760 lb. No change in structural condition.	Loaded to -4010 lb at P _B . No change in structural condition.	Loaded to -883 lb at P. No change in structural condition.
High Humidity (240-hr exposure)	No degradation or change in appearance.	No degradation or change in appearance.	No degradation or change in appearance.
MDPL at Amb After Exposure	Loaded to +2760 lb. No change in structural condition.	Loaded to -4010 lb at P _B . No change in structural condition.	Loaded to -883 lb at P. No change in structural condition.
Fungus Culture (28-day exposure)	No fungus growth on component.	No fungus growth on component.	No fungus growth on component.
MDPL at Amb After Exposure	Loaded to +2760 lb. No change in structural condition.	Loaded to -4010 lb at P _B . No change in structural condition.	Loaded to -883 lb at P. No change in structural condition.
Salt Spray (168-hr exposure)	No degradation of composite. Slight corrosion of metal.	No degradation of composite. Slight corrosion of metal.	No degradation of composite. Slight corrosion of metal.
MDPL at Amb After Exposure	Loaded to +2760 lb. No change in structural condition.	Loaded to -4010 lb at P _B . No change in structural condition.	Loaded to -883 lb at P. No change in structural condition.
Half-Life Fatigue Load No. of cycles MDPL after fatigue	± 420 lb 5.02×10^6 No change in appearance or function.	± 310 lb at P _A 5.01×10^6 No change in appearance or function.	± 175 lb at P 5.05×10^6 No change in appearance or function.
Failure Loading Failure load Margin of safety Failure location and description	5075 lb $\frac{5075 - 2760}{2760} = 0.839$ Linear deflection to failure by tear-out of attachment bushings in lug.	9200 lb at P _B $\frac{9200 - 4010}{4010} = 1.29$ Linear deflection to failure by tearing of pivot bearing.	1600 lb at P $\frac{1600 - 883}{883} = 0.81$ Linear deflection to failure by shear debonding at hub (see Figure 56).

CATEGORY 4 TESTS

This series of tests consisted of vibration tests of three axes at three temperatures, full-life fatigue tests, and crack propagation tests under cyclic load. The vibration tests were conducted in accordance with the requirements of MIL-E-5272C.⁷ The full-life fatigue tests and the crack propagation tests were conducted subsequent to the vibration tests. The components were subjected to an MDPL test prior to the beginning of the test series. All components sustained the MDPL without any apparent change in condition. Table XX summarizes the sequence of testing and the applicable specifications.

TABLE XX. SEQUENCE OF CATEGORY 4 TESTS		
Test No.	Test Description	Specification
1	X-axis vibration at -65°F, ambient, and +160°F	MIL-E-5272C, para 4.7.12, procedure XII
2	Y-axis vibration at -65°F, ambient, and +160°F	Same as above.
3	Z-axis vibration at -65°F, ambient, and +160°F	Same as above.
4	Full-life fatigue	-
5	Crack initiation, propagation, and failure	-

Vibration Tests

The vibration tests were conducted using an MB Electronics Model C210 vibrator. The components were mounted in the equipment to simulate actual aircraft installation and to permit orientation of the components about the three principal axes. A resonance search was performed from 10 to 500 Hz to determine the resonant frequency of the components. Each component was vibration tested for 3 hours (1 hour each at -65°F, at ambient, and at +160°F). A Wyle airconditioner was used to provide the low- and high-temperature air to an enclosure that was placed over the components under test.

The resonance search revealed that only the aft bell crank exhibited a resonant frequency, which was present only in one axis.

During vibration testing of the quadrant assembly, a problem occurred in the plane perpendicular to the flat plane of the sheave (identified as the X axis). The cable attached to the sheave through the attachment groove began to vibrate, transmitting the vibration load to the sheave. The vibration load resulted in high deflections in the sheave, and the groove exhibited evidence of wear from the vibration of the cable. The high deflections in the sheave caused some minor cracking of the sheave spokes near the hub. Figure 57 shows the quadrant assembly after vibration testing. The components sustained the vibration tests and the MDPL after testing with no significant change in condition.

Full-Life Fatigue Tests

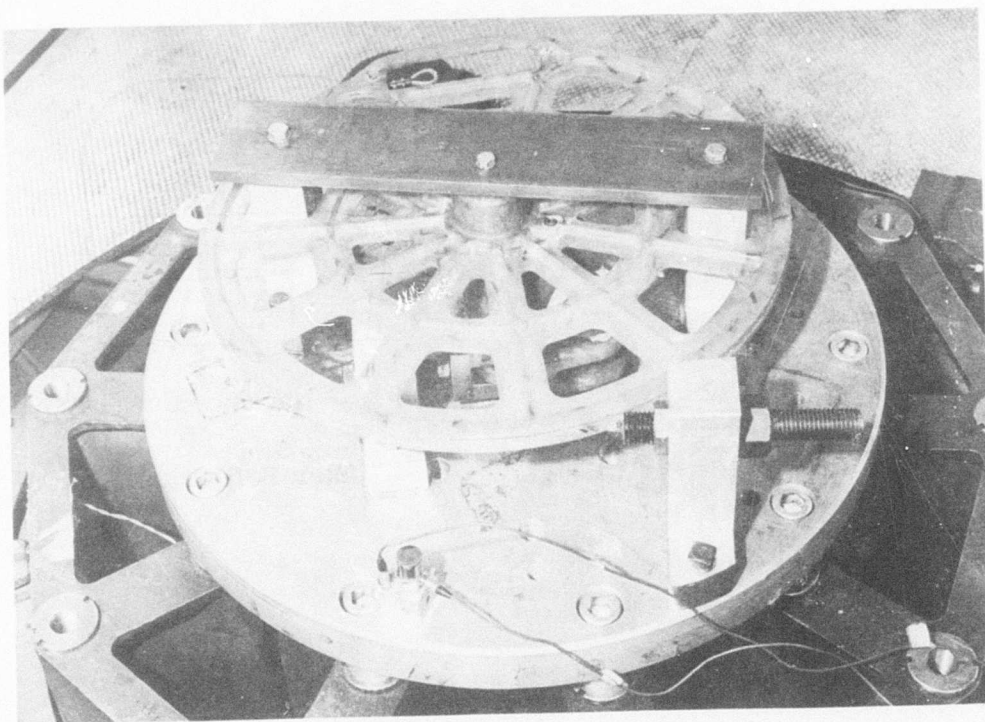
After completion of the vibration tests, the components were subjected to full-life fatigue tests of 10×10^6 operational load cycles. All three components sustained the full 10×10^6 cycles without any apparent degradation to the composite materials, the metal fittings, or the adhesive bonds. All components sustained the MDPL after fatigue testing with no apparent change in condition.

Crack Propagation Tests

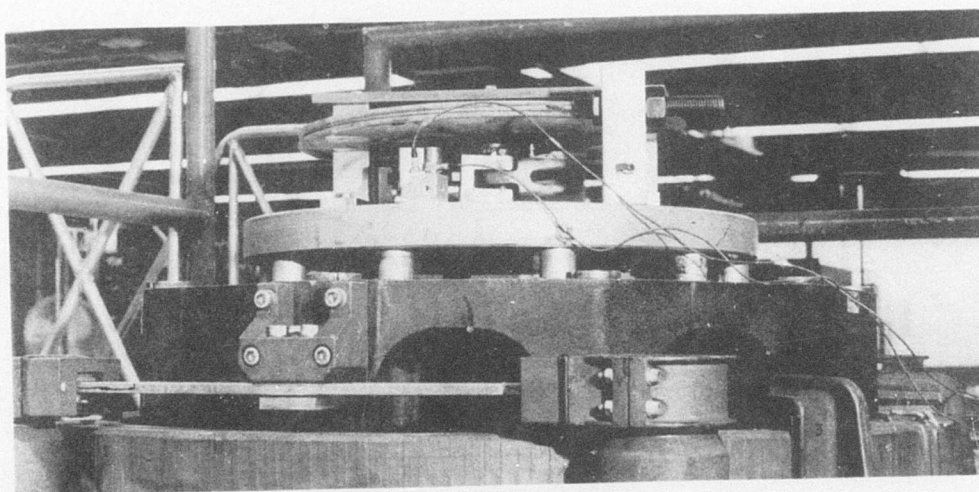
The crack propagation tests were conducted in order to further evaluate the response of the ballistically damaged components to cyclic loads. A precisely dimensioned and located crack was made in each specimen as shown in Figure 58. The crack was located near the area of the ballistic impact in each specimen, since this area is the primary load-carrying member and will put the maximum stress at the tip of the crack. The cracks were initiated by sawing through the component with a hacksaw. The final fine crack was made with a 00 jeweler's saw.

The cracked component was cycled at the operational load for the period of time necessary to simulate 100 hours of operation. Assuming an operational load cycling time of one cycle per minute, 6000 operational load cycles would be required to simulate 100 operating hours.

The load level selected for the crack propagation tests was 6000 operation load cycles. The crack growth was to be measured as a function of applied cycles. However, it was found that the crack would not grow significantly under this operational load, and the tests were modified as necessary to obtain the data.



A. Top View



B. Side View

Figure 57. Quadrant Assembly After Vibration Testing.

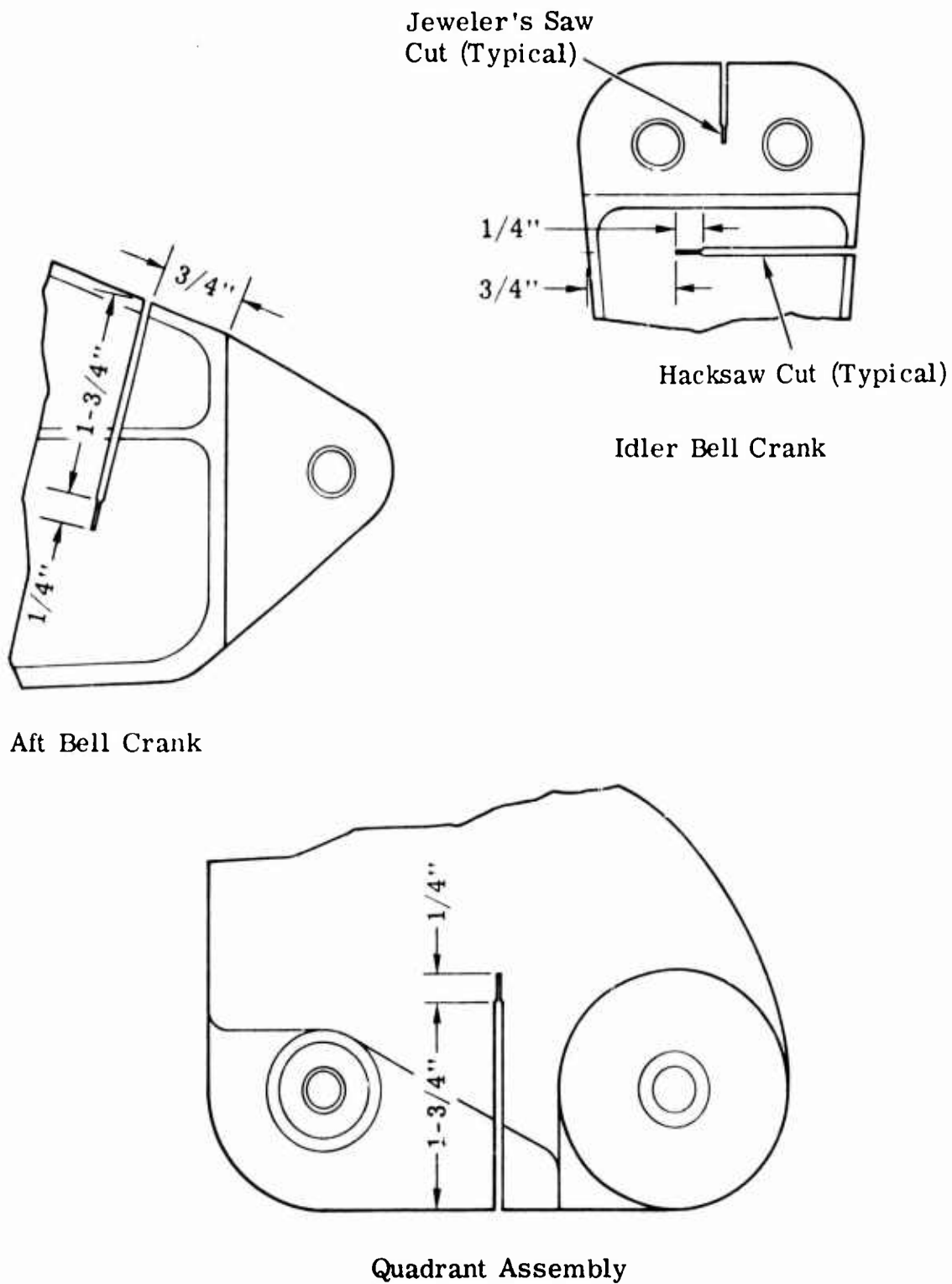


Figure 58. Location of Cracks in Test Specimens for Crack Propagation Tests.

Figure 59 shows the initial crack in the idler bell crank after undergoing 6000 operational load cycles at +420 and -510 pounds. There was no apparent increase in the length of the crack after cycling. The load was incrementally increased to ± 2500 pounds. However, this load did not increase the length of the crack, and it became apparent that the component would fail by tear-out of the bearing attachment holes. Therefore, a crack was initiated between the two attachment holes, and the cyclic load of +420 and -510 pounds was applied for an additional 270 cycles. The additional cyclic loading did not cause any propagation of either crack. The load was again incrementally increased while the crack was monitored. The component failed abruptly during the cycling at 3260 pounds without any observable slow crack propagation. Figure 60 shows the component after failure.

Figure 61 shows the aft bell crank with a crack made through both the primary and secondary load members. The crack was made through these two members to assure that some crack propagation would be achieved during the cyclic loading. The component was loaded to +505 and -670 pounds for 6000 cycles. A slight crack (0.35-inch-long) occurred early in the cyclic loading (<1000 cycles). Crack propagation did not grow beyond this length during the additional 5000 cycles. During the loading, the component exhibited a 0.015-inch deflection under tension load and a 0.027-inch deflection under compression load. To cause additional crack propagation and to determine the failure load in the component, the load was increased to +830 and -1050 pounds while still under the loading cycle, and the data on the load versus deflection and the crack growth versus number of cycles were recorded. The component was loaded to 1990 pounds, at which time the crack propagated abruptly and the component failed. The deflection at failure was 0.075 inch. Figure 62 shows the aft bell crank after failure. Figure 63 shows the load-deflection curve for the aft bell crank. Figure 64 shows the crack propagation curve for the aft bell crank after 6000 cycles and increased load.

Figure 65 shows the quadrant assembly with the initial crack in the crank area after 6000 operational load cycles. The component was subjected to 6000 operational load cycles at +735 and -883 pounds without any evidence of crack propagation (see Figure 65). The load was then increased to +1225 and -1475 pounds in an effort to cause some propagation of the induced crack. However, the component exhibited a bond failure at the hub joint. The failure progressed into the hub portion of the crank as shown in Figure 66 and therefore was not reparable. Propagation testing of the component was terminated at this point.

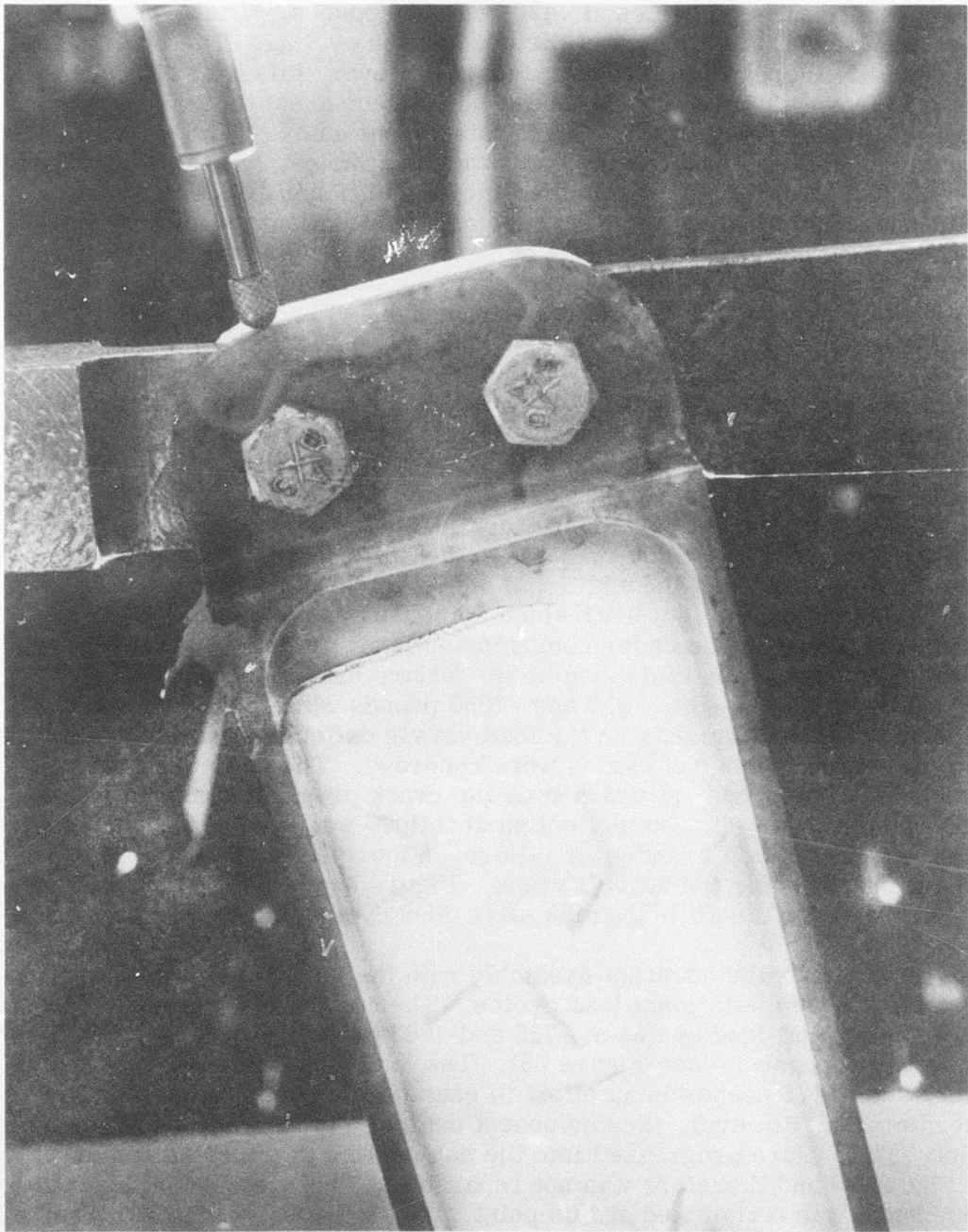


Figure 59. Initial Crack in Idler Bell Crank After 6000 Operational Load Cycles.

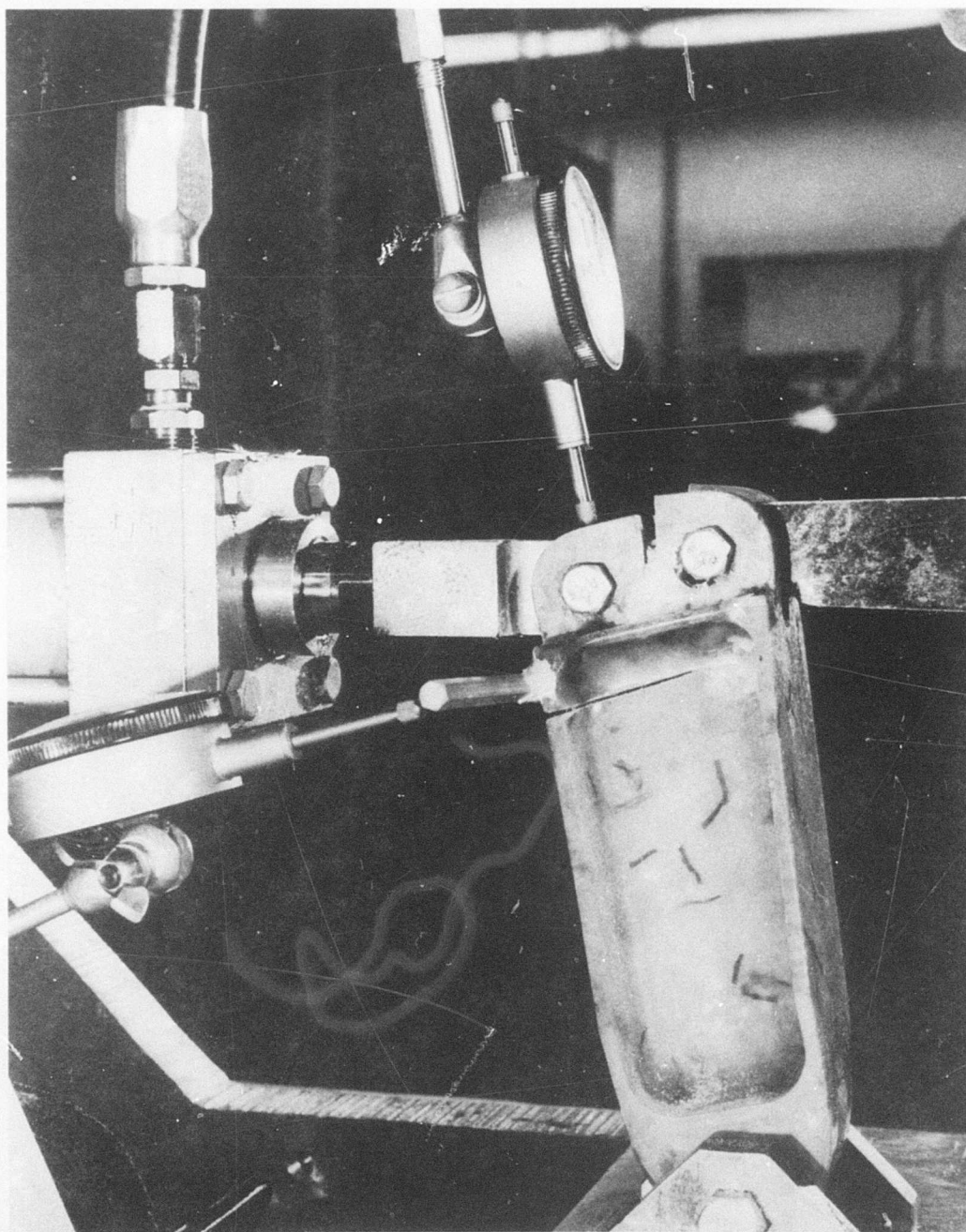


Figure 60. Idler Bell Crank Loaded to Failure -
Crack Propagation Test.

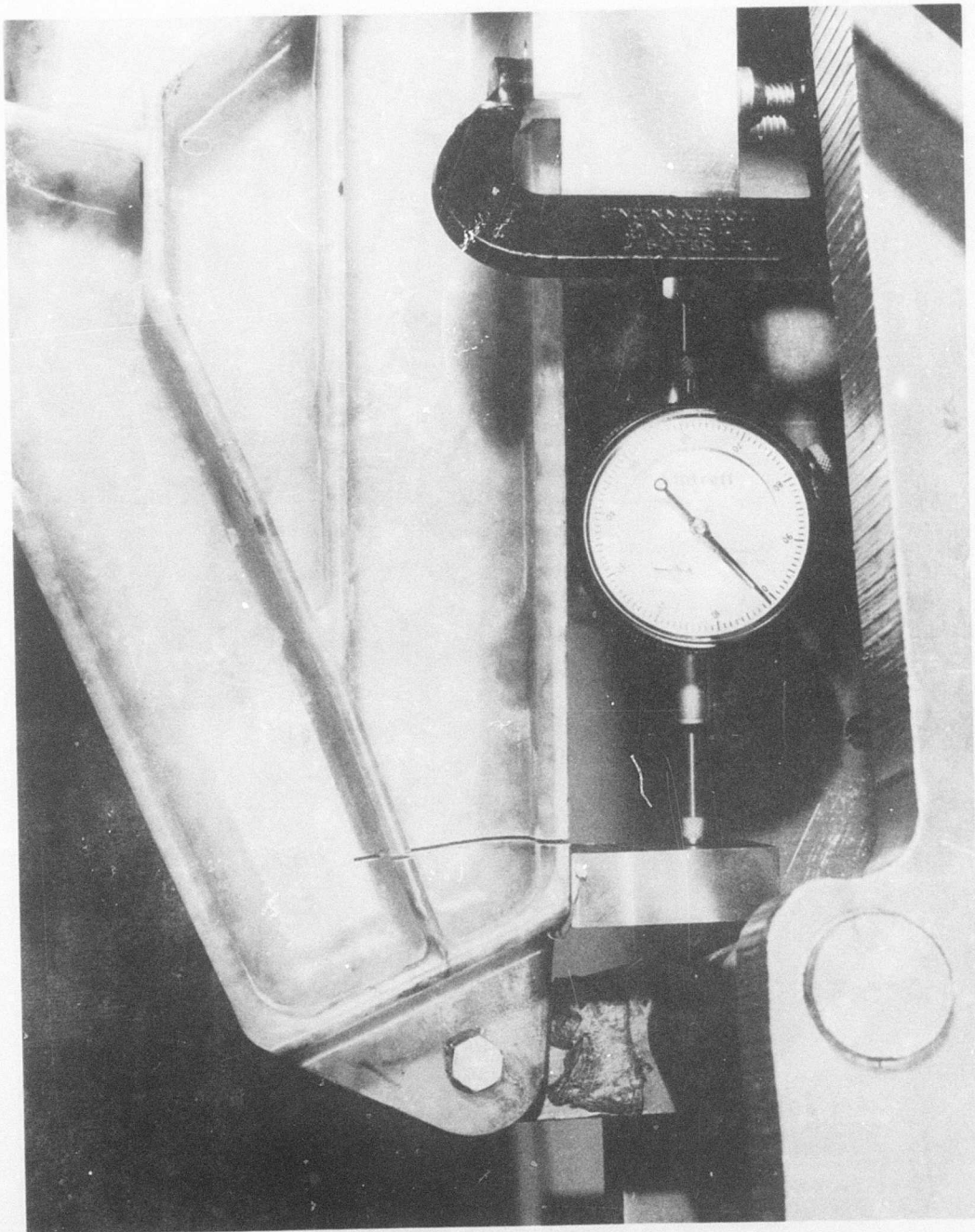


Figure 61. Initial Crack in Aft Bell Crank After 6000 Operational Load Cycles.

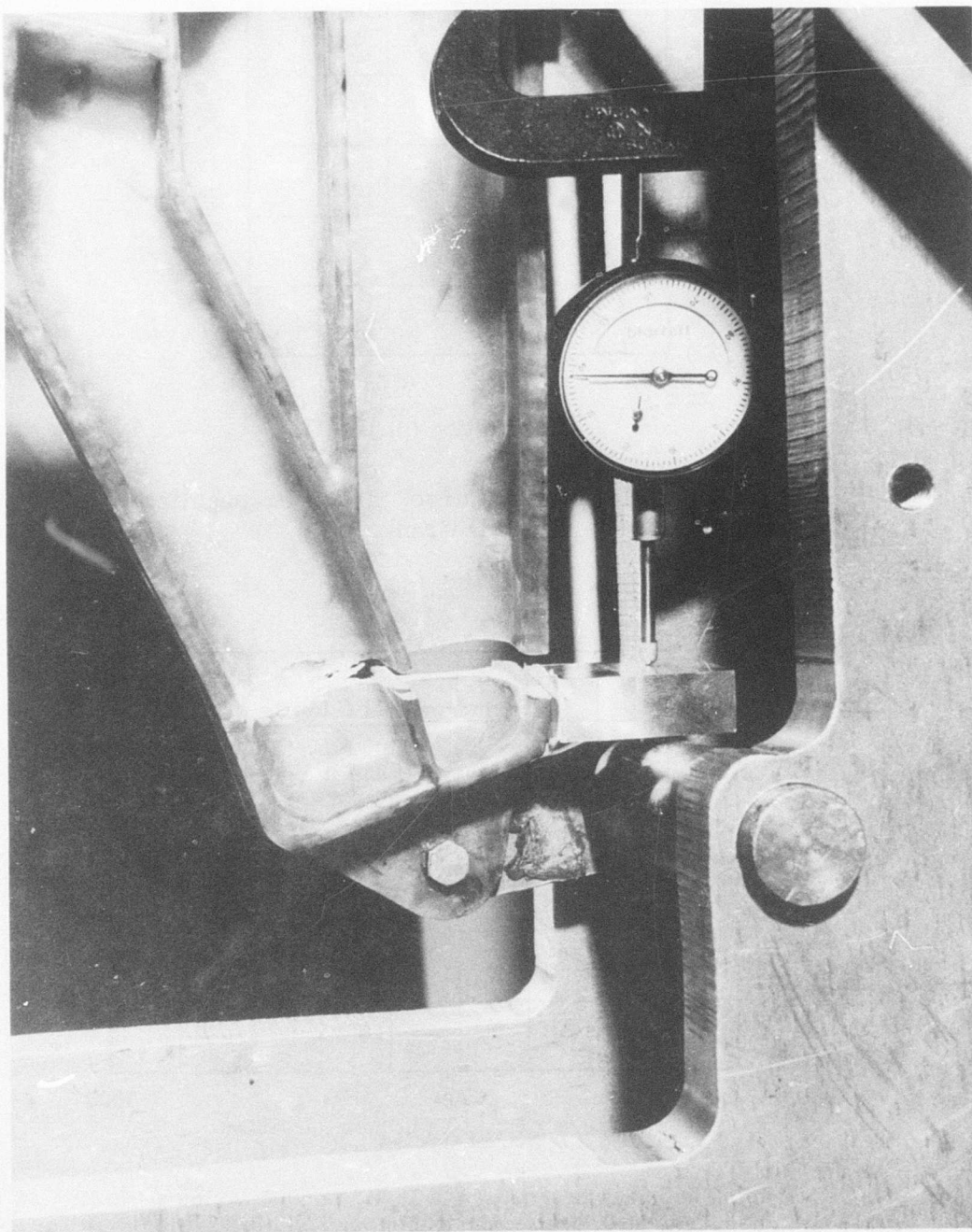


Figure 62. Aft Bell Crank Loaded to Failure - Crack Propagation Test.

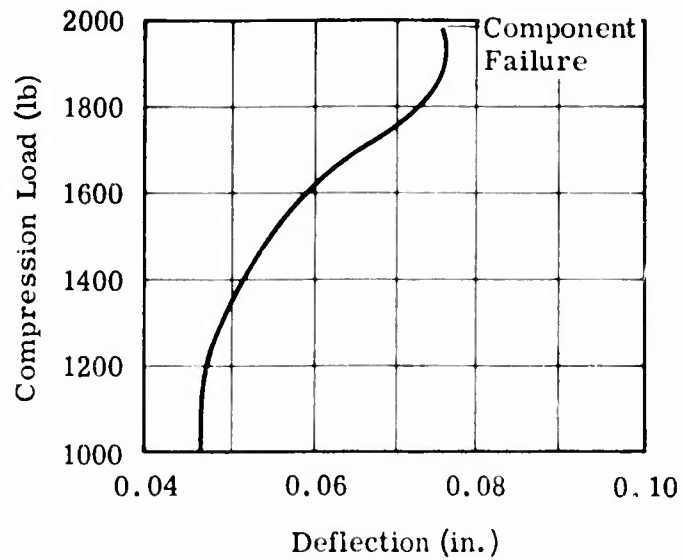
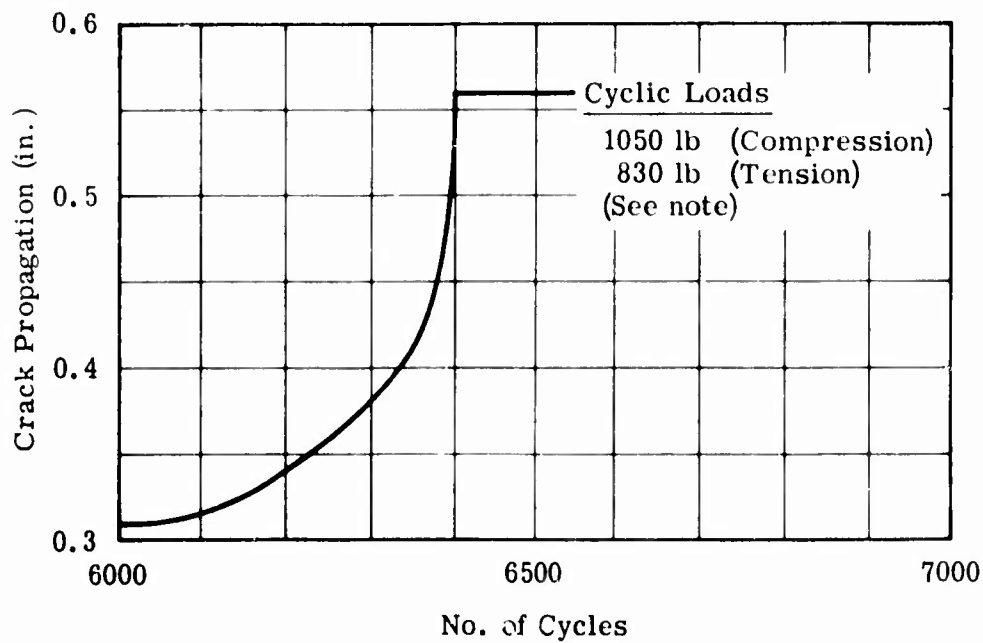


Figure 63. Load-Deflection Curve, Crack Propagation Loading - Aft Bell Crank.



Note: The crack progressed 0.31 in. in 6000 cycles at loads of 670 lb (compression) and 505 lb (tension) before the load was increased.

Figure 64. Crack Propagation Curve - Aft Bell Crank.

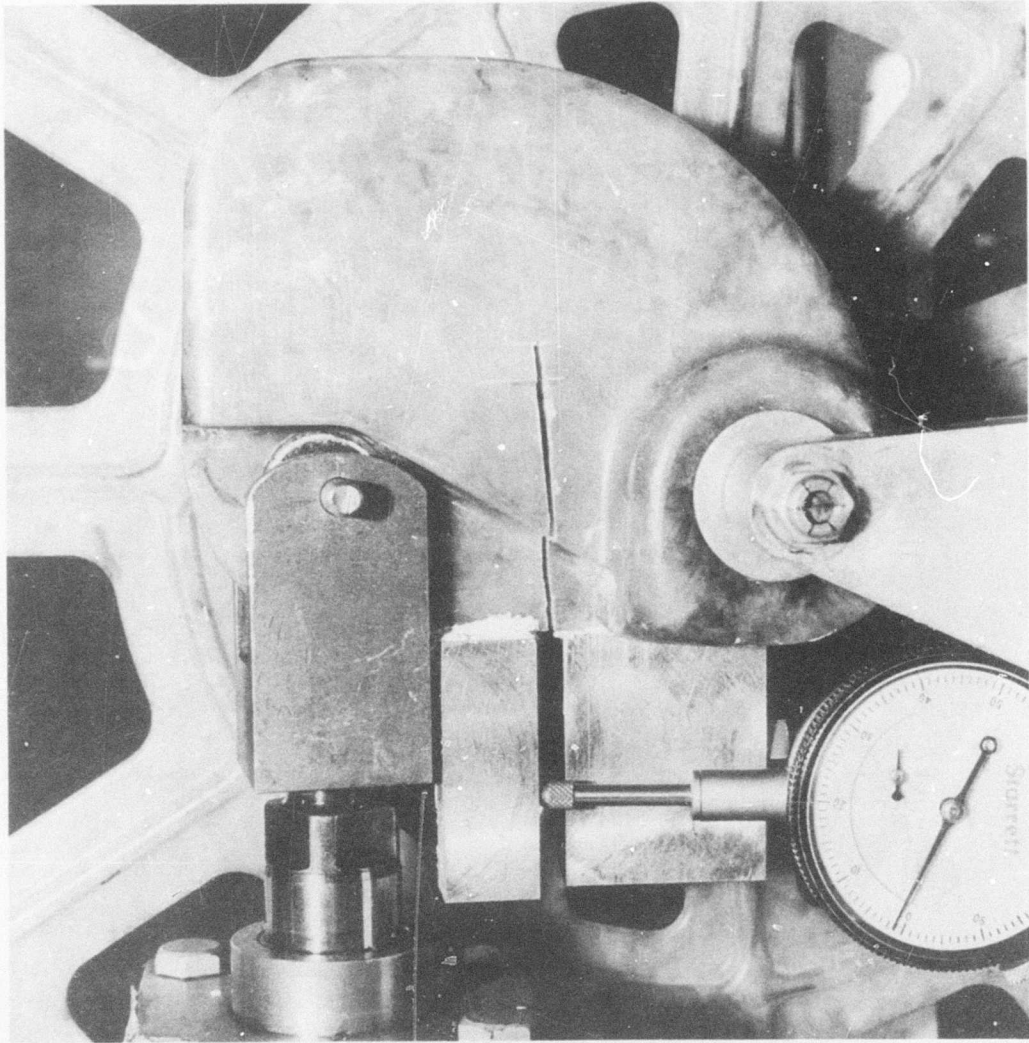


Figure 65. Initial Crack in Crank of Quadrant Assembly
After 6000 Operational Load Cycles.

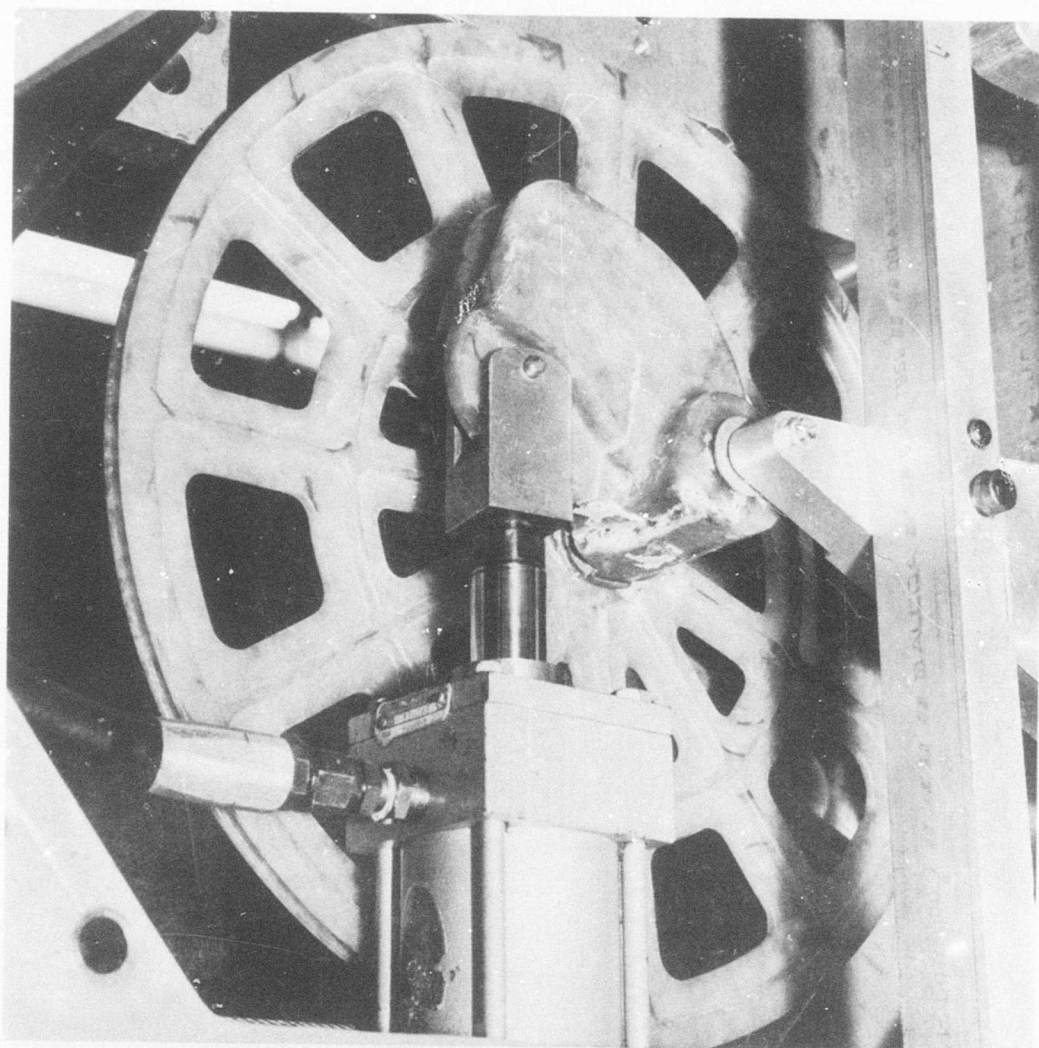


Figure 66. Quadrant Assembly Loaded to Failure - Crack Propagation Test.

A comparison of the cracked component failure loads with the maximum design loads and operational loads is given in Table XXI. It can be seen that the failure loads exceeded the operational loads in all cases. However, the severely cracked bell cranks did not achieve the maximum design loads.

TABLE XXI. COMPARISON OF FAILURE LOADS WITH MAXIMUM DESIGN LOADS AND OPERATIONAL LOADS - CRACK PROPAGATION TESTS

Component	Loads (lb)		
	Maximum Design	Operational	Failure
Idler Bell Crank	+2760	±420	+2450 ^a
Aft Bell Crank	-4010	±602	- 1050
Quadrant Assembly	-883	±175	- 1475
^a Component exhibited dual cracks.			

CATEGORY 5 TESTS

This test series consisted of exposing the components to ultraviolet radiation for 48 hours. The components were subjected to an MDPL test before and after exposure. The ultraviolet radiation tests were conducted in an Atlas Weather-O-Meter, which emits radiant energy in the proper wavelengths conforming to the requirements of MIL-E-5272C, paragraph 4.9.1.⁷ After the 48-hour exposure, no visible degradation or discoloration of the components was apparent. All of the components sustained the MDPL without any apparent change in condition.

CATEGORY 6 TESTS

This test series consisted of sequential immersion of the components in fuel and oil. The tests were to be conducted in accordance with Method 7011 of Federal Test Method Standard No. 406.⁸ Test Method 7011 requires the use of 2-inch-diameter molded discs for conducting the tests. This procedure was modified to use the complete molded component assembly in the immersion tests. The tests were conducted to determine the effects of sequential fuel and oil immersion on the load-carrying ability of the components and to determine if the weight or dimensions of the components are affected as a result of the immersion tests. The components were weighed, and three dimensional measurements (length,

width, and thickness) were taken prior to immersion. The components were subjected to an MDPL test before and after immersion. All of the components sustained the initial MDPL without any apparent change in condition.

Hydraulic Oil Immersion Test

The first oil immersion test was conducted using MIL-H-5606 hydraulic oil. The components were immersed for 7 days in the oil. No significant changes in the weight or dimensions of the components were observed after immersion. No change was observed in the surface condition or appearance of the components. The MDPL test after immersion was conducted without failure.

JP-4 Fuel Immersion Test

The fuel immersion test was to be conducted using TT-S-735 standard test fluids. By agreement with the contracting officer's technical representative, JP-4 fuel was used instead of TT-S-735. It is believed that JP-4 is more representative of aircraft fuel conditions than the standard TT-S-735 hydrocarbon reagents. The components were immersed for 7 days in the fuel. No significant changes in the weight or dimensions of the components were observed after immersion. No change was observed in the surface condition or appearance of the components. The MDPL test after immersion was conducted without failure.

Aircraft Turbine Engine Oil Test

This test was conducted by immersion of the three components in MIL-L-7808 aircraft turbine engine oil for 7 days. Again, no significant changes in the weight or dimensions of the components were observed after immersion. The surface condition and appearance of the components were unaltered. The MDPL test after immersion was conducted without failure.

Summary

The results of the fuel and oil immersion tests are summarized in Table XXII.

**TABLE XXII. SUMMARY OF FUEL AND OIL IMMERSION
TEST RESULTS**

Test Condition	MDPL (lb)	Condition of Component	Wt (g)	Length (in.)	Width (in.)	Thickness (in.)
A. Idler Bell Crank						
Before Immersion	2760	No change	332	2.721	2.028	0.343
After Immersion						
Hydraulic oil	2760	No change	333	2.720	2.027	0.343
JP-4 fuel	2760	No change	334	2.722	2.029	0.344
Aircraft turbine engine oil	2760	No change	332	2.721	2.030	0.344
B. Aft Bell Crank						
Before Immersion	4010	No change	1283	12.031	2.021	0.921
After Immersion						
Hydraulic oil	4010	No change	1283	12.028	2.022	0.922
JP-4 fuel	4010	No change	1282	12.029	2.021	0.922
Aircraft turbine engine oil	4010	No change	1284	12.029	2.023	0.921
C. Quadrant Assembly						
Before Immersion	883	No change	1821	15.602	3.242	0.470
After Immersion						
Hydraulic oil	883	No change	1819	15.606	3.251	0.468
JP-4 fuel	883	No change	1820	15.597	3.248	0.470
Aircraft turbine engine oil	883	No change	1822	15.600	3.245	0.469

CATEGORY 7 TESTS

This test series consisted of subjecting the components to fire-resistance tests. The tests were to be conducted in accordance with Method 2021 of Federal Test Method Standard No. 406.⁸ Test Method 2021 requires the use of small specimens (0.5 inch wide and 5 inches long) ignited with a 30-second exposure to a Bunsen burner flame. The test plan was modified to use the complete molded test components instead of the small specimens. The test plan was further modified during testing when it became apparent that a 30-second exposure to flame would not ignite the components in some cases. An attempt was made to determine the time required to ignite the molded composite material, the burning time after ignition, and the structural capability of the composite after burning.

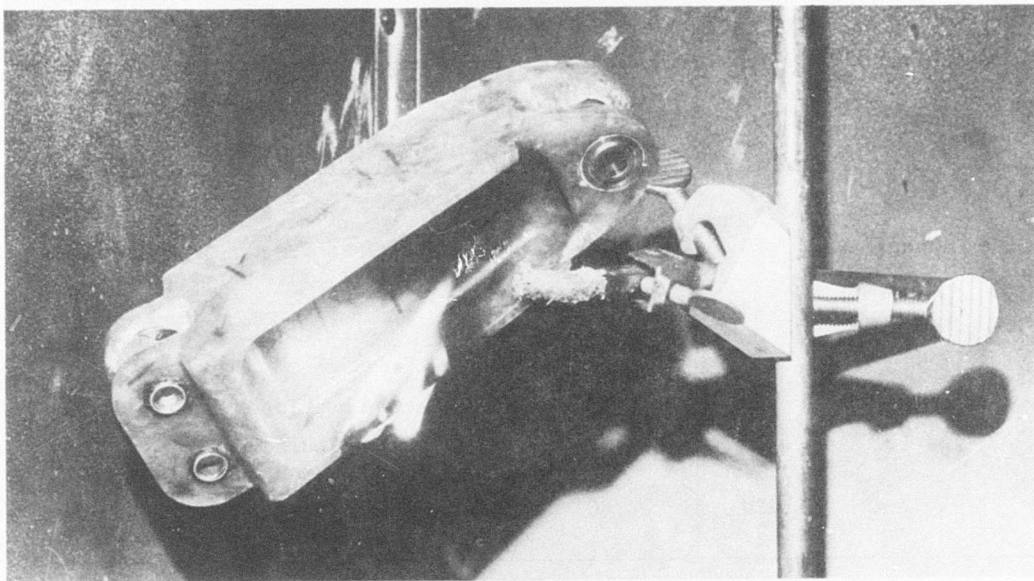
The components were mounted in an exhaust hood, and the Bunsen burner flame was applied at several areas on the components. It was found that the surface resin in the area of ignition burned readily when the flame was applied long enough to ignite the resin. However, in no case was the total component consumed. Only the surface resin burned, and a fiber glass-resin char was formed. Further attempts to ignite the underlying resin were not successful. Table XXIII summarizes the results of the fire-resistance tests.

Figure 67A shows the surface resin of the idler bell crank burning in the area of the 0.150-inch-thick edge member after 30-second exposure to flame. Figure 67B shows the idler bell crank at the conclusion of this test. Figure 68 shows the quadrant assembly after 30- and 60-second exposures to flame in the crank area. The damage was very limited after the 30-second flame exposure and was not at all extensive after the 60-second flame exposure. Figure 69A shows the quadrant assembly burning in the crank area after 315-second exposure to flame. Figure 69B shows the extent of fire damage after this test. Figure 70A shows the surface resin of the quadrant assembly burning in the grooved rim area after 30-second exposure to flame. Figure 70B shows the extent of fire damage after this test.

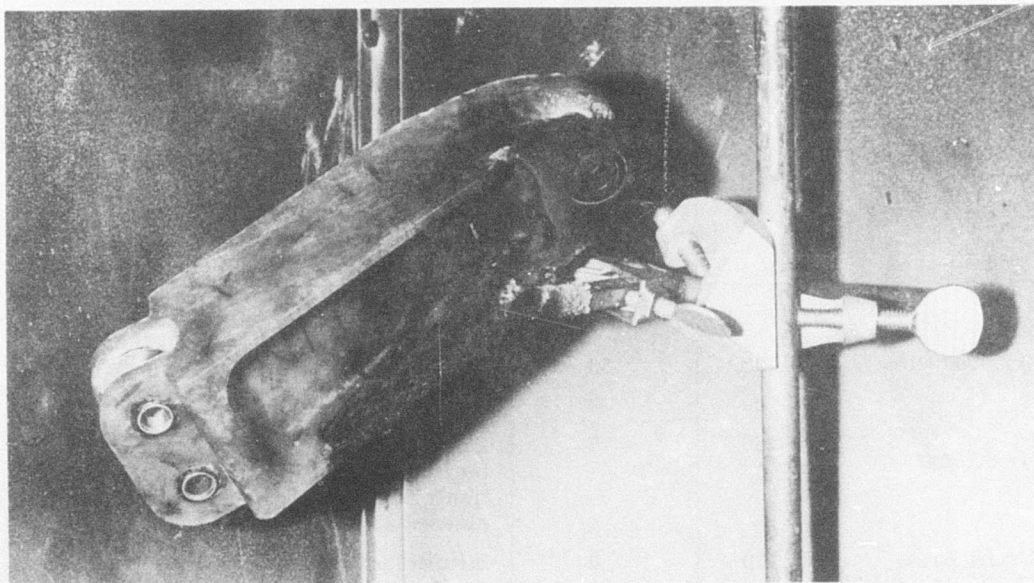
A 30-second flame impingement on thin (<0.150 -inch-thick) sections caused destructive burning of these sections. The time required to ignite the thicker (>0.250 -inch-thick) sections was nearly 3 minutes. These sections burned for 3 to 5 minutes until all surface resin was consumed and a fiber glass-resin char formed, at which time the fire was self-extinguished. Attempts to promote further burning by reapplication of the flame resulted in burning deeper into the component while the flame was applied. When the flame was removed, the fire was

TABLE XXIII. SUMMARY OF FIRE-RESISTANCE TEST RESULTS

Area of Flame Application	Ignition Time (sec)	Burn Time After Ignition (sec)	Remarks
A. Idler Bell Crank			
Edge Member (0.150-in. -thick)	30	311	Surface resin burned readily and ignited resin further up the component.
	60	131	Some continued burning with heavy char formation. Considered structurally unsound.
Attachment Lug (0.346-in. -thick)	30	0	Insufficient heat for ignition of resin.
	60	122	Surface resin burned readily. Flame was extinguished as char formed.
	120	66	Low-level flame with heavy char formation. Considered structurally sound.
B. Aft Bell Crank			
Attachment Lug (0.207-in. -thick)	30	62	Surface resin burned. No burning of resin around metal bushings.
	60	242	Deep burning of resin with heavy char formation. Considered structurally sound.
Attachment Lug (0.375-in. -thick)	30	0	Insufficient heat for ignition of resin.
	60	345	Surface resin burned, spreading flame over entire lug. Heavy char formation.
	300	-	Continued smoking and burning as long as flame was applied. Fire went out almost immediately after removal of flame. Considered structurally sound.
C. Quadrant Assembly			
Grooved Rim	30	33	Local burning of surface resin.
	60	28	Low-level flame over larger area.
	180	17	All surface resin was consumed. Further burning resulted in deeper penetration with heavy char formation. Considered structurally unsound.
Crank Area (0.462-in. -thick)	30	0	Insufficient heat for ignition of resin.
	60	30	Local burning of surface resin.
	315	17	All surface resin was consumed. Further burning resulted in heavy char and smoke. Considered structurally sound.

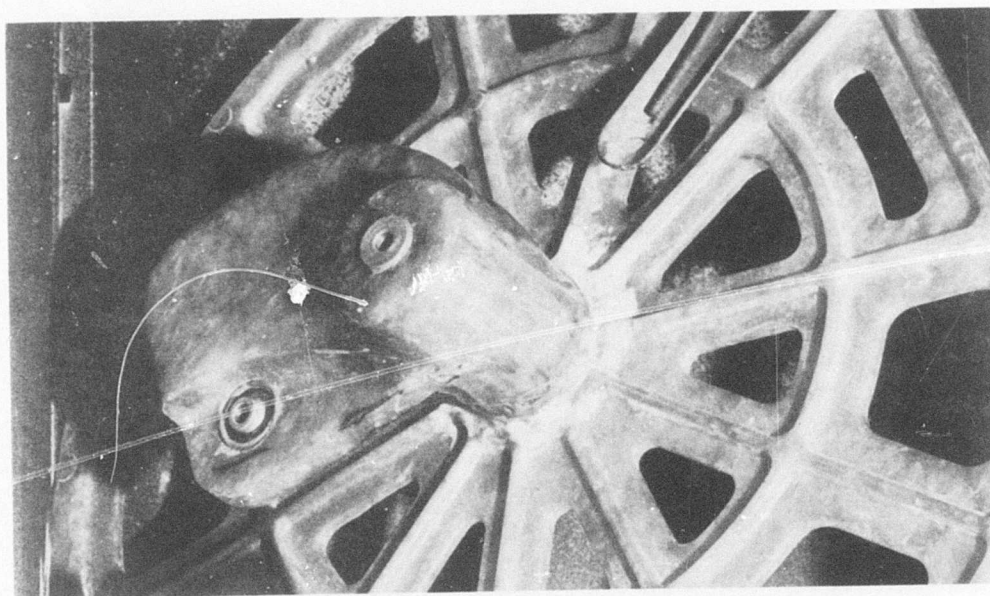


A. Burning After 30-Second Exposure to Flame

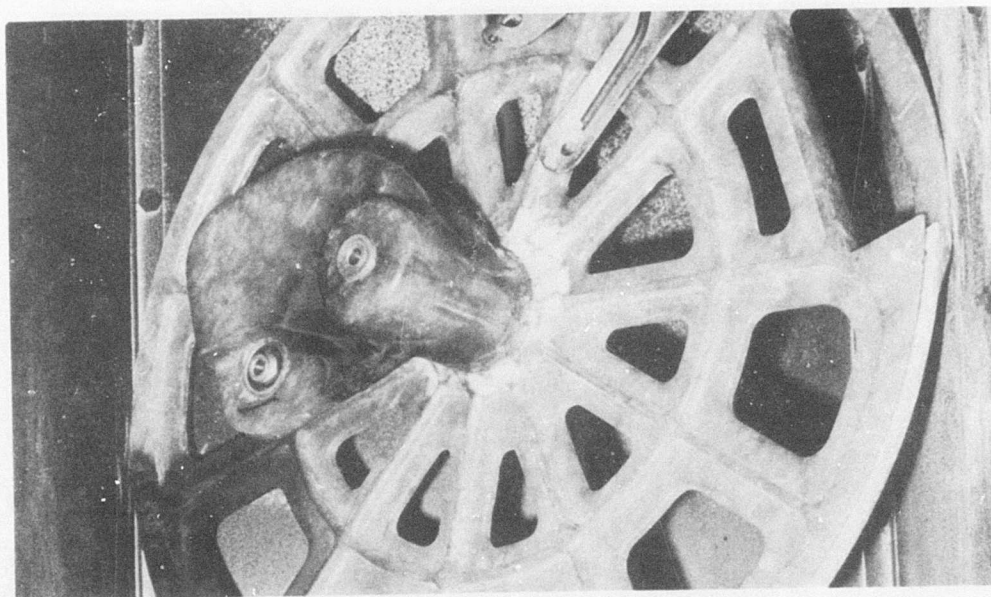


B. Fire Damage After Test

Figure 67. Idler Bell Crank Fire-Resistance Test.

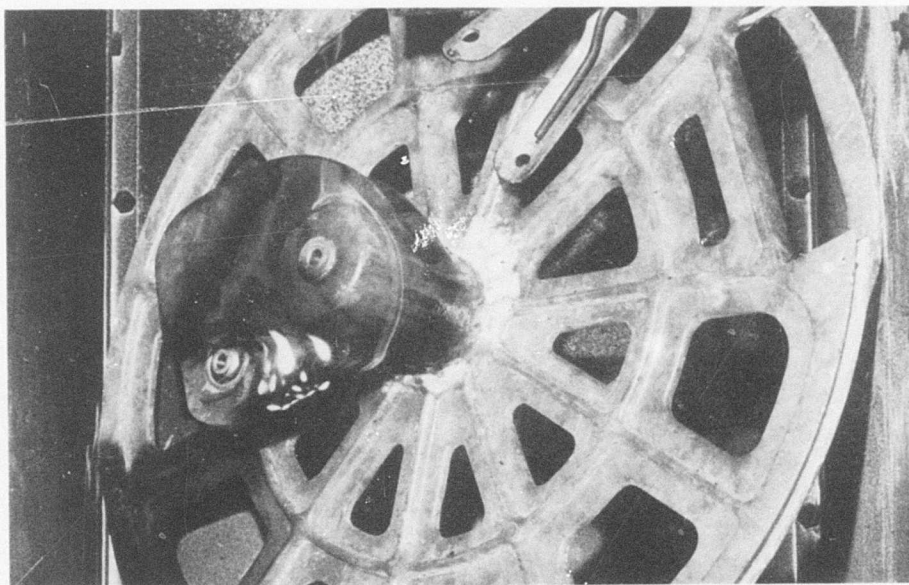


A. After 30-Second Exposure to Flame



B. After 60-Second Exposure to Flame

Figure 68. Quadrant Assembly Fire-Resistance Test (Crank Area).

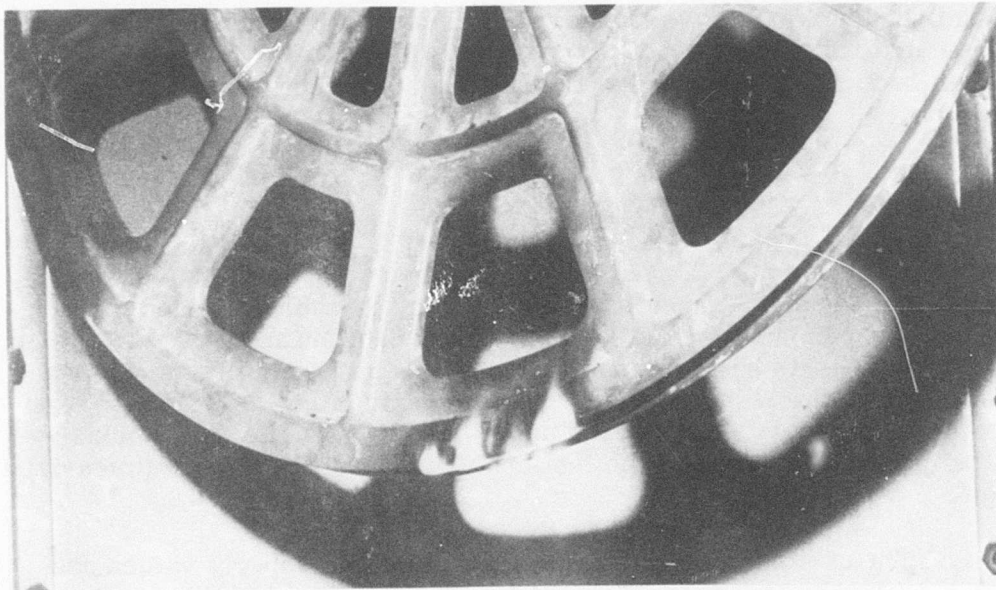


A. Burning After 315-Second Exposure to Flame

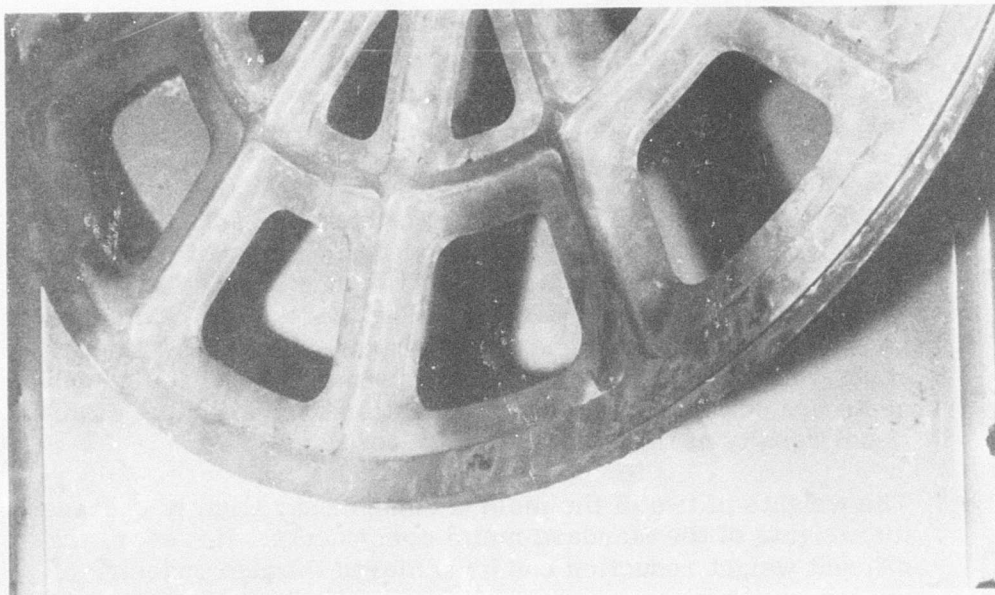


B. Fire Damage After Test

Figure 69. Burning and Extent of Fire Damage in the Crank Area of the Quadrant Assembly.



A. Burning After 30-Second Exposure to Flame



B. Fire Damage After 270-Second Exposure to Flame

Figure 70. Quadrant Assembly Fire-Resistance Test
(Grooved Rim Area).

extinguished within a few seconds. The thick sections were considered to have structurally sound load-carrying capabilities after the test; however, the thin sections were sufficiently consumed to be considered structurally unsound.

SUMMARY OF TEST RESULTS

The results of the tests conducted on the three components have demonstrated the excellent capability of compression-molded, short-fiber glass-epoxy composites for ballistic-damage-tolerant flight control components. The tests performed on the components and the response of the components to the test conditions are summarized in Table XXIV. (Confidential ballistic data are presented in Volume II.) The conclusions that can be drawn as a result of the test and evaluation effort are summarized below.

1. The use of conservative design allowable property values and conservative design approaches has resulted in components with high margins of safety. The exception is the marginal design condition of the quadrant assembly at its hub joint.
2. The short-fiber molding materials used for fabricating the components are easily formed and molded. Components produced from the short-fiber molding materials have predictable and reliable strength values.
3. The components met or exceeded all strength value requirements in the undamaged and damaged conditions and sustained all temperature and environmental tests without any significant evidence of degradation except in the fire-resistance tests. The components are not fireproof, but in no case was the entire component consumed. Only the surface resin burned, forming a fiber glass-resin char. These test results indicate that the components are suitable for flight qualification except for the conditional results of the fire-resistance tests.
4. The weights of two of the molded components slightly exceeded the weights of the standard metal components. However, significant weight reduction can be achieved through redesign of the components.

TABLE XXIV. SUMMARY OF TEST RESULTS

Test Condition	General Response of the Components
High-Cycle Fatigue Loading	<ul style="list-style-type: none"> ● Components are not affected by fatigue cycling at operational loads for 5×10^6 to 10×10^6 cycles. ● Bushings and bearings may become unbonded if not properly installed. ● Attachment bolts, bushings, and bearings exhibit some metal fatigue.
Vibration in Three Axes	<ul style="list-style-type: none"> ● Components are unaffected by vibrational loading. ● Input loads from attachment cables or linkages may cause structural damage.
Temperature Extremes	<ul style="list-style-type: none"> ● Components are capable of carrying the maximum design loads at temperature extremes of -80° to $+160^{\circ}\text{F}$. Temperature shock at these extremes is tolerable.
Adverse Environment	<ul style="list-style-type: none"> ● Components are unaffected by exposure to sand and dust, high humidity, fungus, and salt spray and can carry the maximum design loads after exposure.
Ultraviolet Radiation	<ul style="list-style-type: none"> ● Components are unaffected by ultraviolet (solar) radiation and can carry the maximum design loads after exposure.
Fuel and Oil Immersion	<ul style="list-style-type: none"> ● Components are unaffected by immersion in MIL-H-5606 hydraulic fluid, JP-4 fuel, and MIL-L-7808 aircraft turbine engine oil and can carry the maximum design loads after immersion.
Fire Resistance	<ul style="list-style-type: none"> ● Components are not fireproof but can be considered to be self-extinguishing. Components with thin ($<0.150\text{-in.}$-thick) sections are destructively consumed when set afire. Components with thick ($>0.250\text{-in.}$-thick) sections form heavy surface char but may continue to carry load.

LITERATURE CITED

1. Cully, D. C., and Kolarik, R. V., DEVELOPMENT OF BALLISTIC-DAMAGE-TOLERANT FLIGHT CONTROL COMPONENTS MOLDED OF A SHORT-FIBER REINFORCED COMPOSITE MATERIAL, PHASE I SUMMARY REPORT: COMPOSITE MATERIAL FORMATION, EVALUATION, AND CHARACTERIZATION, Goodyear Aerospace Corporation, Akron, Ohio; USAAMRDL Technical Report 72-28, Eustis Directorate, U.S. Army Air Mobility Research and Development Laboratory, Fort Eustis, Va., September 1972, AD 752918.
2. Cully, D. C., and Boller, T. J., DEVELOPMENT OF BALLISTIC-DAMAGE-TOLERANT FLIGHT CONTROL COMPONENTS MOLDED OF A SHORT-FIBER REINFORCED COMPOSITE MATERIAL (U), PHASE II SUMMARY REPORT: COMPONENT DESIGN, FABRICATION, TESTING, AND EVALUATION (U), Goodyear Aerospace Corporation, Akron, Ohio; USAAMRDL Technical Report 73-27, Eustis Directorate, U.S. Army Air Mobility Research and Development Laboratory, Fort Eustis, Va., March 1973. (Confidential Report)
3. Whinery, D. G., BALLISTICALLY TOLERANT REPLACEMENT AIRCRAFT COMPONENTS (U), North American Rockwell Corporation, Columbus, Ohio; USAAVLABS Technical Report 71-4, U.S. Army Air Mobility Research and Development Laboratory, Fort Eustis, Va., April 1971, AD 516178L. (Confidential Report)
4. McArdle, E., Jr., INCREASED SURVIVABILITY FOR FLIGHT CONTROL SYSTEMS (U), The Boeing Company, Vertol Division, Philadelphia, Pa.; USAAVLABS Technical Report 69-57, U.S. Army Aviation Materiel Laboratories, Fort Eustis, Va., November 1969, AD 506 695L. (Confidential Report)
5. Russc, A., FLIGHT CONTROLS ANALYSIS BOEING-VERTOL MODEL YHC-1B, 114-S-10, The Boeing Company, Vertol Division, Philadelphia, Pa., March 1961.
6. FABRICATION SPECIFICATION FOR BALLISTIC-DAMAGE-TOLERANT FLIGHT CONTROL COMPONENTS MOLDED OF A SHORT-FIBER GLASS REINFORCED EPOXY RESIN COMPOUND. (To be published as a Government Specification.)
7. GENERAL SPECIFICATION FOR ENVIRONMENTAL TESTING OF AERONAUTICAL AND ASSOCIATED EQUIPMENT, MIL-E-5272C, 20 January 1960.

8. FEDERAL TEST METHOD STANDARD, PLASTICS: METHODS OF TESTING, Federal Test Method Standard No. 406, 5 October 1961.
9. Dotseth, Walter D., SURVIVABILITY DESIGN GUIDE FOR U.S. ARMY AIRCRAFT, VOLUME I: SMALL-ARMS BALLISTIC PROTECTION, North American Rockwell Corporation, Los Angeles, California; USAAMRDL Technical Report 71-41A, Eustis Directorate, U.S. Army Air Mobility Research and Development Laboratory, Fort Eustis, Va., November 1971, AD 891122L.
10. Fritzsche, H. J., FABRICATION AND TEST OF HIGH SURVIVABILITY FLIGHT CONTROL COMPONENTS (U), The Boeing Company, Vertol Division, Philadelphia, Pa; USAAMRDL Technical Report 72-23, Eustis Directorate, U. S. Army Air Mobility Research and Development Laboratory, Fort Eustis, Va., August 1972, AD 522884L. (Confidential Report)

APPENDIX

COMPOSITE MATERIAL SYSTEM PROPERTIES

Composite material system properties are summarized in tabular and graphic form in this appendix. The data presented are a result of the test program conducted under Contract DAAJ02-70-C-0062 and reported in the Phase II Summary Report² for that program. The specific material system evaluated is a composite molded of randomly oriented, chopped-fiber, glass-epoxy materials. The composite material constituents are described in Table XXV.

TABLE XXV. COMPOSITE MATERIAL CONSTITUENTS		
Constituents	Materials	Content (v/o)
Fiber	S Glass/470 Finish	52
Matrix	DEN 438	48
Mold Charge	Prepreg Ribbon ($\ell = 0.5$ in.)	-

The key properties for the composite material system are summarized in Table XXVI. Typical tensile, compression, and panel shear stress-strain curves for the composite material system are shown in Figures 71, 72, and 73, respectively.

The following design curves for the composite material system are included in this appendix:

<u>Property</u>	<u>Figure No.</u>
Flexural strength	74
Interlaminar shear strength	75
Tensile strength	76
Compressive strength	77
Panel shear strength	78
Bearing strength	79

These design curves are based on a statistical analysis of the test data. The curves represent values that will be exceeded 99 percent of the time with a confidence level of 95 percent.

TABLE XXVI. SUMMARY OF KEY PROPERTIES FOR THE COMPOSITE MATERIAL SYSTEM			
<u>Material System:</u> S glass/DEN 438		<u>Orientation:</u> Random	
<u>Fiber Content:</u> 52 v/o		<u>Density:</u> 0.068 lb/in. ³	
Properties	Temperature		
	-80°F	75°F	180°F
A. Tensile Properties			
Tensile Ultimate (psi x 10 ³)	24.2	20.1	17.4
Proportional Limit (psi x 10 ³)	11.2	8.4	6.5
Tensile Modulus (psi x 10 ⁶)	3.7	3.4	2.6
Ultimate Strain (μin./in.)	9,100	8,600	11,700
B. Compression Properties			
Compression Ultimate (psi x 10 ³)	49.1	36.5	24.0
Proportional Limit (psi x 10 ³)	27.5	20.6	11.5
Compression Modulus (psi x 10 ⁶)	3.1	2.9	2.3
C. Panel Shear Properties			
Shear Ultimate (psi x 10 ³)	23.7	17.4	15.4
Proportional Limit (psi x 10 ³)	5.4	4.4	3.6
Shear Modulus (psi x 10 ⁶)	1.3	1.1	1.1
D. Interlaminar Shear Properties			
Shear Ultimate, Short Beam (psi x 10 ³)	7.4	7.8	5.1

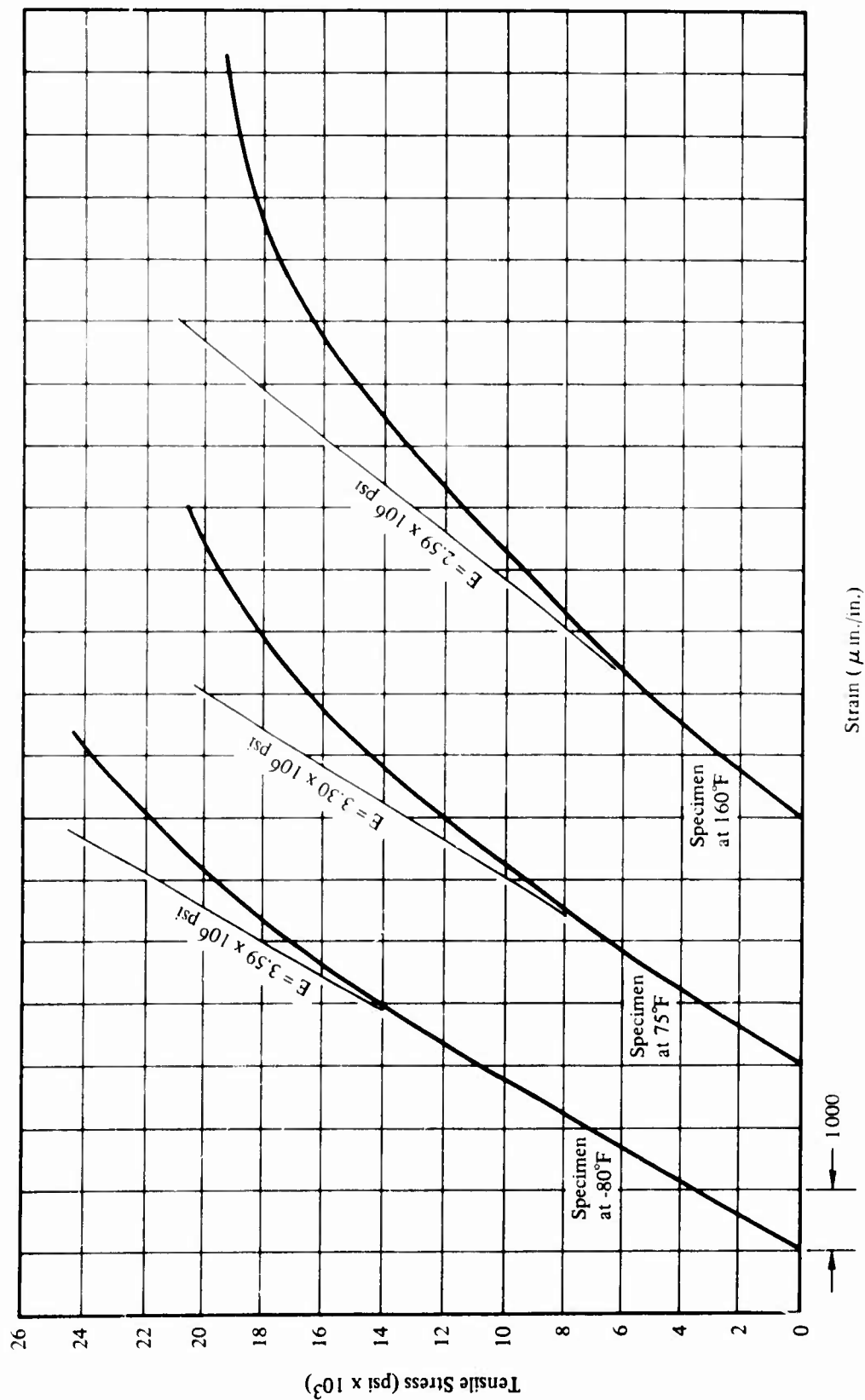


Figure 71. Typical Tensile Stress-Strain Curves for the Composite Material System.

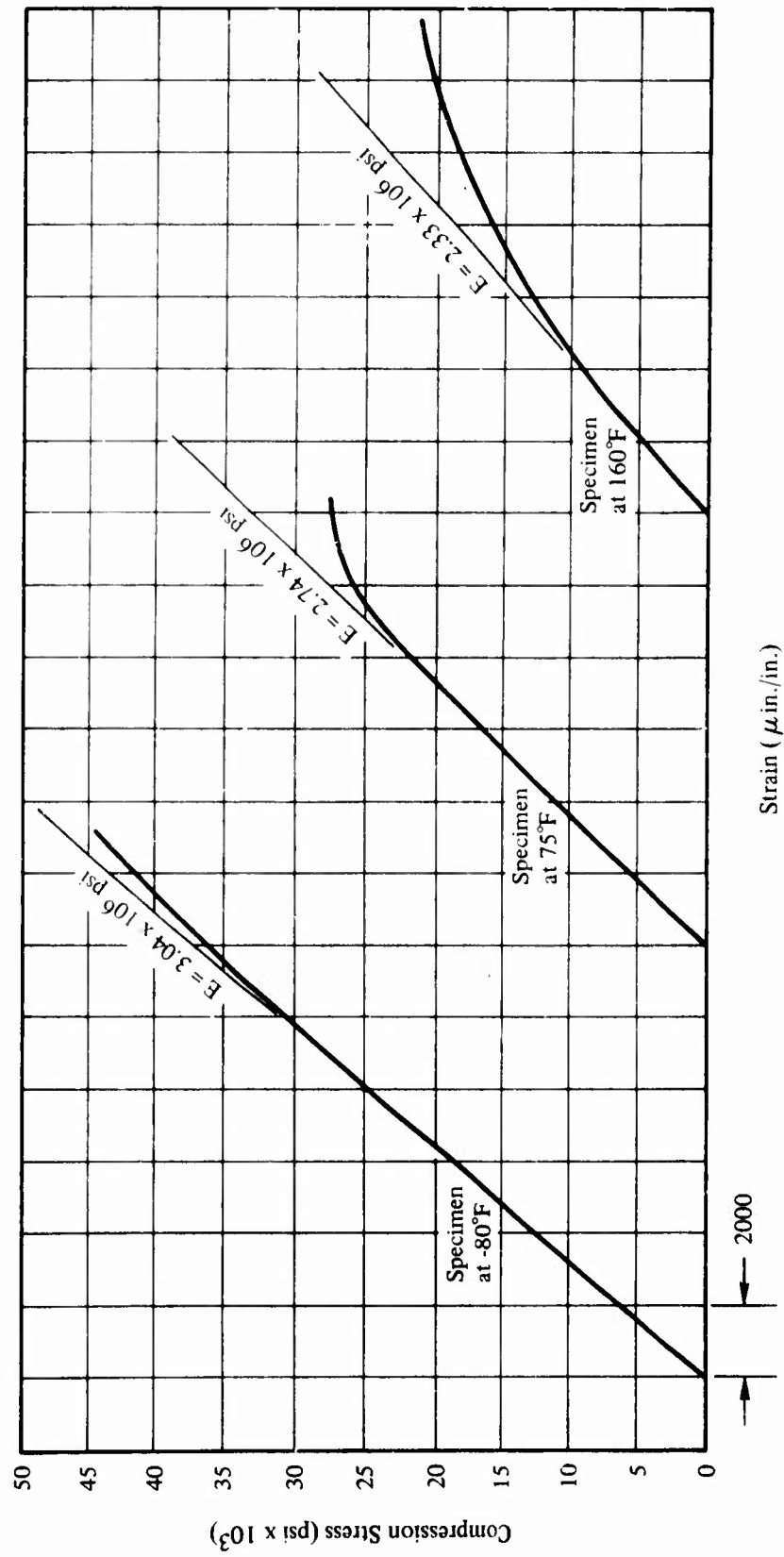


Figure 72. Typical Compression Stress-Strain Curves for the Composite Material System.

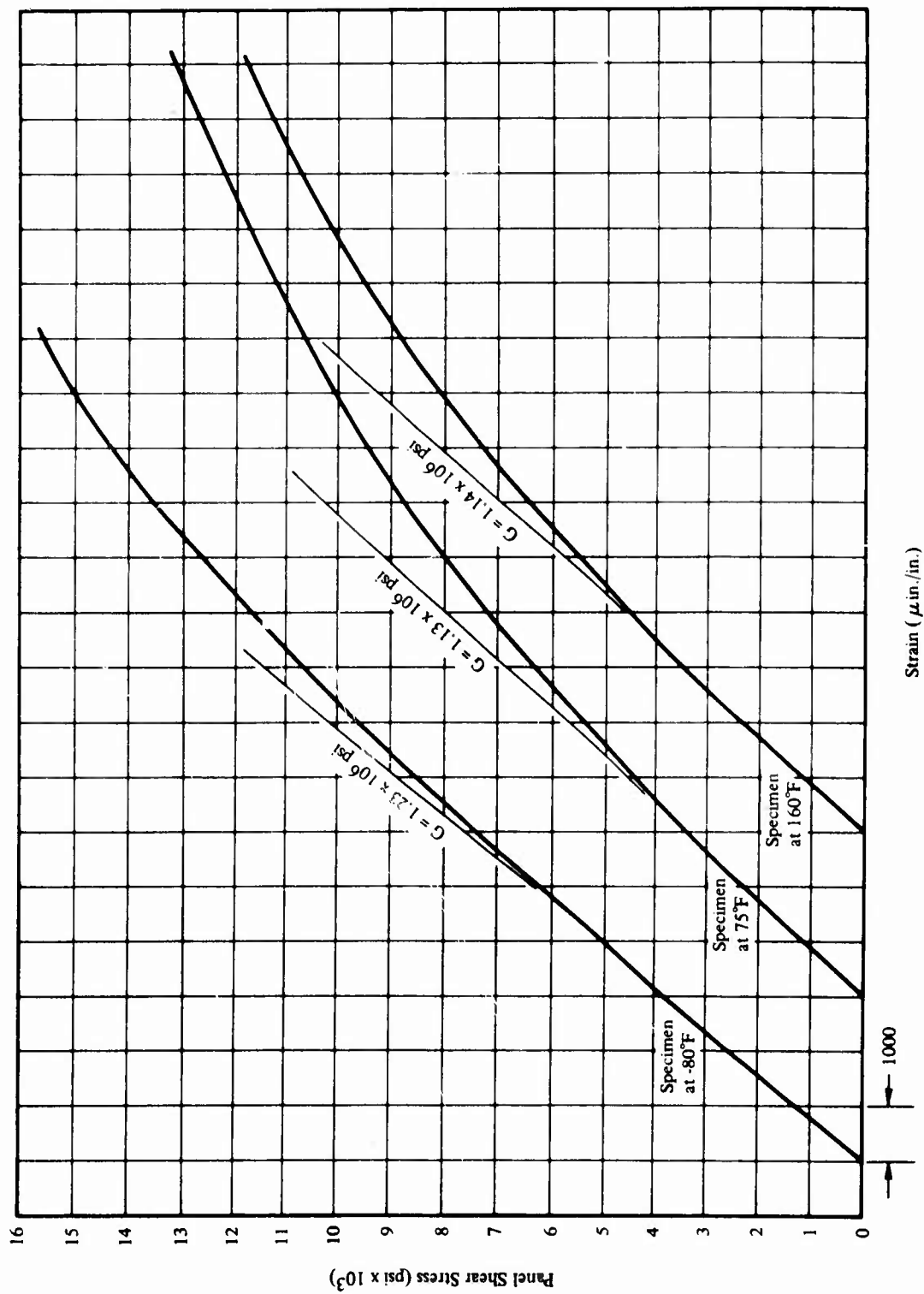


Figure 73. Typical Panel Shear Stress-Strain Curves for the Composite Material System.

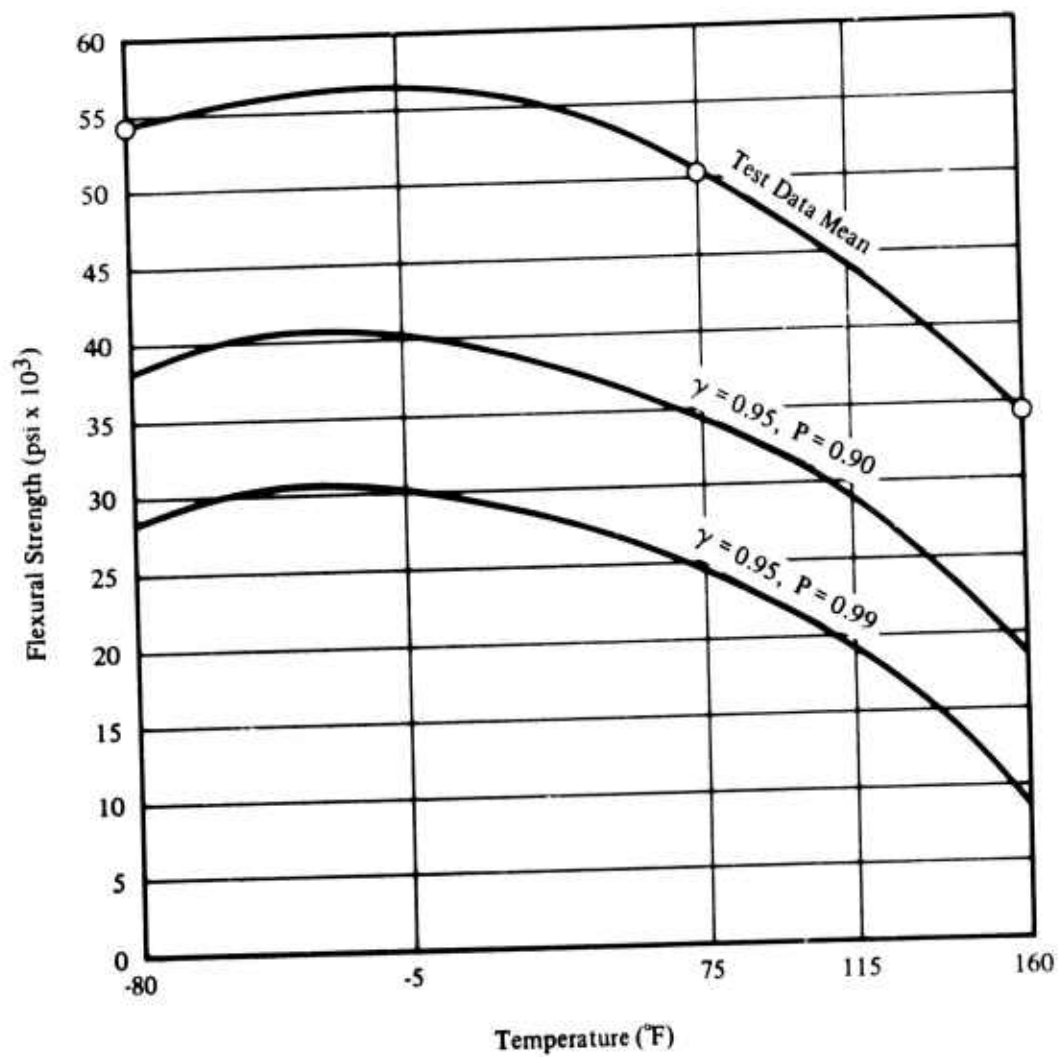


Figure 74. Flexural Strength Design Curves for the Composite Material System.

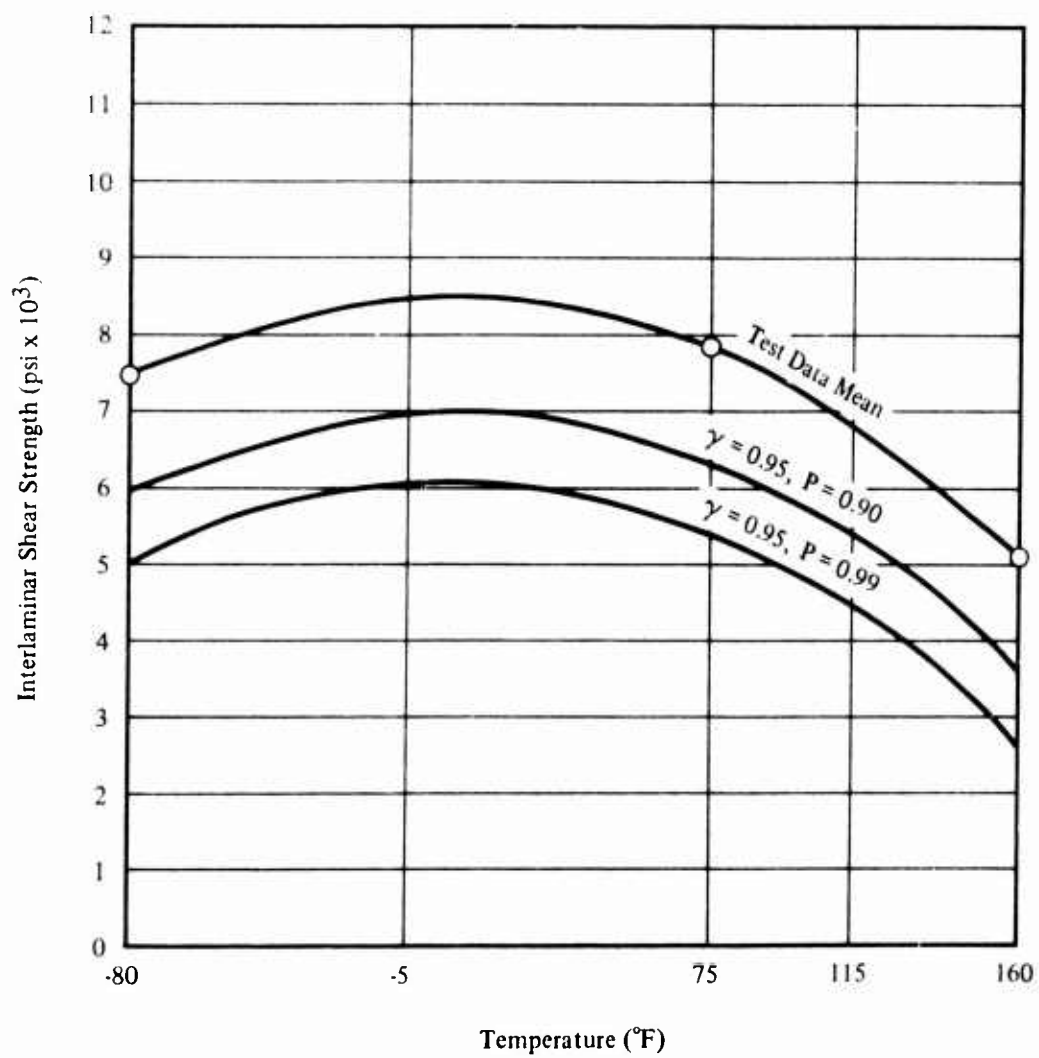


Figure 75. Interlaminar Shear Strength Design Curves for the Composite Material System.

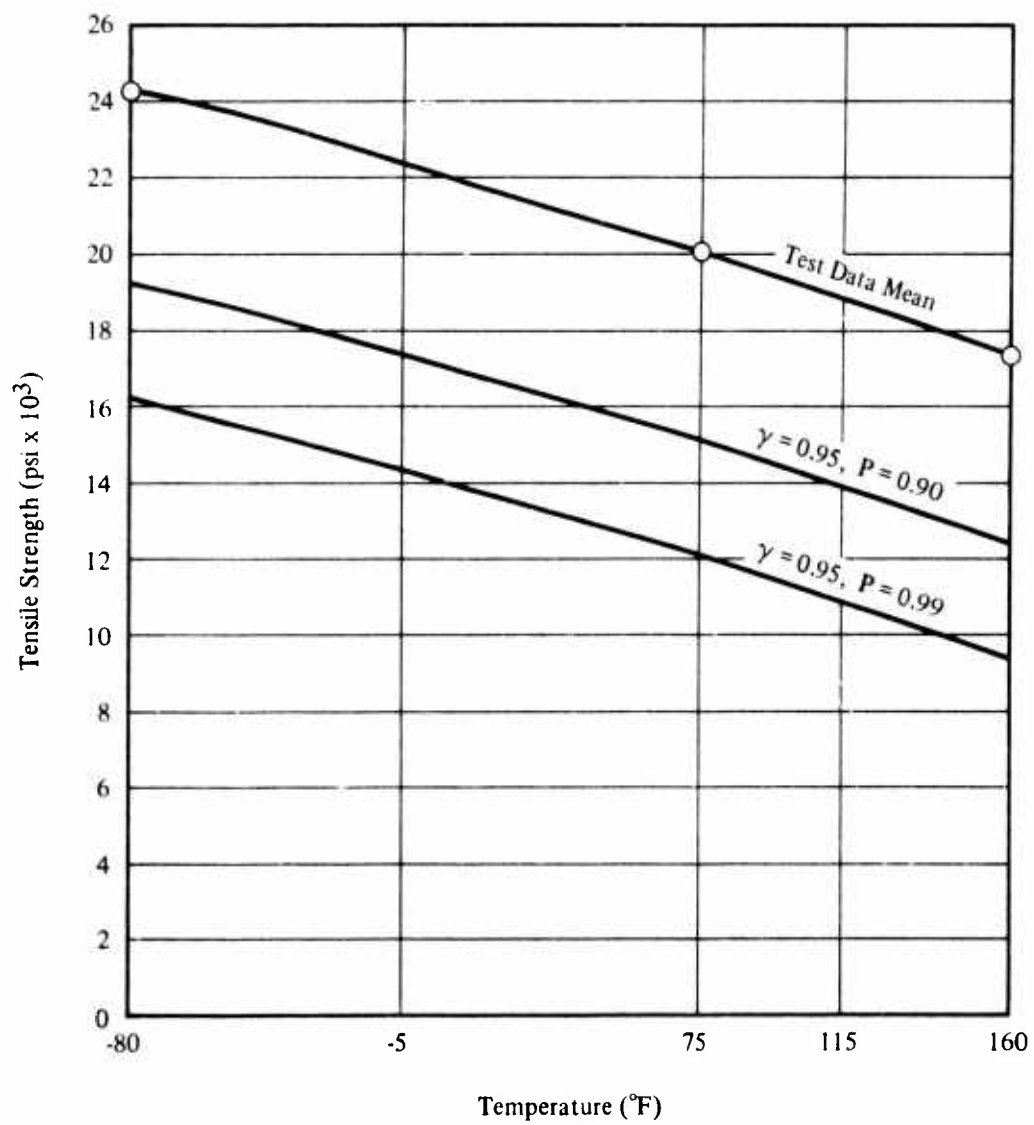


Figure 76. Tensile Strength Design Curves for the Composite Material System.

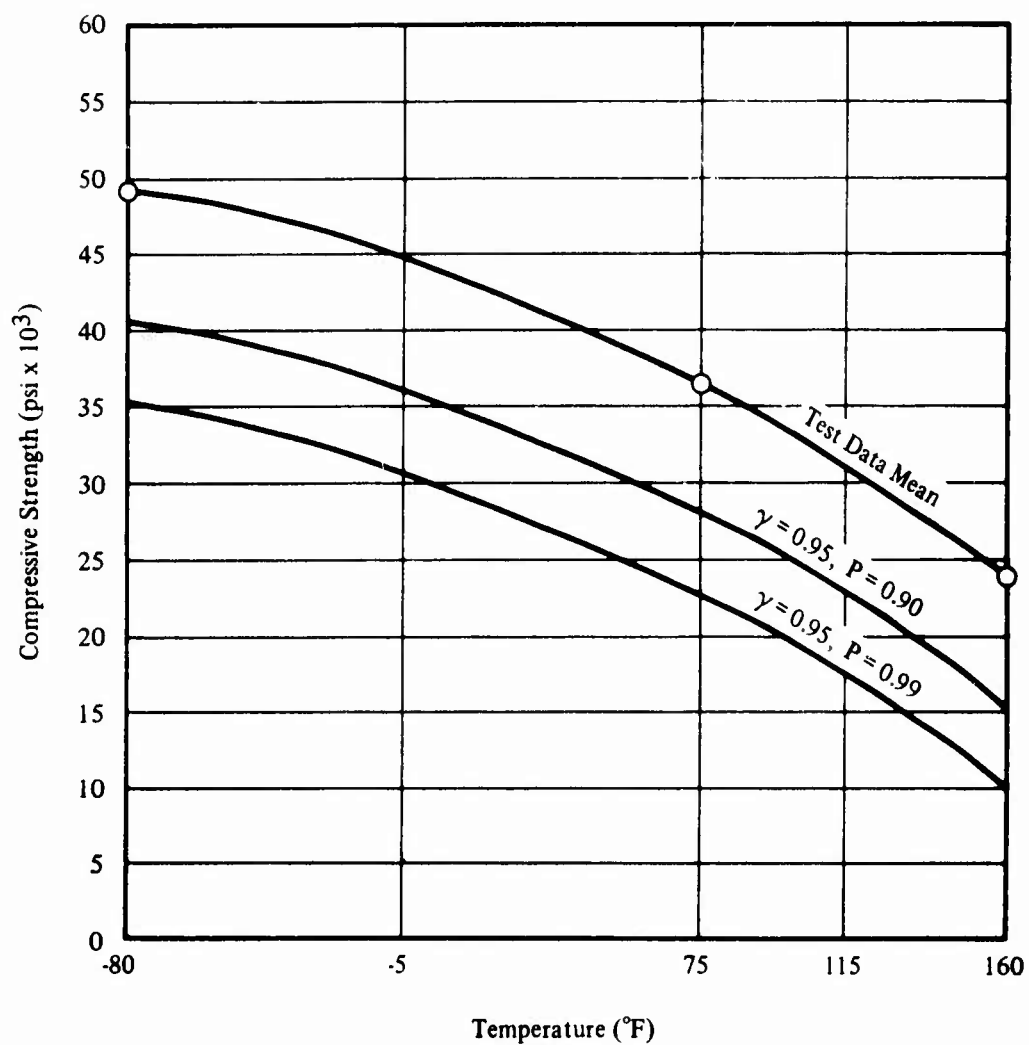


Figure 77. Compressive Strength Design Curves for the Composite Material System.

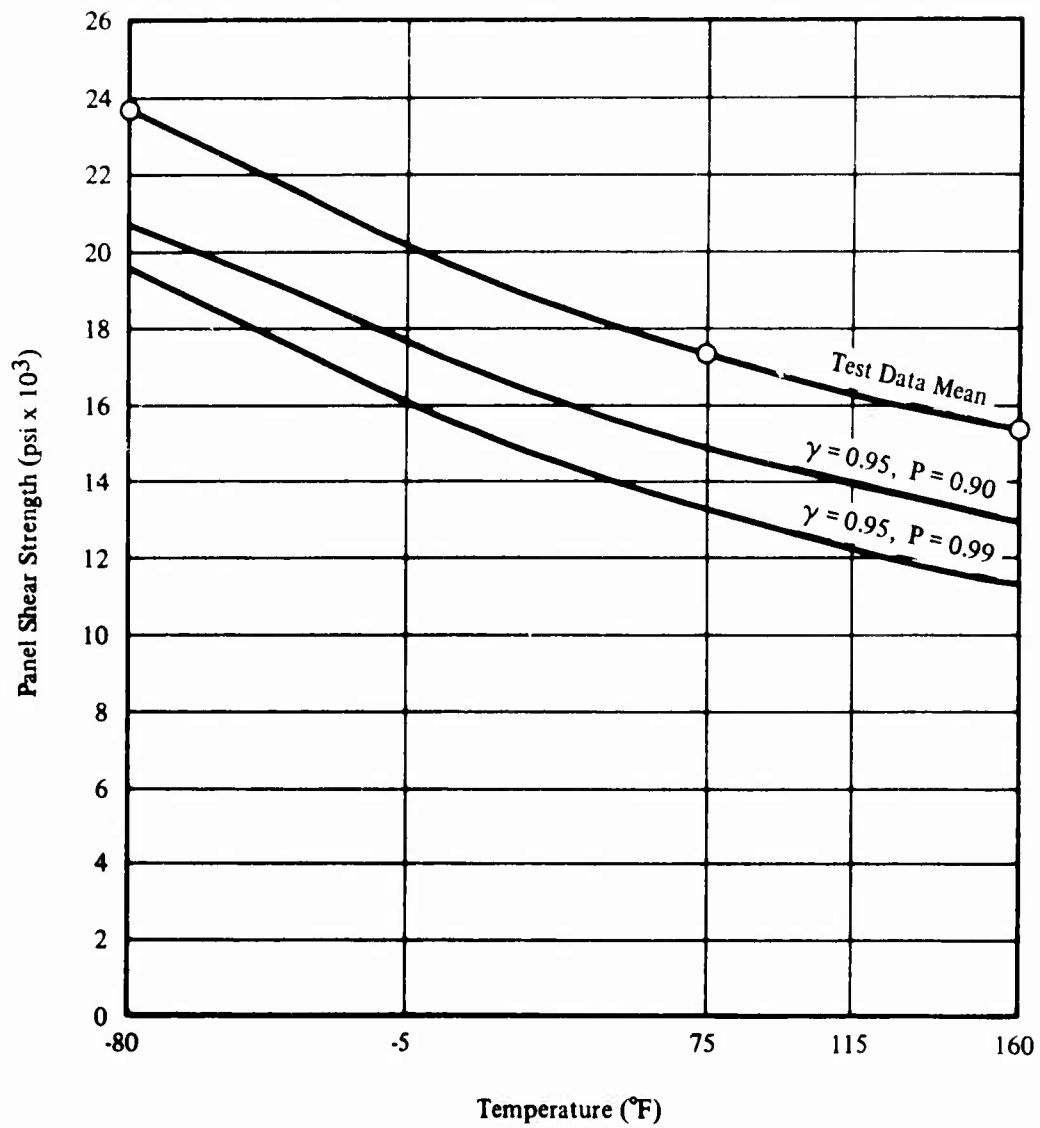


Figure 78. Panel Shear Strength Design Curves for the Composite Material System.

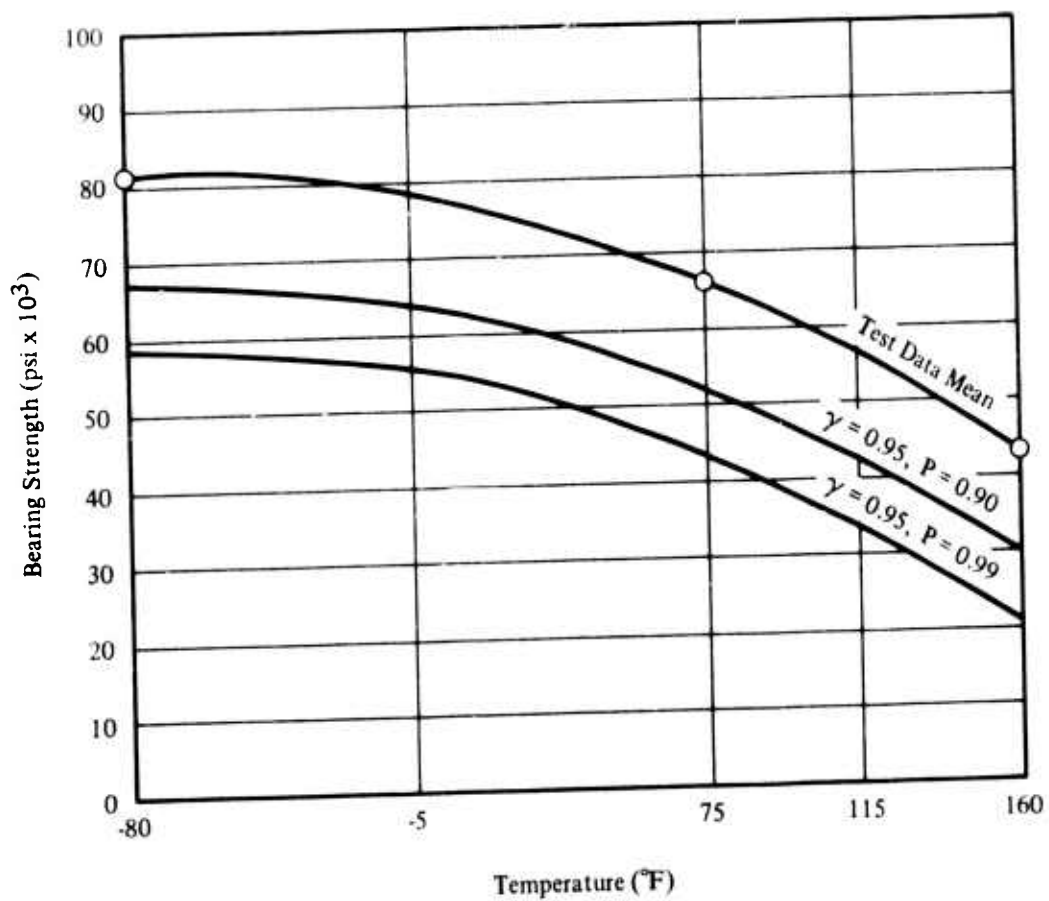


Figure 79. Bearing Strength Design Curves for the Composite Material System.

Unclassified

Security Classification

DOCUMENT CONTROL DATA - R & D

(Security classification of title, body of abstract and indexing annotation must be entered when the overall report is classified)

1. ORIGINATING ACTIVITY (Corporate author) Goodyear Aerospace Corporation Akron, Ohio 44315		2a. REPORT SECURITY CLASSIFICATION Unclassified	
		2b. GROUP	
3. REPORT TITLE DESIGN GUIDE HANDBOOK FOR THE DESIGN OF BALLISTIC-DAMAGE-TOLERANT SHORT-FIBER-MOLDED AIRCRAFT FLIGHT CONTROL SYSTEM COMPONENTS VOLUME I - DESIGN CRITERIA, CONCEPTS, TOOLING, FABRICATION, TESTING, AND EVALUATION			
4. DESCRIPTIVE NOTES (Type of report and inclusive dates) Design Guide Handbook, November 1972 thru April 1973			
5. AUTHOR(S) (First name, middle initial, last name) Donald C. Cully and Theodore J. Boller			
6. REPORT DATE August 1973	7a. TOTAL NO. OF PAGES 160	7b. NO. OF REFS 10	
8a. CONTRACT OR GRANT NO. DAAJ02-70-C-0062	9a. ORIGINATOR'S REPORT NUMBER(S) USAAMRDL Technical Report 73-62A		
b. PROJECT NO. Task 1F162203A15003	9b. OTHER REPORT NO(S) (Any other numbers that may be assigned this report) GER 15881, Volume I		
c.			
d.			
10. DISTRIBUTION STATEMENT Distribution limited to U.S. Government agencies only; test and evaluation; August 1973. Other requests for this document must be referred to the Eustis Directorate, U.S. Army Air Mobility Research and Development Laboratory, Fort Eustis, Virginia 23604.			
11. SUPPLEMENTARY NOTES Volume I of a two-volume report		12. SPONSORING MILITARY ACTIVITY Eustis Directorate, U.S. Army Air Mobility Research and Development Laboratory Fort Eustis, Virginia	
13. ABSTRACT The design guide has been prepared to provide the design engineer, structural analyst, manufacturing engineer, and test engineer with the engineering know-how and technology to design, analyze, manufacture, and test ballistic-damage-tolerant flight control components molded of a short-fiber glass-epoxy composite material. The design guide provides data on the effects of variable material parameters such as resin type, fiber length, fiber type, fiber finish, and composite thickness on the ballistic response of the composite (i.e., the extent of damage and residual load capacity after damage). Fully tumbled caliber .30 ball M2 and untumbled caliber .50 AP M2 projectiles were evaluated at several impact temperatures and velocities. Methods of design to maximize ballistic tolerance and design analysis techniques are described. Designs, tooling and manufacturing techniques, and a test and evaluation program for three typical flight control components are presented. The design guide is organized in two volumes. The greatest amount of the design guide information is unclassified and is presented in this document (Volume I) to facilitate its availability and use by individual designers. The essential classified information is presented in Volume II for sources of pertinent and/or related information that may be required by the designer.			

DD FORM 1473

REPLACES DD FORM 1473, 1 JAN 64, WHICH IS OBSOLETE FOR ARMY USE.

Unclassified

Security Classification

Unclassified

Security Classification

14	KEY WORDS	LINK A		LINK B		LINK C	
		ROLE	WT	ROLE	WT	ROLE	WT
	Aircraft Control System Design Aircraft Structural Design Ballistic-Damage-Tolerant Components Ballistic-Damage-Tolerant Designs Aircraft Survivability Aircraft Safety Helicopter Control System Survivability Composites, Fiber-Glass Reinforced Composites, Short-Fiber Reinforced Impact Damage Small-Arms Fire Design Allowables Fatigue, Cyclic						

Unclassified

Security Classification